Development of the detoxification method for zinc plant leach residues by removing heavy metals using coupled extraction-cementation (CEC) process

A dissertation submitted in partial fulfillment of the requirements for the degree of
Doctorate in Engineering

By

MARTHIAS SILWAMBA

Laboratory of Mineral Processing and Resources Recycling,
Division of Sustainable Resources Engineering,
Graduate School of Engineering,
Hokkaido University, Japan
March 2021

Declaration

I, **Marthias SILWAMBA**, hereby declare that, except where specific reference is made in the text, this dissertation is my own research work and it has never—in its entirety or in parts—submitted to any university for academic qualification.

Signature: _____
M. Silwamba

Date: _____

Acknowledgments

Firstly, I would like to express my wholeheartedly thanks to my Ph.D. supervisor, Assoc. Prof. Mayumi ITO, for her support, constructive and critical advice during my study period. She made me believe in myself and mature as a researcher. Apart from science and engineering, my other invaluable take-homes for working under her supervision are kindness, planning, managing, and organization.

To my co-supervisor, Prof. Naoki HIROYOSHI, he made complex phenomena seem easy. The saying by Albert Einstein “If you can't explain it simply, you don't understand it well enough” was realized after working under him. I am forever grateful and at the same time amazed by how you used to bring those numerous ideas during those long discussions.

I would like also to extend my sincere thanks to Dr. Carlito Baltazar TABELIN who was the assistant professor when I joined the Laboratory of Mineral Processing and Resource Recycling. His views and knowledge about science and engineering are just amazing. I cannot forget to mention his mentorship in academic writing. Furthermore, I would like to pass my sincere gratitude to Assis. Prof. Ilhwan PARK for his generous help and suggestions during my Ph.D. scholar journey. Special thanks go to Ph.D. co-examiners, Prof. Tsutomu SATO and Assoc. Prof. Masatoshi SAKAIRI for their advice and comments that helped improve the quality of this dissertation.

My sincere appreciation also goes to the President of Hokkaido University for Hokkaido University President’s Fellowship scholarship. Additionally, a partial scholarship from MEXT Honors (JASSO) is also highly appreciated. I would like also to acknowledge the research funds from the Japan International Cooperation Agency (JICA)/Japan Science and Technology Agency (JST), and Science and Technology Research Partnership for Sustainable Development (SATREPS).

Many thanks to all members of the Laboratory of Mineral Processing and Resources Recycling for their kindness and for making my life easy and fun in Japan. Special mention of Mr. Tomoki FUKUSHIMA and Mr. Ryota HASHIZUME of Zambia Researcher Group for assistance on this research.

Lastly but not the least, I would love to wholeheartedly thank my wife, Salome MUSANSE-SILWAMBA, and our sons, Salifyanji Marthias SILWAMBA and Isreal Ivwananji SILWAMBA, for their, love, sacrifices, encouragements, and prayers. It was painful and in many times disturbing to do this Ph.D. miles away from them. My lovely wife did everything possible to take good care of our sons while I was away. Special thanks also go to my parents (Mr. E. H. Silwamba and Mrs. J. N. Silwamba), brothers and sisters for always being there for me. Finally, my heart is full of gratitude and praise to the Almighty God for my life and EVERYTHING, indeed I am just the pencil in His hands.

Abstract

Enormous amounts of solid wastes are generated annually as the result of extensive mining, mineral processing, and metal extraction operations. For example, zinc (Zn) metal extraction via hydrometallurgical processes—leaching of calcine or zinc oxide minerals followed by electrowinning of Zn—generate huge amounts of zinc plant leach residues (ZPLRs) which are often stockpiled, and in many instances abandoned after closure of mining/metallurgical processing operations. With the rapid depletion of high-grade geogenic ores, ZPLRs are now considered as secondary resources because they contain significant amounts of valuable metals such as Zn, copper (Cu), lead (Pb), and silver (Ag) depending on the original ores processed. From an environmental point of view, however, ZPLRs are considered toxic wastes because they contain hazardous heavy metals such as Pb, Zn, and cadmium (Cd), among others. The environmental and resource concerns of the ZPLRs can be addressed by removing/or recovering heavy/or valuable metals. In this study, an innovative method, a coupled extraction-cementation (CEC) process that combines two stages (i.e., extraction and recovery of extracted valuable/heavy metals thereby minimizing the operation stages and amounts of lixiviant) is investigated to detoxify high-Pb and Zn ZPLRs obtained from Kabwe, Zambia. The outline and abstract of each chapter are as below:

In Chapter 1, the background, problem description, and objectives of the study are presented.

In Chapter 2, a review of previous studies on methods and techniques used in the concentration of valuable minerals and recovery of valuable and critical metals from ZPLRs and other Zn hydrometallurgical solid wastes such as iron removal purification residues and metal cementation filter cake was conducted.

Chapter 3 reported on the detoxification of ZPLRs by the Fe-based CEC process using microscale zero-valent iron (mZVI) and acidified chloride (HCl-NaCl) solution. For the Fe-based CEC process, only Pb (the most toxic) was targeted for cementation in leaching pulp before solid-liquid separation. Lead removal was evaluated in different solution compositions with and without the addition of mZVI. Cementation products were separated from the leaching pulp by magnetic separation. The addition of mZVI during ZPLRs leaching (i.e., Fe-based CEC) increased Pb removal from 3% to 24%, 1.3% to 27.5%, 5.2% to 34.9%, and 6.5% to 55.8% when NaCl concentration was fixed at 0.86 M and HCl concentrations were 0 M, 0.01 M, 0.05 M and 0.1 M, respectively, after 12 h. Analysis of the Pb-loaded mZVI (magnetic fraction) by scanning electron microscopy with energy-dispersive X-ray spectroscopy (SEM-EDX) and X-ray photoelectron spectroscopy (XPS) revealed that Pb was recovered during leaching via cementation as zero-valent Pb (Pb^0). The toxicity characteristic leaching procedure (TCLP) for Pb of ZPLRs before and after CEC treatment decreased from 11.3 to 3.5 mg/L (below 5 mg/L threshold).

In Chapter 4, selective agglomeration of zero-valent Pb, Zn, Al was investigated. This was necessary to evaluate the applicability of the Al-based CEC process for ZPLRs because the hypothesized cementation product (Pb-Zn-Al) cannot be separated physically from the leaching pulp using a magnet. When Zn, Al, and Pb metal powders were shaken in 0.1 M HCl, only Pb agglomerated. Further investigation showed that Pb agglomeration occurred in acidified chloride (HCl-NaCl) solution, but not in non-acidified chloride (NaCl) solution. Agglomeration was proposed to be a result of the removal of the brittle oxide film and the metallurgical bond formation ('solid-state cold welding') between Pb particles because Pb is a soft metal whose crystallization occurs even at room temperature. To investigate selective agglomeration of fine Pb metal particles in presence of other fine particles, fixed amounts of Pb metal powder were mixed with various amounts of fine quartz particles (–53 μm). Aluminum metal powder was also added to cement dissolved Pb^{2+}. Separation of agglomerated Pb from quartz was done by sieving. Around 98% of Pb metal powder was selectively agglomerated and could be separated effectively from quartz even for the as high mass ratio of quartz to Pb metal as 24 g to 0.15 g. This implied that Al-based CEC could be applied to ZPLRs because the cementation product could be separated from the leaching pulp by sieving.

Chapter 5 investigated the removal of both Pb and Zn from ZPLRs by an Al-based CEC process using zero-valent aluminum (ZVAl) in acidified chloride solution. The reasons for using ZVAl were (1) to cement both Pb and Zn since thermodynamic potential shows that ZVAl can favorably cement Pb and Zn, and (2) to use stronger reducing agent metal to increase the rate of the electrochemical reaction of cementation of Pb and Zn. The fact that ZVAl and targeted cemented metals (i.e., Pb and Zn) are non-ferromagnetic, separation of cementation product from the leaching pulp was via sieving since cemented product agglomerated. The results showed that for 2 h Pb removal significantly increased when ZVAl was added using low chloride concentration (e.g., for 0.1 M HCl, the addition of ZVAl increased Pb removal from 3% to 69% and 9% to 72% for 0.5 M and 1 M NaCl). The dramatic increase of Pb removal at low NaCl concentration was attributed to the leaching solution not attaining saturated with dissolved Pb^{2+} and Pb-Cl complexes. However, Zn removal, which was independent of NaCl concentration and addition of ZVAl, was not cemented out of the leaching pulp despite it being thermodynamic favorable. The suppression of cementation of Zn by ZVAl was attributed to proton (H^{+}) competition for electrons from ZVAl. The leachability test results using TCLP protocol for detoxified residues showed that Pb and Zn in solution were as low as 0.12 mg/L (below 5 mg/L threshold) and 21.5 mg/L (below 25 mg/L threshold), respectively. A treatment flowchart for detoxification of ZPLRs using Al-based CEC was proposed.

And finally, Chapter 6 summarizes the important findings of this dissertation and proposes possible future research works.

Table of Contents

List of Figures

List of Tables

CHAPTER 1: GENERAL INTRODUCTION

1.1. Background

The ever-increasing demand for metals is as the results of explosive population growth in the past decades which has led to an increase in economic activities such as construction and modernization of communication equipment, transportation, and advancement in agricultural and medical sectors where metals are used extensively (Daigo et al., 2014; Halada et al., 2008; Mohr et al., 2018). This high demand has led to enormous increase of amounts of solid wastes and residues that are generated from metals extraction by metallurgical processes. Zinc (Zn) metal extraction, for example, from sulfide or oxide ores by classical hydrometallurgical route (i.e., roast-leach-electrowinning for sulfide ores or direct leach-electrowinning processes) generates huge amounts of metallurgical solid wastes (Zn plant leach residues and purification residues) of 0.5–0.9 tonnes per tonne of Zn metal produced (Pelino et al., 1996; Rämä et al., 2018).

Zinc hydrometallurgical solid wastes, particularly the Zn plant leach residues and purification residues, are usually stockpiled, and in some instances abandoned after the closure of extraction operations (Gutiérrez et al., 2016). The stockpiled Zn hydrometallurgical wastes pose serious threats to the existent of life in the biosphere because they contain toxic heavy metals and metalloid such as residual Zn, lead (Pb), arsenic (As), copper (Cu), and cadmium (Cd) among others (Behnajady and Moghaddam, 2017; Li et al., 2017; Lu et al., 2014; Ruşen et al., 2008; Sethurajan et al., 2016). However, Zn hydrometallurgical wastes are currently considered as a secondary resource of the said metals as well as current critical metals such cobalt (Co), indium (In), germanium (Ge), and gallium (Ga) due to the depletion of high-grade geogenic ores (Fattahi et al., 2016; Licht et al., 2015; Safarzadeh et al., 2011). Thus, heavy metals removal/recovery from Zn hydrometallurgical wastes tackles the environmental and resource concerns all together.

Although pyrometallurgical processes can be employed to remove/recover heavy metals from Zn hydrometallurgical wastes (Mombelli et al., 2019, 2018; Wang et al., 2013), they are not preferred processes because (1) they are energy-intensive as they are operated at high temperatures, (2) they produce toxic and greenhouse gases, and (3) they are not suitable for feed materials containing low grade of valuable metals like the Zn hydrometallurgical wastes without any concentration. Hydrometallurgical processes, on the other hand, are relatively less energy-intensive, produce solid residues as well as gases that may cause less or no secondary environmental pollution, and can be used to treat low grade Zn hydrometallurgical wastes economically. This could be the reason why

numerous studies have been published on the removal/recovery of heavy metals/valuable metals from Zn residue wastes using hydrometallurgical processes (Li et al., 2018; Reyes et al., 2017; Ruşen et al., 2008; Sethurajan et al., 2016; Zhang et al., 2019). However, all the studied hydrometallurgical processes follow the conventional sequence of (1) leaching, (2) solid-liquid separation, and (3) finally recovery of dissolved metals from leachates. Although hydrometallurgical processes that follow the conventional sequence achieve the intended purpose of toxic heavy metal removal or valuable metals recovery from Zn wastes, there are two serious drawbacks. Firstly, at the leaching stage, highly concentrated lixiviants are required to extract the target metal(s) (Farahmand et al., 2009; Guo et al., 2010). Secondly, resultant leaching residues contain heavy metal-rich residual solution due to difficulties and inherently incomplete solid-liquid separation partly exacerbated by silica gel formation and the presence of very fine particles in Zn residues wastes (Bodas, 1996; He et al., 2011). To remove residual solutions from generated solid residues after solid-liquid separation, extensive washing or stabilization before disposal should be carried out, requiring complex treatment processes that increase operating costs.

1.2. Objectives of the study

This dissertation proposes and investigates coupled extraction-cementation (CEC) hydrometallurgical processes that address the limitations of conventional hydrometallurgical sequences of processes to remove heavy metals from abandoned Zn plant leach residues (ZLPRs) in Kabwe, Zambia. For CEC hydrometallurgical process, extracted metals are captured/sequestered by cementation before the solid-liquid separation hence eliminating the need for extensive washing of resultant residues to remove residual heavy metal-rich solution (Fig. 1-1). Additionally, a low concentrated solution is used to achieve high removal/recovery as the solution would not be saturated with dissolved metals. The specific objectives are to:

1. Detoxify ZPLRs by removal of Pb via Fe-based CEC process using micro-scale zero-valent iron (mZVI) as the Pb^{2+} cementation agent in acidified chloride solution.
2. Investigate removal of both Pb and Zn from ZPLRs by Al-based CEC process using zero-valent aluminum (ZVAl) in acidified chloride solution.

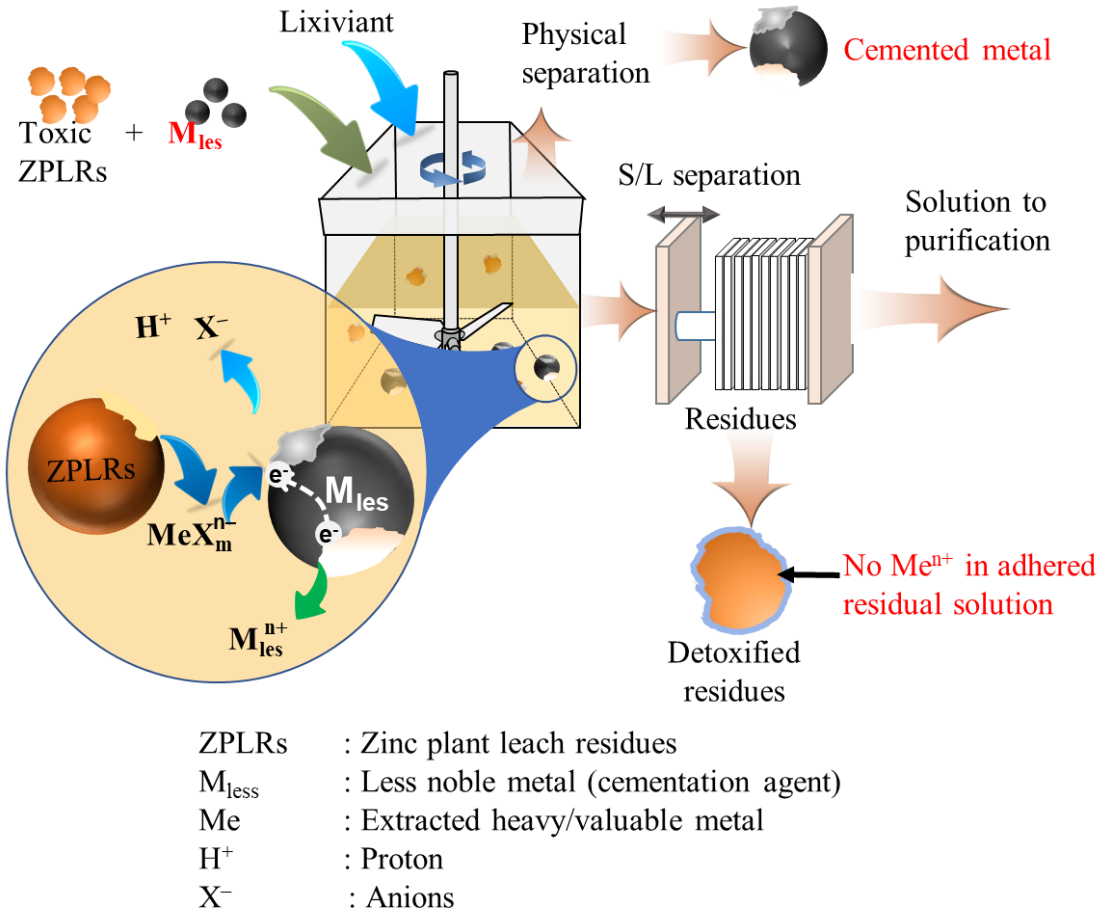

Fig. 1-1. Schematic of CEC process for zinc plant leach residues

1.3. Study area

The Zn plant leach residues were obtained from abandoned Pb-Zn mine wastes from Kabwe, Zambia (Fig. 1-2). Kabwe is known to be among the Pb polluted towns due to the mining activities that took place for 90 years (1904-1994) and continued transportation of the Pb-Zn mine wastes, particularly Zn plant leach residues since it composed of fine particles, from the dumpsite to residential areas by wind and water erosion. This is partly the reason why topsoil of most residential areas close to the mine dumpsite have elevated amount of Pb above 2000 mg/kg (Kříbek et al., 2019; Tembo et al., 2006) and children's blood lead level as high as 4.28 mg/L (Yabe et al., 2019, 2015) which is way above the revised recommended 0.05 mg/L by Centers for Diseases Control and Prevention (CDC, 2012).

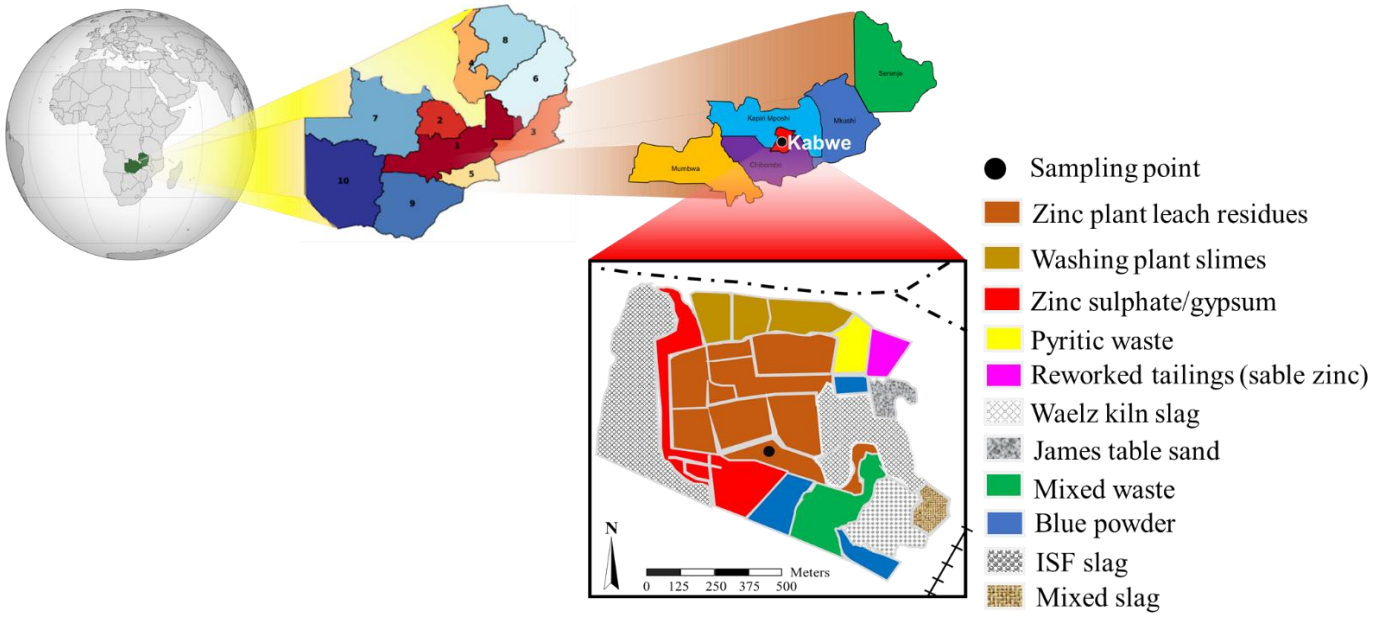

Fig. 1-2. Schematic geographic map of Africa superimposed with map of Zambia superimposed and the location of the Kabwe as well as different types of historic Pb-Zn mine wastes.

1.4. Dissertation outline

Chapter 1 gives a general background, objectives of the study, and study area description.

Chapter 2 reviews previous studies on removal/recovery of heavy/valuable metals from Zn hydrometallurgical wastes.

Chapter 3 reports on the detoxification of ZPLRs by Fe-based CEC process using microscale zero-valent iron (mZVI) in chloride solution to simultaneously recover extracted Pb.

Chapter 4 investigates selective agglomeration of zero-valent Pb, Zn, and Al. This was necessary to evaluate the applicability of the Al-based CEC process for ZPLRs because the hypothesized cementation product (Pb-Zn-Al) cannot be separated physically from the leaching pulp using magnet

Chapter 5 investigates removal of both Pb and Zn via Al-based CEC process using zero-valent aluminum zero-valent aluminum (ZVAl) in acidified chloride solution.

Chapter 6 gives the summary and general conclusion of the dissertation and proposes future research works.

References

Behnajady, B., Moghaddam, J., 2017. Selective leaching of zinc from hazardous As-bearing zinc plant purification filter cake. Chemical Engineering Research and Design 117, 564–574. https://doi.org/10.1016/j.cherd.2016.11.019

Bodas, M.G., 1996. Hydrometallurgical treatment of zinc silicate ore from Thailand. Hydrometallurgy 40, 37–49. https://doi.org/10.1016/0304-386X(94)00076-F

CDC, 2012. Low level lead exposure harms children: a renewed call for primary prevention. Report of the Advisory Committee on Childhood Lead Poisoning Prevention of the Centers for Disease Control and Prevention (the Centers for Disease Control and Prevention (CDC)), the Centers for Disease Control and Prevention (CDC). Atlanta.

Daigo, I., Osako, S., Adachi, Y., Matsuno, Y., 2014. Time-series analysis of global zinc demand associated with steel. Resources, Conservation and Recycling 82, 35–40. https://doi.org/10.1016/j.resconrec.2013.10.013

Farahmand, F., Moradkhani, D., Safarzadeh, M.S., Rashchi, F., 2009. Brine leaching of lead-bearing zinc plant residues: Process optimization using orthogonal array design methodology. Hydrometallurgy 95, 316–324. https://doi.org/10.1016/j.hydromet.2008.07.012

Fattahi, A., Rashchi, F., Abkhoshk, E., 2016. Reductive leaching of zinc, cobalt and manganese from zinc plant residue. Hydrometallurgy 161, 185–192. https://doi.org/10.1016/j.hydromet.2016.02.003

Guo, Z., Pan, F., Xiao, X., Zhang, L., Jiang, K., 2010. Optimization of brine leaching of metals from hydrometallurgical residue. Transactions of Nonferrous Metals Society of China 20, 2000–2005. https://doi.org/10.1016/S1003-6326(09)60408-8

Gutiérrez, M., Mickus, K., Camacho, L.M., 2016. Abandoned PbZn mining wastes and their mobility as proxy to toxicity: A review. Science of The Total Environment 565, 392–400. https://doi.org/10.1016/j.scitotenv.2016.04.143.

Halada, K., Shimada, M., Ijima, K., 2008. Forecasting of the Consumption of Metals up to 2050. Materials Transactions 49, 402–410. https://doi.org/10.2320/matertrans.ML200704.

He, S., Wang, J., Yan, J., 2011. Pressure leaching of synthetic zinc silicate in sulfuric acid medium. Hydrometallurgy 108, 171–176. https://doi.org/10.1016/j.hydromet.2011.04.004.

Kříbek, B., Nyambe, I., Majer, V., Knésl, I., Mihaljevič, M., Ettler, V., Vaněk, A., Penížek, V., Sracek, O., 2019. Soil contamination near the Kabwe Pb-Zn smelter in Zambia: Environmental impacts and remediation measures proposal. Journal of Geochemical Exploration 197, 159–173. https://doi.org/10.1016/j.gexplo.2018.11.018.

Li, B., Wang, X., Wei, Y., Wang, H., Barati, M., 2018. Extraction of copper from copper and cadmium residues of zinc hydrometallurgy by oxidation acid leaching and cyclone electrowinning. Minerals Engineering 128, 247–253. https://doi.org/10.1016/j.mineng.2018.09.007.

Li, M., Zheng, S., Liu, B., Du, H., Dreisinger, D.B., Tafaghodi, L., Zhang, Y., 2017. The leaching kinetics of cadmium from hazardous Cu-Cd zinc plant residues. Waste Management 65, 128–138. https://doi.org/10.1016/j.wasman.2017.03.039.

Licht, C., Peiró, L.T., Villalba, G., 2015. Global Substance Flow Analysis of Gallium, Germanium, and Indium: Quantification of Extraction, Uses, and Dissipative Losses within their Anthropogenic Cycles. Journal of Industrial Ecology 19, 890–903. https://doi.org/10.1111/jiec.12287.

Lu, D., Jin, Z., Shi, L., Tu, G., Xie, F., Asselin, E., 2014. A novel separation process for detoxifying cadmium-containing residues from zinc purification plants. Minerals Engineering 64, 1–6. https://doi.org/10.1016/j.mineng.2014.03.026.

Mohr, S., Giurco, D., Retamal, M., Mason, L., Mudd, G., 2018. Global Projection of Lead-Zinc Supply from Known Resources. Resources 7, 17. https://doi.org/10.3390/resources7010017.

Mombelli, D., Mapelli, C., Barella, S., Gruttadauria, A., Spada, E., 2019. Jarosite wastes reduction through blast furnace sludges for cast iron production. Journal of Environmental Chemical Engineering 7, 102966. https://doi.org/10.1016/j.jece.2019.102966.

Mombelli, D., Mapelli, C., Di Cecca, C., Barella, S., Gruttadauria, A., Ragona, M., Pisu, M., Viola, A., 2018. Characterization of cast iron and slag produced by jarosite sludges reduction via Arc Transferred Plasma (ATP) reactor. Journal of Environmental Chemical Engineering 6, 773–783. https://doi.org/10.1016/j.jece.2018.01.006.

Pelino, M., Cantalini, C., Abbruzzese, C., Plescia, P., 1996. Treatment and recycling of goethite waste arising from the hydrometallurgy of zinc. Hydrometallurgy 40, 25–35. https://doi.org/10.1016/0304-386X(95)00004-Z.

Rämä, M., Nurmi, S., Jokilaakso, A., Klemettinen, L., Taskinen, P., Salminen, J., 2018. Thermal Processing of Jarosite Leach Residue for a Safe Disposable Slag and Valuable Metals Recovery. Metals 8, 744. https://doi.org/10.3390/met8100744.

Reyes, I.A., Patiño, F., Flores, M.U., Pandiyan, T., Cruz, R., Gutiérrez, E.J., Reyes, M., Flores, V.H., 2017. Dissolution rates of jarosite-type compounds in H2SO4 medium: A kinetic analysis and its importance on the recovery of metal values from hydrometallurgical wastes. Hydrometallurgy 167, 16–29. https://doi.org/10.1016/j.hydromet.2016.10.025.

Ruşen, A., Sunkar, A.S., Topkaya, Y.A., 2008. Zinc and lead extraction from Çinkur leach residues by using hydrometallurgical method. Hydrometallurgy 93, 45–50. https://doi.org/10.1016/j.hydromet.2008.02.018.

Safarzadeh, M.S., Dhawan, N., Birinci, M., Moradkhani, D., 2011. Reductive leaching of cobalt from zinc plant purification residues. Hydrometallurgy 106, 51–57. https://doi.org/10.1016/j.hydromet.2010.11.017.

Sethurajan, M., Huguenot, D., Lens, P.N.L., Horn, H.A., Figueiredo, L.H.A., van Hullebusch, E.D., 2016. Leaching and selective copper recovery from acidic leachates of Três Marias zinc plant (MG, Brazil) metallurgical purification residues. Journal of Environmental Management 177, 26–35. https://doi.org/10.1016/j.jenvman.2016.03.041.

Tembo, B.D., Sichilongo, K., Cernak, J., 2006. Distribution of copper, lead, cadmium and zinc concentrations in soils around Kabwe town in Zambia. Chemosphere 63, 497–501. https://doi.org/10.1016/j.chemosphere.2005.08.002.

Wang, X.Q., Xie, K.Q., Ma, W.H., Yang, M.Y., Zeng, P., Cao, Y.C., 2013. Recovery of zinc and other valuable metals from zinc leach residue by top blowing fuming method. Mineral Processing and Extractive Metallurgy 122, 174–178. https://doi.org/10.1179/1743285513Y.0000000045.

Yabe, J., Nakayama, S.M.M., Ikenaka, Y., Yohannes, Y.B., Bortey-Sam, N., Oroszlany, B., Muzandu, K., Choongo, K., Kabalo, A.N., Ntapisha, J., Mweene, A., Umemura, T., Ishizuka, M., 2015. Lead poisoning in children from townships in the vicinity of a lead–zinc mine in Kabwe, Zambia. Chemosphere 119, 941–947. https://doi.org/10.1016/j.chemosphere.2014.09.028.

Yabe, J., Nakayama, S.MM., Nakata, H., Toyomaki, H., Yohannes, Y.B., Muzandu, K., Kataba, A., Zyambo, G., Hiwatari, M., Narita, D., Yamada, D., Hangoma, P., Munyinda, N.S., Mufune,

T., Ikenaka, Y., Choongo, K., Ishizuka, M., 2019. Current Trends of Blood Lead Levels, Distribution Patterns and Exposure Variations among Household Members in Kabwe, Zambia. Chemosphere 125412. https://doi.org/10.1016/j.chemosphere.2019.125412.

Zhang, Y., Jin, B., Song, Q., Chen, B., Wang, C., 2019. Leaching Behavior of Lead and Silver from Lead Sulfate Hazardous Residues in NaCl-CaCl2-NaClO3 Media. JOM 71, 2388–2395. https://doi.org/10.1007/s11837-019-03472-1

CHAPTER 2: ZINC HYDROMETALLURGICAL SOLID WASTES THE HAZARDOUS MATERIALS AND SECONDARY RESOURCE OF VALUABLE AND CRITICAL METALS: A REVIEW

2.1. Introduction

Zinc (Zn) is the fourth highest consumed metal globally, whose use spans from steel galvanizing, brass casting, bronze casting, manufacture of medicines, rubbers, and pigments (Daigo et al., 2014; Kaya et al., 2020). Zinc has been extracted from Roman times from widespread deposits of different geochemical and mineralogical compositions (Gutiérrez et al., 2016) (Fig. 2-1). Around 85% of Zn metal is produced by hydrometallurgical processes—leach-purification-electrowinning processes—(after pretreatment of zinc sulfide (ZnS) concentrate via the oxidative roasting process for sulfide ores or direct leaching for zinc oxide ores) (Abkhoshk et al., 2014). The calcine—roasting product of zinc sulfide (ZnS) concentrate—contains around 56-65 wt% Zn and the remaining 35-44 wt% are gangue minerals (e.g., iron (Fe), silicon (Si), and calcium (Ca), Sulfur (S)), accompanied valuable metals (e.g., Zn, copper (Cu), lead (Pb), silver (Ag), cadmium (Cd), and nickel (Ni)) and currently listed critical metals (e.g., cobalt (Co), indium (In), gallium (Ga), vanadium (V), and germanium (Ge)) depending on the origin of the ores (Behnajady and Moghaddam, 2017a; Fan et al., 2019; Khosravirad et al., 2020a; Kumar Sahu et al., 2020; Safarzadeh et al., 2009c; Zhu et al., 2018a). For Zn oxide ores the content of target Zn metal is even lower in the range of 10-30 wt% (Abkhoshk et al., 2014) and the remaining being gangue minerals and other minerals containing valuable and critical metals. Gangue minerals and minerals containing valuable and critical metals constitute the enormous amounts of zinc hydrometallurgical solid wastes that are generated as leaching residues or purification residues at different stages of Zn metal production.

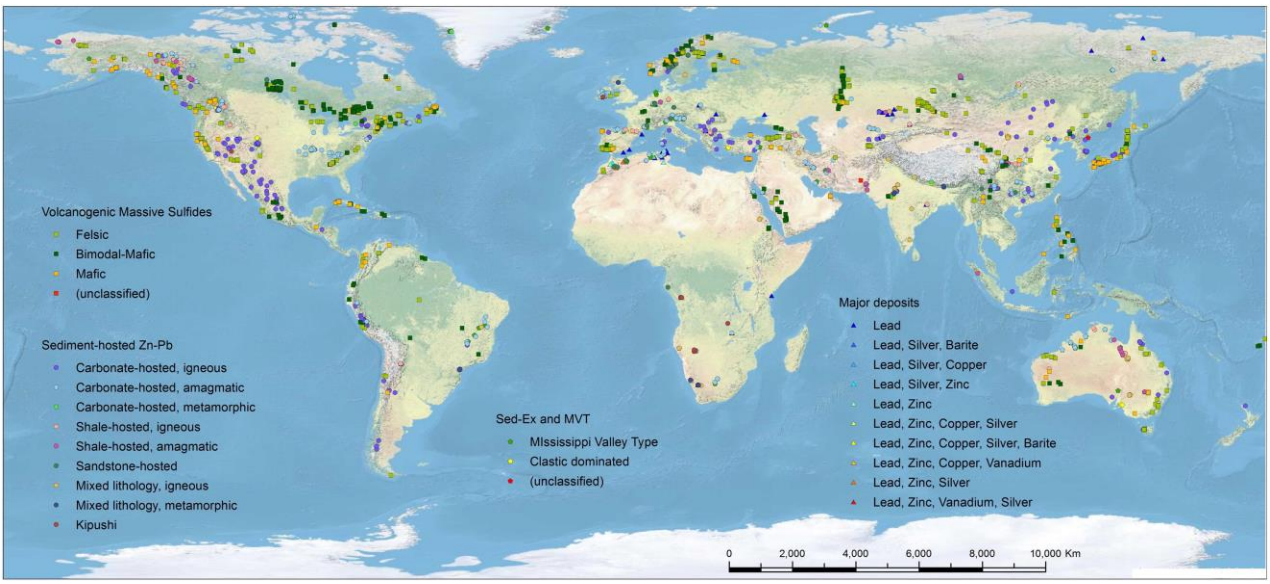

Fig. 2-1. Global occurrence of Pb-Zn ore deposits (reprinted with permission from Gutiérrez et al. (2016), copyright (2021) Elsevier)

Zinc hydrometallurgical solid wastes are usually dumped in ponds near the processing plants where they take up much space. Although these wastes contain valuable and critical metals, they are a nuisance to the biosphere because they contain toxic heavy metals/metalloids such as Cd, Pb, Ni, mercury (Hg), and arsenic (As) among others. These toxic metals/metalloids leach out from Zn hydrometallurgical solid wastes and contaminate surrounding topsoils and ground as well as surface waters (Anju and Banerjee, 2011; Demır et al., 2008; Gutiérrez et al., 2016; Sethurajan et al., 2016a). The toxicity and public health significance of these heavy metals even at low exposure concentrations are well documented (Needleman, 2004; Tabelin et al., 2018).

Treatment of Zn hydrometallurgical solid wastes is broadly categorized into two (1) immobilization of heavy metals and (2) heavy/valuable metals removal/recovery by either phytoextractions or various metallurgical techniques. The initial cost of immobilization of heavy metals by addition of chemical adsorbents/stabilizers (Erdem and Özverdi, 2011; Tangviroon et al., 2020) or by bio-immobilizer (Mwandira et al., 2019) may be relatively low, but this usually needs constant monitoring and maintenance. Besides, valuable and critical metals are lost to immobilized products. Meanwhile, heavy metals removal from Zn hydrometallurgical solid wastes by phytoextraction (Kumar et al., 1995; Lorestani et al., 2013; Roshanfar et al., 2020) is a slow process and valuable metals are equally lost to the biomass. In addition, challenges of plant growth in residues with high heavy metals have been reported (Leteinturier et al., 2001).

With the advent of the depreciation of the high-grade geogenic ores, the recovery of valuable and critical metals from zinc metallurgical solid wastes by various metallurgical processes has attracted much attention (Ju et al., 2011a; Kumar Sahu et al., 2020; Ruşen et al., 2008a; Sethurajan et al., 2017a; Tang et al., 2019; Zhang et al., 2016). Besides, the environmental threats posed by these wastes are indirectly eliminated by reprocessing and extraction of metals by metallurgical processes. Another benefit of metal extraction from Zn hydrometallurgical solid wastes is the reduction of carbon dioxide (CO_2) emitted per ton of metals produced compared to CO_2 emitted from the extraction of Zn and other valuable metals from primary ores (Kaya et al., 2020; Ng et al., 2016). Reviews published recently have only discussed the recovery of a single given metal from general industrial and domestic solid wastes, thus, the secondary resource potential of Zn hydrometallurgical solid wastes for many valuable and critical metals are not discussed in depth (Jha et al., 2001; Kaya et al., 2020; Matinde et al., 2018; Ng et al., 2016). Besides, a review of the environmental significance of Zn hydrometallurgical solid wastes has been covered by only a few researchers (Gutiérrez et al., 2016). The aim of this is chapter is to give a comprehensive overview of the resource and environmental importance of different types of Zn hydrometallurgical solid wastes that are generated during Zn metal production. In particular, this chapter focuses on the effects of these wastes on the environment where they are dumped, recent novel metallurgical techniques applied to recover/remove valuable/critical/heavy metals from Zn hydrometallurgical solid wastes.

2.2. Zinc production and generation of hydrometallurgical solid wastes

Figure 2-2 shows a simplified process flowchart of Zn metal production by hydrometallurgical processes from zinc sulfide minerals (sphalerite (ZnS), iron-bearing sphalerite ((Zn,Fe)S), lead-bearing sphalerite ((Zn,Pb)S), etc.,) which account for almost 95% of global Zn metal (Kaya et al., 2020). Zinc content in mined ore is around 5-15% and it is concentrated to around 55% by froth flotation before subjecting it to the pretreatment stage, oxidative roasting. During oxidative roasting of Zn sulfide concentrate at around 800°C (dead roasting), Zn sulfide minerals are converted to Zn oxide minerals. Similarly, gangue sulfide minerals, as well as valuable (including critical elements) sulfide minerals, are equally converted to their respective oxide minerals. Simplified chemical reactions that occur during oxidative roasting are depicted by Eq. 2-1 to 2-14 (here Me is Cu, Pb, Co, Ni, Ag, and Cd, etc.,) (Balarini et al., 2008; Boyanov et al., 2014).

$$2ZnS + 3O_2 = 2ZnO + 2SO_2 \quad (2\text{-}1)$$

$$ZnS + 2O_2 = ZnSO_4 \quad (2\text{-}2)$$

$$ZnSO_4 = ZnO + SO_3 \quad (2\text{-}3)$$

$$MeS + 3/2O_2 = MeO + SO_2 \quad (2\text{-}4)$$

$$MeS + 2O_2 = MeSO_4 \quad (2\text{-}5)$$

$$MeSO_4 = MeO + SO_3 \quad (2\text{-}6)$$

$$SO_3 = 1/2O_2 + SO_2 \quad (2\text{-}7)$$

$$2FeS_2 + 2O_2 = 2FeS + 2SO_2 \quad (2\text{-}8)$$

$$FeS + 2O_2 = FeSO_4 \quad (2\text{-}9)$$

$$3FeS + 5O_2 = Fe_3O_4 + 3SO_2 \quad (2\text{-}10)$$

$$2FeSO_4 = Fe_3O_4 + SO_2 + SO_3 \quad (2\text{-}11)$$

$$4Fe_3O_4 + O_2 = 6Fe_2O_3 \quad (2\text{-}12)$$

$$ZnO + Fe_2O_3 = ZnFe_2O_4 \quad (2\text{-}13)$$

$$2ZnO + SiO_2 = Zn_2SiO_4 \quad (2\text{-}14)$$

The formation of $ZnFe_2O_4$ (Eq. 2-13) and Zn_2SiO_4 (Eq. 2-14) are undesirable because their refractoriness hence requires strong acid solutions to dissolve Zn. Furthermore, for the indium(in)-bearing Zn ores the formed $ZnFe_2O_4$ mineral during roasting incorporates In by isomorphic substitution of Fe in the lattice (Fan et al., 2019; Rao and Rao, 2005) which leads to loss of In unless $ZnFe_2O_4$ is dissolved.

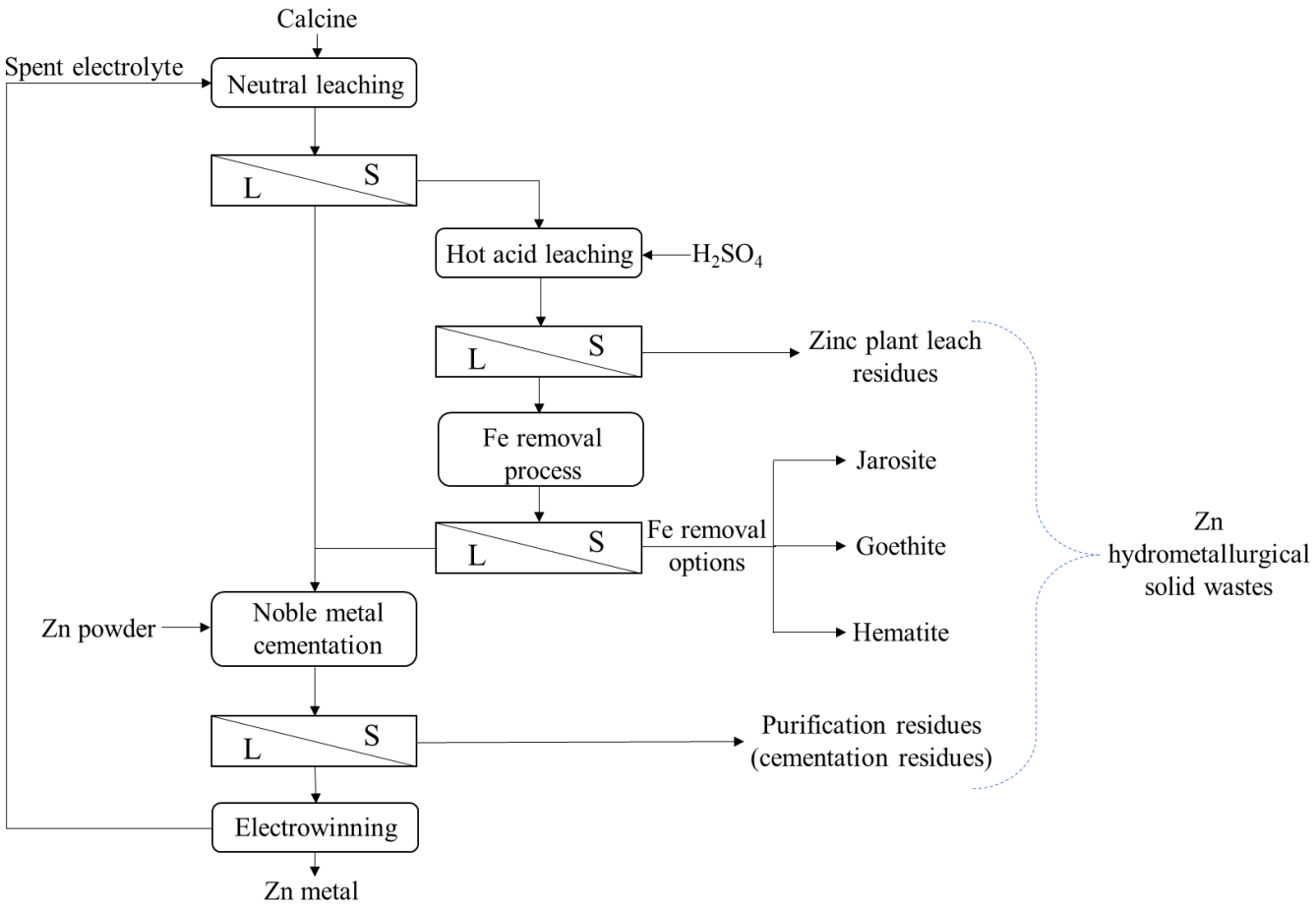

Fig. 2-2. Simplified zinc extraction process flowchart.

2.2.1. Leaching of calcine/oxide ore and generation of zinc plant leach residues

The roasted Zn concentrate (calcine) or concentrated Zn oxide ore is subjected to neutral leaching where ZnO and MeO (here Me is Cu, Cd, Co, Ni and small amounts of Pb and Ag) are dissolved in spent sulfate electrolyte leaving a hard to dissolve minerals like SiO_2, Zn_2SiO_4, $ZnFe_2O_4$, and Fe_2O_3 in residues. Accompanied Pb (PbO) in calcine/Zn oxide ore is leached at neutral leaching and precipitate as $PbSO_4$, thus it is removed together with neutral residues. Neutral leach residues are then treated with the hot H_2SO_4 to possibly leach $ZnFe_2O_4$ and Zn_2SiO_4. The co-dissolved Fe and Si make downstream purification challenging due to the formation of voluminous purification wastes and silica gel formation, respectively. The leach residues generated at the hot H_2SO_4 leaching stage are usually stockpiled and they contain undissolved $ZnFe_2O_4$ and Zn_2SiO_4, $PbSO_4$, and other adsorbed valuable and critical metals. For In-bearing Zn calcine, In is lost in the matrix of the undissolved $ZnFe_2O_4$.

2.2.2. Leachate purification and generation of purification residues

Dissolved Fe is removed from the leachate by precipitating it as jarosite, goethite, or hematite and the Zn hydrometallurgical process is named after the adopted Fe removal process (Pelino et al., 1996). The removal of Fe by precipitation represents considerable amounts of loss of Zn and co-dissolved valuable metals as well as critical metals.

The jarosite process is the widely used Fe removal process due to it being relatively simple and low cost. However, huge amounts of Fe purification residues are produced per ton of Zn metal (i.e., 0.4t/t ore). Jarosite precipitation (Eq. 2-15) occurs at pH 0.5–2 and temperature of 95°C after addition of monovalent cation reagents, for example, ammonium or sodium salts (Han et al., 2014a; Pelino et al., 1996).

$$3Fe^{3+} + 2SO_4^{2-} + M^+ + 6H_2O = MFe_3(SO_4)_2(OH)_6 + 6H^+ \quad (2\text{-}15)$$

Here M in jarosite is cations like Na^+, NH_4^+, Ag^+, $1/2Pb^{2+}$, and H_3O^+. The loss of valuable and critical metals in jarosite is due to the replacement of Fe in the crystal lattice of jarosite with Zn, Cd, Cu, and Co (Dutrizac, 1984; Han et al., 2014a; Pelino et al., 1996). Since the Jarosite process produces acid, calcine is added to neutralize the leachate as the result the unreacted minerals in calcine (e.g., $ZnFe_2O_4$, SiO_4, Zn_2SiO_4) and $PbSO_4$ precipitates are removed together with jarosite.

Meanwhile, the hematite process is carried out at high pressure (2Mpa) and temperature (200°C) with the addition of oxygen to precipitate Fe as iron oxide, hematite (Fe_2O_3) (Eq. 2-16). The volume of residues produced per ton of Zn metal by the hematite process is low (i.e., 0.18t/t ore) with minimal loss of Zn and other valuable and critical metals by adsorption to hematite (Pelino et al., 1996).

$$2Fe^{2+} + 1/2O_2 + 2H_2O = Fe_2O_3 + 4H^+ \quad (2\text{-}16)$$

The Fe removal from Zn sulfate solution by the goethite process (Eq. 2-17) is done at elevated leachate temperature of around 90°C, pH 3, and in the presence of oxygen to oxidize ferrous to ferric catalyzed by copper in the leachate. Zn calcine is added to the Zn sulfate leachate, just like the jarosite process, to neutralize the produced acid and maintain pH at 3 (Han et al., 2014b).

$$4Fe^{2+} + O_2 + 6H_2O = 4FeOOH + 8H^+ \quad (2\text{-}17)$$

Although the goethite produces relatively low amounts of residues per ton of Zn metal (i.e., 0.25 t/t ore) than the jarosite process, the loss of Zn is high as generated residues contain as high as 5-10%

Zn (Pelino et al., 1996). In addition, much of the valuable and critical metals are lost to goethite residues. The high loss of valuable metals to goethite residues is due to it having the high capacity (large specific surface area) for adsorption for valuable cations (Forbes et al., 1976; Liu et al., 2014).

The next stage of purification of the Zn sulfate leachate before electrowinning is reductive precipitation (cementation) of dissolved noble metals by Zn metal powder. Cementation of noble metals by Zn metal powder is as shown in Eq. 2-18

$$Me^{2+} + Zn = Me + Zn^{2+} \quad (2\text{-}18)$$

here Me is noble metal in the sulfate leachate which may include Pb, Ag, Cu, Cd, Ni, Co, and Arsenic (As). The unreacted Zn metal is removed together with the cemented metals. Thus, the cementation purification residues (purification cake) generated at this stage are polymetallic.

2.3. Environmental and resource importance of Zn hydrometallurgical solid wastes

2.3.1. Toxicity of heavy metals in Zn hydrometallurgical solid wastes

Zinc hydrometallurgical solid wastes have diverse elemental and mineralogical compositions depending on the primary ore processed and the stage at which they were generated. Table 2-1 shows few selected Zn hydrometallurgical solid wastes of different mineralogy, elemental composition and toxicity characteristics. These wastes were/or are discriminatorily stockpiled near the metallurgical plant, and are in most cases abandoned after the closure of plant operations with no proper environmental management (Gutiérrez et al., 2016). Although not all of the Zn hydrometallurgical solid wastes are characterized for the mobility of heavy metals (e.g., Zn, Cu, Pb, As, Ni, etc.,), those that are characterized by leachability tests (also by sequential extraction) show high mobility of heavy metals and toxicity level (Bevandić et al., 2021; Çoruh et al., 2013; Gutiérrez et al., 2016; Karbassi et al., 2016; Kerolli–Mustafa et al., 2015; Kříbek et al., 2019; Martínez-Sánchez et al., 2019; Rodríguez et al., 2009; Schaider et al., 2007).

Table 2-1. Different types of selected few Zn hydrometallurgical solid wastes and their major minerals, total valuable/toxic metal content, and toxicity

Type of Zn hydrometallurgical solid wastes	Zn Metallurgical plant and location	Mineral, elemental composition, and potential toxicity				References
		Major mineral phases	Valuable/heavy metals content (wt%)	Other major elements (wt%)	Potential toxicity (mg/L)	
Zinc plant leach residues	NILZ plant, Zanjan, Iran	$ZnSO_4 \cdot H_2O$, $PbSO_4$, SiO_2, Fe_2O_3, $CaSO_4 \cdot 2H_2O$, $KAl_2(Si_3Al)O_{10}(OH)_2$	Zn: 9.2, Pb: 12.4.	Fe: 4.3, Si: 8.8, Ca: 10.2, Al: 3.4, S: 9.8	—	(Farahmand et al., 2009b)
	Zn hydrometallurgical plant, China	$ZnFe_2O_4$, $ZnSO_4$, $ZnFe_2O_4$, $CaSO_4$, PbS, $PbSO_4$, Pb_3SiO_5	Zn: 19.6, Pb: 4.2, Cu: 0.9	Fe: 24, Ca: 2, Mn: 1.4	(TCLP 1311) Zn: 4589, Pb: 1.4, Cd: 93.5, As: 0.3	(M. Li et al., 2013)
	Bafgh Zn smelting plant, Yazd, Iran	$ZnSO_4 \cdot 7H_2O$, $ZnFe_2O_4$, $PbSO_4$, SiO_2, Fe_2O_3, $CaSO_4 \cdot 2H_2O$, $KFe_3(SO_4)_2(OH)_6$	Zn: 7, Pb: 14.2, Ag_2O: 0.16, CuO: 0.77	Fe2O3: 16.9, SiO_2: 15.1, CaO: 4.7, SO_3: 24, Al_2O_3: 2.5	—	(Behnajady et al., 2012)
	Unnamed plant, Três Marias, Brazil	(ZPLRs produced for (a) >30, (b) 5-30 and (c) <2 years), SiO_2, Fe_2O_3, $CaSO_4 \cdot 2H_2O$,	Zn: 2.5-5, Pb: 1.5-2.4, Cd: 0.02-0.06, Cu: <1	Fe: 6.7-11.5, Ca: 7-8.6, S: 27-32, SiO_2: 25-30	(TCLP 1311) Zn: 94-1053, Pb: 3-11, Cd: 3-27, Cu: 2-28	(Sethurajan et al., 2016a, 2017a)
	Çinkur plant, Turkey	(Blend) $ZnSO_4 \cdot 7H_2O$, $ZnFe_2O_4$, Zn_2SiO_4, $PbSO_4$, SiO_2, Fe_2O_3, $CaSO_4 \cdot 1/2H_2O$, $CaSiO_4$	Zn: 11.9, Pb: 16.5, Cd: 0.04	SO_3: 19.8, SiO_2: 15.9, CaO: 8.5, Al_2O_3: 3.9	(TCLP 1311) Zn: 420, Pb: 21, Cd: 9.2	(Çoruh and Ergun, 2010; Ruşen et al., 2008a; Rüşen and Topçu, 2018)

Table 2-1 (continued)

Type of Zn hydrometallurgical solid wastes	Zn Metallurgical plant and location	Mineral, elemental composition, and potential toxicity				References
		Major mineral phases	Valuable/heavy metals content (wt%)	Other major elements (wt%)	Potential toxicity (mg/L)	
	Zinc plant of Kayseri, Turkey	$PbSO_4$, $CaSO_4{\cdot}2H_2O$, $ZnSO_4{\cdot}2H_2O$,	ZnO: 12.3, PbO: 21.4, CuO: 0.1	Fe_2O_3: 11, SiO_2: 12.5, CaO: 6.7, SO_3: 15.4, Al_2O_3: 6.2	(TCLP 1311) Zn: 362, Pb: 65.1, Cd: 2.8, Mn: 3.5	(Çoruh et al., 2013; Özverdİ and Erdem, 2010)
	Kabwe Pb-Zn plant, Kabwe, Zambia	$ZnSO_4{\cdot}7H_2O$, $PbSO_4$, SiO_2, Fe_2O_3, FeOOH, $CaSO_4{\cdot}2H_2O$, $PbCO_3$, $PbCa_2Zn_3(SiO_4)_2$	Zn: 2.5, Pb: 6.2, Cu: 0.2	Fe: 17, Ca: 7.3, SO_3: 18.2, SiO_2: 31.4	(TCLP 1311) Zn: 473.5, Pb: 12.93	Investigated in this study
	Unnamed plant, Yunnan province, China	$ZnFe_2O_4$, $PbSO_4$, SiO_2	Zn: 12.5, Pb: 12.2	Fe: 21.2, SiO_2: 7	—	(Xin et al., 2013)
	Lead and Zinc plant, Zhuzhou, China	$ZnSO_3{\cdot}5/2H_2O$, ZnS, $PbSO_4$, Pb_2O_3, $Fe_2(SO_4)_2(OH)_5(H_2O)$	Zn: 5.4, Pb: 4.7, Cd: 0.2, Cu: 0.2, As: 0.2	Fe: 13.5, Ca: 3.3, Mn: 0.4	(GB 3085.3-2007, pH 3.25) Pb: 5.3, Cd: 68, Zn: 3500, Cu: 82	(Min et al., 2013)
Jarosite	Unnamed plant in Europe.	$NaFe_3(SO_4)_2(OH)_6$, $PbSO_4$, ZnS	Zn: 2.4, Pb: 4, Cu: 0.09	Fe: 17.4, S: 28, Ca: 2.5, Na: 1.8	—	(Palden et al., 2019b, 2019a)
	Baiyin Nonferrous Metals Group, China.	$ZnFe_2O_4$, $PbSO_4$, $K_2Fe_6(SO_4)_4(OH)_{12}$, $CaSO_4{\cdot}1/2H_2O$, SiO_2	Zn: 7.1, Pb: 4, Ag: 0.009, Cu: 0.2, As: 0.2, Cd: 0.1	Fe: 19.9, SiO_2: 10.12, SO_3: 38.2	—	(Ju et al., 2013, 2011b)
	Zijin Smelting Plant, Neimenggu, China	$ZnFe_2O_4$, $KFe_3(SO_4)_2(OH)_6$, $PbSO_4$,	Zn: 5.9, Pb: 8.5, Ag: 0.022, Cu: 0.2, Cd: 3.6	Fe: 28.8, S: 10.8, Si: 1.2	—	(Han et al., 2014a)

Table 2-1 (continued)

Type of Zn hydrometallurgical solid wastes	Zn Metallurgical plant and location	Mineral, elemental composition, and potential toxicity				References
		Major mineral phases	**Valuable/heavy metals content (wt%)**	**Other major elements (wt%)**	**Potential toxicity (mg/L)**	
	Unnamed plant, Southern, China	$ZnSO_4 \cdot H_2O$, $ZnSO_4 \cdot 7H_2O$, $NaFe_3(SO_4)_2(OH)_6$	Zn: 3.6, Cu: 0.11, Pb: 0.07, Cd: 0.01, In: 490 g/t, Ga: 160 g/t.	Fe: 28.3, S: 12.8, Na: 1.4	—	(Zhu et al., 2018b)
	Hindustan Zinc Limited, Khetri Rajasthan, India	$KFe_3(SO_4)_2(OH)_6$, $NH_4Fe_3(SO_4)_2(OH)_6$, $2Fe_2O_3SO_3 \cdot 5H_2O$, $FeSO_4$, $Fe(OH)_3$, $PbSO_4$, $CaSO_4$	ZnO: 9.2, PbO: 1.9	Fe_2O_3: 32.1, SiO_2: 6.8, Al_2O_3: 6.8, CaO: 6.9, MgO: 1.9	(TCLP 1311) Pb: 35.9, Cd: 27.3, Ni: 3.4, Cr: 64, As: 3.3, Ag: 3.3	(Asokan et al., 2010, 2006; Pappu et al., 2006)
	Cartegna, SE, Spain	$ZnFe_2O_4$, $NaFe_3(SO_4)_2(OH)_6$, $NH_4Fe_3(SO_4)_2(OH)_6$, $CaSO_4 \cdot 2H_2O$, $PbSO_4$, ZnS	ZnO: 4-16, PbO: 2.5-4.5, Cd: 430-970 (mg/Kg), As: 579-1530 (mg/Kg)	Fe_2O_3: 12.4-35, Al_2O_3: 1.3-2.4, SO_3: 19.2-40, SiO_2: 7.1-10.3, CaO: 1.8-8.7	—	(Martínez-Sánchez et al., 2019)
Goethite	Nuova Samin plant, Sardinia, Italy	γ-Fe_2O_3, α-FeOOH, Fe_3O_4, β-$Ca_2SiO_4 \cdot H_2O$, $Fe_2(SO_4)_3 \cdot H_2O$	ZnO: 13.3, PbO: 6.3, CdO: 0.08, As_2O_3: 0.3, CuO: 0.46, NiO: 0.3	Fe_2O_3: 51.3, SiO_2: 2.91	—	(Pelino et al., 1996; Romero and Rincón, 1997)
	Nyrstar Zn plant, Balen, Belgium	$ZnFe_2O_4$, Zn_2SiO_4, $PbSO_4$, SiO_2, $CaSO_4 \cdot 2H_2O$, $Ca(OH)_2$, $KFe_3(SO_4)_2(OH)_6$	Zn: 5.9, Pb: 1.8, Cu: 0.4	Fe: 24.1, Ca: 5.5		(Abo Atia and Spooren, 2020a; Rodriguez et al., 2020)
	Unnamed plant, Norway	—	Zn: 5.9-12.9, Pb: 1.5-3.7, trace In, Ge, Ag.	Fe: 24-23, SiO_2: 3.7-8.4, CaO: 0.7-6.1	—	(Di Maria and Van Acker, 2018a)

Table 2-1 (continued)

Type of Zn hydrometallurgical solid wastes	Zn Metallurgical plant and location	Mineral, elemental composition, and potential toxicity				References
		Major mineral phases	Valuable/heavy metals content (wt%)	Other major elements (wt%)	Potential toxicity (mg/L)	
Zn cementation filter cake	Unnamed plant, Três Marias, Brazil	Cu_2O, $Cu_3(CO_3)_2(OH)_2$, $PbSO_4$	Zn: 28.5, Cu: 47.2, Cd: 9.3, Pb: 4.9, Ni: 0.3, Co: 0.3.	Fe: 0.12, Mn: 0.21	(TCLP 1311) Cd: 718.8, Pb: 39.8	(Sethurajan et al., 2016b)
	NILZ plant, Zanjan, Iran	Zn, $ZnSO_4$, $ZnSO_3{\cdot}2.5H_2O$, CdO, ZnO	Zn: 44.3, Cd: 15.2, Ni: 3.9, Cu: 1.4, Pb: 1.1	Mn: 0.08, Ca: 2.2	—	(Safarzadeh et al., 2009a)
	Zanjan Zinc Khales sazan Industries Company, Zanjan, Iran	Zn, $Zn_4O_3{\cdot}(SO_4){\cdot}7H_2O$, $ZnSO_4{\cdot}3Zn(OH)_2{\cdot}4H_2O$, Pb, $PbSO_4$	Zn: 55.7, Pb: 2.6, As: 1.9, Co: 0.5, Ni: 1, Cd: 0.17, Cu: 0.05	Fe: 0.3, Mg: 0.3	—	(Behnajady and Moghaddam, 2017b)
	Unnamed plant, Tak province, Thailand.	Zn, ZnO, Cd, $Cd(OH)_2$, CdO, PbO, Pb, Cu	Zn: 10.8, Pb: 6, Cd: 43.6, Cu: 6.1, Co: 0.8, Ni: 0.5, In: 0.073%, Ga: 0.023.	Fe: 0.5, Sn: 0.08	–	(Nusen et al., 2015)
	Çinkur plant, Turkey	$ZnSO_3{\cdot}2.5H_2O$, $Zn_3O(SO_4)_2$, $ZnSO_4{\cdot}7H_2O$, PbO, $Pb_3O_2SO_4$, $PbSiO_3{\cdot}xH_2O$, $Pb_3O_2SO_4$, CuO, $(Zn,Cu)_2(AsO_4)OH$, $Cu_{24}As_{12}S_4$	Zn: 15.6, Pb: 2.6, As: 12.6, Cu: 15.3, Cd: 1.7, Ni: 1.3, Co: 0.6, Ge: 700 ppm.	SiO_2: 3.4, Fe: 0.3		(Kul and Topkaya, 2008)
	Bafgh Zn smelting plant, Bafgh, Iran		18.5% Zn, 1.1% Co, 0.18% Cd, 1.8% As	7.3% Mn, 2.5% Fe, 6.2% Ca, 2.3% Si		(Khosravirad et al., 2020b)

Lead is among the most toxic heavy metals in Zn hydrometallurgical solid wastes. High amounts of Pb in the blood (i.e., > 5 µg/dL) of adults and children affect the functionalities of the central nervous system, kidney, and reproductive organs. The effects are more severe to children as it disrupts and causes irreparable neural development (Tabelin et al., 2018; Wani et al., 2015). The possible pathway of Pb poisoning from Zn hydrometallurgical solid wastes is by ingesting particles of solid wastes or soil contaminated with transported Zn hydrometallurgical solid wastes and drinking water contaminated with mobilized Pb from Zn hydrometallurgical solid waste (Oyedele et al., 1995; Wani et al., 2015; Yabe et al., 2015; Zhang et al., 2012). The mobile fraction of Pb in Zn metallurgical solid wastes is mainly controlled by the dissolution of host minerals such as anglesite ($PbSO_4$), massicot (PbO), jarosite (K^+-, NH_4^+-, Na^+-jarosite), and cerussite ($PbCO_3$). Easy dissolution of these Pb minerals follow the order of PbO = $PbCO_3$ > $PbSO_4$ > jarosite (Bataillard et al., 2003; Sethurajan et al., 2016b). The release of the Pb into solution is also controlled by desorption from hydrous Fe-Mn oxyhydroxide (Glover et al., 2002; Wu et al., 2020).

Cadmium in Zn hydrometallurgical solid wastes is equally as toxic as Pb. Exposure to bioaccessible Cd leads to cancer and it also impairs many organ systems like respiratory, urinary, skeletal, cardiovascular, and central nervous systems (Rafati Rahimzadeh et al., 2017; Tabelin et al., 2018). The pathways of Cd poisoning to humans from Zn hydrometallurgical solid wastes is similar to Pb (i.e., ingesting particles of solid wastes or soil contaminated with transported Zn hydrometallurgical solid wastes and drinking water contaminated with mobilized Cd). Although crystalline Cd minerals in Zn hydrometallurgical solid wastes are not reported probably due to composition being below the detection limits of X-ray Powder Diffraction (XRD), dissolution of Cd from Zn hydrometallurgical solid wastes depends on pH (acid extractable) and redox potential which entails association with oxide minerals and desorption from hydrous ferric oxyhydroxide (Behnajady and Moghaddam, 2017a; Sethurajan et al., 2016a).

Another toxic and carcinogen element in Zn hydrometallurgical solid waste is Arsenic. Arsenic in Zn hydrometallurgical solid wastes is arsenic-containing mined and processed ores (Smedley and Kinniburgh, 2002), or it is added during leachate purification as cobalt and nickel cementation activator (Boyanov et al., 2004). Arsenic crystalline minerals in Zn hydrometallurgical solid wastes are not reported but its leachability as the function of pH shows a ‘U’-shaped curves (i.e., it's mobilized/leached in strong acid and strong alkaline solutions) (Behnajady and Moghaddam, 2017a; Tabelin et al., 2018).

Other metals such as Cu and Zn in Zn hydrometallurgical solid wastes are not toxic to humans if they are not ingested in excess. Enzymes and proteins of humans and animals contain Cu as one of the vital elements for functionality. Zinc is equally important for the good immune system, reproduction, and physiological growth (Tabelin et al., 2018 and references therein). Zinc mobility and dissolution from Zn metallurgical solid wastes are controlled by the dissolution of minerals such as hydrated zinc sulfate ($ZnSO_4 \cdot xH_2O$), zinc oxide (ZnO), and desorption from hydrous ferric oxyhydroxide and jarosite (Srivastava and Srivastava, 1990). Dissolution of Zn from relatively stable minerals like zinc ferrite ($ZnFe_3O_4$), zinc silicate (Zn_2SiO_4), galena (ZnS), and zero-valent Zn in weak acid solution (e.g., acid rainwater) is low unless they are being subjected to aggressive solution in reductive and oxidative conditions (Sethurajan et al., 2017b, 2016a). Identified copper minerals, especially in purifications residues, that control mobility and leachability of Cu are zero-valent Cu, cuprite (Cu_2O), and azurite ($Cu_3(CO_3)_2(OH)_2$) (Sethurajan et al., 2016b).

2.3.2. Zinc hydrometallurgical solid wastes as valuable resources

Table 2-1 shows that most of Zn hydrometallurgical solid wastes contain considerable amounts of valuable metals (i.e., Cu, Pb, Zn, Ni, Ag, and Cd) as well as current critical metals (i.e., Co, In, Ge, and Ga). The demand outlook of most of these critical and valuable metals shows a sharp increase through to 2030 and 2050 (Fig. 2-3). The driver for the projected high demand is associated with forecasted population increase, stock dynamics, and growth of gross domestic product (Watari et al., 2020). Besides, critical metals such as Co, In, Ge, and Ga have become an integral part of new developments in low-carbon technologies (Tabelin et al., 2021; Watari et al., 2020). With the advent of the depreciation of the high-grade geogenic ores, zinc metallurgical solid wastes are now considered as a secondary resource of the said valuable metals and critical metals. Various techniques have been developed and applied to reprocess Zn hydrometallurgical solid wastes to recovery these metals which in return solves the environmental concerns (heavy metals pollution) associated with these wastes.

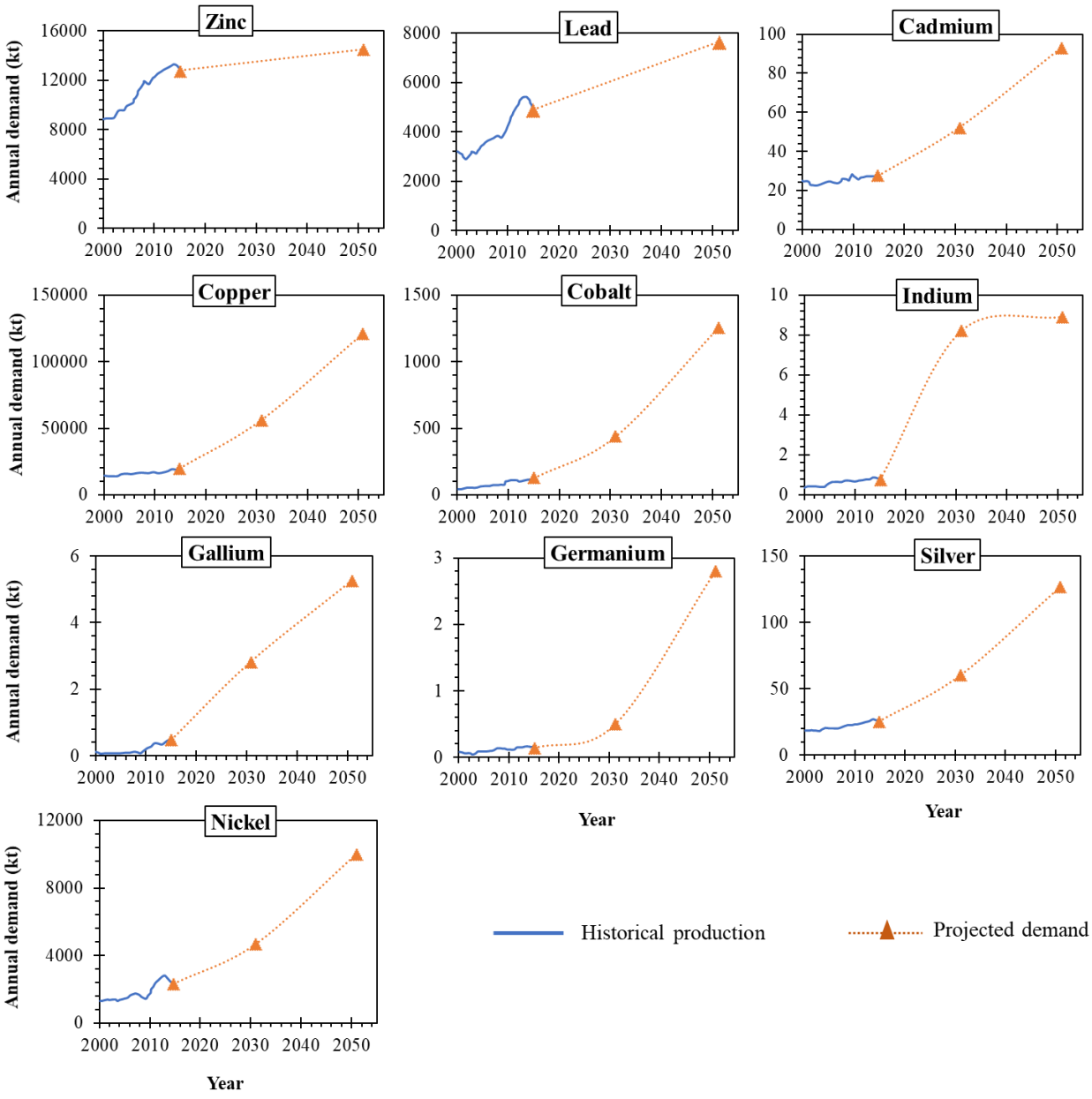

Fig. 2-3. Global valuable and critical metal outlook through 2030 and 2050 (Watari et al., 2020)

2.4. Recovery of valuable and critical metals from Zn hydrometallurgical solid wastes

2.4.1. Concentration of valuable minerals from Zn hydrometallurgical solid wastes by froth flotation

Zinc hydrometallurgy solid wastes contain high amounts of the gangue/unwanted minerals that make extraction of valuable metals by hydrometallurgy processes, pyrometallurgy processes, or the combination of the processes complex and expensive. Thus, investigations to concentrate valuable

minerals by froth flotation before metals extraction processes have been carried out (Kim et al., 1991; Rashchi et al., 2005; Yao et al., 2019; Zheng et al., 2015). Froth flotation (a well-known process in mineral processing) is the physico-chemical concentration technique that uses the hydrophobicity difference between the gangue and valuable minerals. The hydrophobic particles—in most cases this hydrophobicity is enhanced by the addition of flotation reagents called collectors—are separated from hydrophilic particles by attaching to introduced rising air bubbles and are collected on the froth (Wills and Finch, 2015).

2.4.1.1. Sulfidation-flotation of valuable minerals from Zn hydrometallurgical solid wastes

Most of the valuable minerals in Zn hydrometallurgical solid wastes are in the oxidized state. Conventional flotation sulfhydryl collectors (e.g., xanthates) which are well researched and widely used in the flotation of sulfide minerals cannot be directly used to impart and enhance hydrophobicity to the sulfates and oxides minerals in Zn hydrometallurgical solid wastes. In order to use sulfhydryl collectors, Zn hydrometallurgical solid wastes are pretreated by the addition of sulfidation agents, hydrothermal, or sulfidation roasting so that surfaces of valuable oxide/sulfate minerals are modified to behave as sulfide minerals (Han et al., 2014a; Min et al., 2020; Rashchi et al., 2005).

The commonly used sulfidation agents include sodium sulfide (Na_2S), sodium hydrogen sulfide (NaHS), and ammonium sulfide ($(NH_4)_2S$) as the sources of S^{2-} and HS^- to attach to the surface of sulfates and oxides minerals before the addition of sulfhydryl collectors. For example, when Na_2S is added to water it dissociates as depicted by Eqs. 2-19 to 2-21 and species abundance depend on pH (Wills and Finch, 2015).

$$Na_2S + 2H_2O = 2NaOH + H_2S \quad (2\text{-}19)$$

$$H_2S = H^+ + HS^- \quad (2\text{-}20)$$

$$HS^- = H^+ + S^- \quad (2\text{-}21)$$

Surfaces of carbonate and sulfate minerals in Zn hydrometallurgical solid wastes, for example, are activated by the S^- and HS^- as shown in Eq. 2-22 to 2-27 (Liu et al., 2020; Wu et al., 2017).

$$MeCO_{3(surf)} + S^{2-} = MeS_{(surf)} + CO_3^{2-} \quad (2\text{-}22)$$

$$MeCO_{3(surf)} + HS^- = MeS_{(surf)} + CO_2 + OH^- \quad (2\text{-}23)$$

$$MeSO_{4(surf)} + S^{2-} = MeS_{(surf)} + SO_4^{2-} \quad (2\text{-}24)$$

$$MeSO_{4(surf)} + HS^- = MeS_{(surf)} + SO_4^{2-} + H_2O \quad (2\text{-}25)$$

To achieve a satisfactory concentration of oxidized valuable minerals from Zn hydrometallurgical solid wastes, it is imperative to control the pH and dosage of sulfidation agents. Under acidic pH, sulfidation efficiency is low because S^- reacts with H^+ to form HS^- (Eq. 2.21), and the latter (i.e., HS^-) further reacts with H^+ to forms H_2S as the stable species (Eq. 2.20). Additionally, valuable carbonate minerals dissolve at low pH and dissolved metal ions react with sulfhydryl collector which result in a decrease of the available collector to impart hydrophobicity to oxide minerals. For amphoteric metals such as Zn and Pb, dissolve in high alkaline pH and cause a similar problem of collector consumption and suppression of flotation efficiency. The importance of the control of the dosage of sulfidation agent is attributed to low sulfidation at a low dosage and suppressing effects due to desorption of collector on surface sulfurized by S^- via replacement as shown in Eq. 2-26 ($MeX_{2(surf)}$ denote the surface of adsorbed xanthate on the surface of sulfurized mineral) (Rashchi et al., 2005).

$$PbX_{(surf)} + S^{2-} = PbS_{(surf)} + 2X^- \quad (2\text{-}26)$$

Rashci et al (2005) and Dashti and Rashci (2005) studied the flotation of $PbSO_4$ from the zinc leach residues via sulfidation-flotation using Na_2S as the sulfidation agent and they could obtain Pb recovery of around 66% at optimum condition. They noted the importance critical control of pH and Na_2S dosage at narrow optimum values (pH 9.6) and dosage (Na_2S 7000 g/t) below and above which Pb recovery dramatically decreases.

Valuable mineral concentration from jarosite residues by froth flotation cannot be carried out by sulfidation-flotation process without pretreatment. This is because valuable minerals are encapsulated or masked by jarosite and other precipitates hence thermal decomposition is carried out before sulfidation-flotation. The decomposition of jarosite (i.e., K-jarosite, Pb-jarosite, and Ag-jarosite) under reductive environment is represented by Eq. 2-27 to 2-29 (Han et al., 2014a).

$$2KFe_3(SO_4)_2(OH)_6 = 3Fe_2O_3 + K_2SO_4 + 3SO_3 + 6H_2O \quad (2\text{-}27)$$

$$PbFe_6(SO_4)_4(OH)_{12} = 3Fe_2O_3 + PbSO_4 + 3SO_3 + 6H_2O \quad (2\text{-}28)$$

$$2AgFe_3(SO_4)_2(OH)_6 = 3Fe_2O_3 + Ag_2SO_4 + 3SO_3 + 6H_2O \quad (2\text{-}29)$$

Han and coworkers (Han et al., 2014a) demonstrated that thermal decomposition (reductive roasting) of jarosite increased recovery and concentrate grade of Pb from 30% and 13 wt% for unroasted

jarosite to 67% and 44 wt% for roasted jarosite, respectively, at optimum roasting (temperature 600–700ºC) and sulfidation-flotation conditions.

Although sulfidation of valuable oxide minerals using sulfidation agent and flotation using sulfhydryl collectors is effective, the application of this technique needs strict and rigorous control of pH and sulfidation dosage within narrow ranges. Another drawback is the generation of toxic gas, H_2S, at a pH lower than 8 (Eq. 2.20) (Park et al., 2020). Generated H_2S is very harmful to human beings because inhalation causes excessive fluid in the lung due to its irritant effects. Additionally, it causes abrupt physical collapse (knockdown) it attacks the brain by preventing intercellular utilization of oxygen (Milby and Baselt, 1999; Park et al., 2020). Hydrothermal sulfidation which mimics the formation of sulfide ore at high pressure and high temperature overcomes the challenges of atmospheric sulfidation using sulfidation agents. The hydrothermal sulfidation is carried out under alkaline pH so that the added sulfur can disproportionate to produce sulfurizing species like S^{2-}, HS^- and $S_2O_3^{2-}$ depicted by Eq. 2-30 and Eq. 2-31 (Gallagher and Lei, 1989; Ke et al., 2014; Liang et al., 2012b, 2012a).

$$4S + 6OH^- = 2S^{2-} + S_2O_3^{2-} + 3H_2O \quad (2\text{-}30)$$

$$4S + 4OH^- = 2HS^{2-} + S_2O_3^{2-} + H_2O \quad (2\text{-}31)$$

The produced sulfurizing agents sulfurize surfaces of the carbonate and sulfate minerals in a similar mechanism as previously described in Eq. 2-22 to 2-25. Moreover, dissolved metals in alkaline react with the sulfurizing agent to form metal sulfide as shown in Eq. 2-32.

$$Me^{n+} + S^{2-} = Me_2S_n \quad (2\text{-}32)$$

Gallagher and coworkers (Gallagher and Lei, 1989) investigated hydrothermal sulfidation-flotation of jarosite to concentrate Pb and Ag. They demonstrated that at optimum sulfidation conditions (i.e., 150ºC, 7% S, and 1 h.) 75–93% and 80–94% of Pb and Ag could be recovered to concentrate and the grade of concentrate was around 43wt% Pb and 24.49 g/kg Ag. However, Ke et al. (2014) could only recover 31.5% Zn and 34.7% Pb to concentrate of grade 21.3wt% Zn and 3.4wt% Pb although the conversion was 82.66% and 95.6%, respectively when the mixture of neutralization sludge and zinc plant leach residues were hydrothermally sulfurized.

Even though hydrothermal sulfidation can achieve high conversion of carbonate/sulfate minerals to sulfide in Zn hydrometallurgical solid wastes, recovery of resultant sulfurized minerals via flotation is low. The low recovery is due to the production of very fine sulfide particles (Liang et

al., 2012b) which respond poorly to flotation due to the low collision probability between fine mineral particles and air bubbles (Hornn et al., 2020). The lost fine sulfurized minerals to tailings is not only a concentration efficiency problem, but is an environmental concern as it poses threat to the generation of acid mine drainage (Park et al., 2020).

Another technique of sulfidation of valuable oxidized minerals in Zn hydrometallurgical solid wastes without using sulfidation agent (i.e., activator Na_2S, NaHS, or $(NH_4)_2S$) is by sulfidation roasting (Ke et al., 2018; Min et al., 2016a, 2020). Pyrite (FeS_2), the gangue mineral in sulfide mineral processing, is used in sulfidation roasting as the source of sulfur. The sulfidation roasting mechanism of oxide/sulfate minerals is a complex gas-solid-solid reaction. For example, the reactions that occur when the mixture of Zn ferrite ($ZnFe_2O_4$) and pyrite is roasted under an inert environment are (1) decomposition of pyrite and formation of the oxygen-deficient environment (Eq. 2-30), (2) sulfur-induced migration of O^{2-} and transformation of sulfur vapor (Eq. 2-33 to 2-36), and (3) sulfidation reaction through O^{2-} and S^{2-} exchange (Eq. 2.37 to 2.39) (Ke et al., 2018; Min et al., 2016a).

$$FeS_2 = Fe_{(1-x)} + S_2 \quad (2\text{-}33)$$

$$ZnFe_2O_4 + S_2 = ZnFe_2O_{(4-\beta)} + SO_2 \quad (2\text{-}34)$$

$$ZnFe_2O_{(4-\beta)} + S_2 = xZnO + ZnFe_2O_{(4-x)} + SO_2 \quad (2\text{-}35)$$

$$Zn_xFe_{(3-x)}O_4 + S_2 = ZnO + Fe_3O_4 + SO_2 \quad (2\text{-}36)$$

$$ZnO + S_2 = ZnS + SO_2 \quad (2\text{-}37)$$

$$ZnO + Fe_{(1-x)} = ZnS + Fe_3O_4 \quad (2\text{-}38)$$

$$Zn_xFe_{(3-x)}O_4 + Fe_{(1-x)} = ZnS + Fe_3O_4 \quad (2\text{-}39)$$

Min et al. (2020) investigated sulfidation roasting to concentrate valuable Zn oxide minerals as well as iron in Zn plant leach residues using pyrite as the source of sulfur. They showed that at optimum conditions of sulfidation roasting (i.e., 30% FeS_2 roasting at 900ºC), around 92% of Zn was converted to ZnS while Fe was converted to Fe_3O_4. Magnetic separation of the roasted product yielded 90.5% recovery Fe of grade 52wt% Fe. Zinc minerals were concentrated by froth flotation from magnetic separation tailing and the recovery and grade Zn in the concentrate was around 76.6 % and 31.7%, respectively, using sulfhydryl collector, sodium butyl xanthogenate.

2.4.1.2. Flotation of valuable oxide minerals from zinc hydrometallurgical solid wastes using oxyhydryl collectors

Sulfidation roasting produces harmful SO_x gas which requires gas capture and gas cleaning facility before venting. Additionally, a high amount of energy is required to heat the materials to the required

temperature and maintain the reactor at a given high pressure which increases the operating costs. Therefore, many researchers have investigated oxyhydryl collectors that can selectively render hydrophobicity on the surface of valuable oxide minerals without sulfidation (Nagaraj and Farinato, 2016). Oxyhydryl collectors, particularly using hydroxamic acids, render hydrophobicity on the surface of valuable oxide minerals by binding on the mineral surface via the formation of chelates/complex with specific metal cations on surface sites. The hydroxamic acids that have been investigated as collectors for anglesite (most abundant Pb mineral in zinc hydrometallurgical solid wastes) include benzohydroxamic acid (BHA), octanohydroxamic acid (OHA), and salicylhydroxamic acid (SHA).

Yao and coworkers (2019) demonstrated that recovery and grade of about 76.4% of Pb could be recovered to concentrate of grade 47.2wt% Pb when 50 mg/L of SHA at pH range of 4–10 were applied. The obtained results were comparable to reagent grade anglesite flotation (90% recovery) (Yao et al., 2018). When Elizondo-Álvarez et al. (2020) compared BHA and OHA collectors on the flotation of anglesite, they found that OHA gives much better recovery than BHA (70% recovery for OHA against 20% recovery for BHA at pH 5-7) and attributed this to stronger bonds the former forms with Pb cations on the surface of anglesite than the bonds latter collector forms.

Although the hydroxamic acids have been investigated as collectors in the flotation of lead oxide minerals they have limitations such as (1) low solubilities because of their high molecular weight (C6–C14), (2) high dosage is required to achieve relatively high recovery and grade of Pb minerals in concentrate, and (3) low selectivity (Elizondo-Álvarez et al., 2020; Marion et al., 2017).

2.4.2. Hydrometallurgical route for valuable and critical metals recovery from zinc hydrometallurgical solid wastes

Recovery of valuable metals from Zn hydrometallurgical solid wastes has been extensively investigated by applying hydrometallurgical processes involving leaching, purification, and recovery of metals from the leachate (Fan et al., 2020; Koleini et al., 2010; Lu et al., 2014; Ntumba Malenga et al., 2015; Raghavan et al., 1998a; Ruşen et al., 2008a; Safarzadeh et al., 2009c; Şahin and Erdem, 2015; Stanojević et al., 2000; Wang et al., 2015; Wardell and Davidson, 1987; Xia and Pickles, 1999; Xin et al., 2013). The advantages of using hydrometallurgical processes for Zn hydrometallurgical wastes include (1) able to treat low-grade residues economically (2) selectivity of valuable metals over gangue minerals depending on lixiviant(s) used during leaching and purification method(s), (3) relatively low energy input as most of the processes are carried out at or near room temperature, and (4) causes relatively low secondary pollution. The studied hydrometallurgical processes for recovery

of valuable metals from Zn hydrometallurgical wastes can broadly be categorized into two (1) acid leach/recovery and (2) alkaline leach/recovery.

2.4.2.1. Acid leaching and valuable and critical metals recovery from Zn hydrometallurgical solid wastes

Most of the valuable minerals in zinc hydrometallurgical solid wastes are in oxidized mineral forms, hence dissolution of valuable and critical metals can be achieved by nonoxidative acid leaching reactions. The selection of the anions for acid leaching is very cardinal because some valuable metals are extracted and reprecipitate depending on the anions of acid. For example, cations such as Pb^{2+}, Ca^{2+}, and Ba^{2+} forms insoluble salts with sulfate ions (SO_4^{2-}) from sulfuric acid (H_2SO_4), while the same anions forms soluble compounds with cations such as $Fe^{2+/3}$, Zn^{2+}, Cu^{2+}, Cd^{2+}, Ni^{2+}, Co^{2+}, In^{3+}, Ga^{3+}, Ge^{4+}, and Al^{3+}. Meanwhile, the chloride (Cl^-) anions from hydrochloric acid (HCl) and brines form soluble compounds with most of the cations (e.g., Fe^{2+}, Fe^{3+}, Zn^{2+}, Cu^{2+}, Al^{3+}, Pb^{2+}, Ag^+, $Ba^{2+,}$ and Ca^{2+}) especially in highly concentrated chloride solutions. This solubility dependence of cations on the anions from the acid is sometimes used to selectively extract some valuable metals from zinc hydrometallurgical wastes while precipitating other valuable metals thereby enriching them in leaching residues.

2.4.2.1.1. Sulfuric acid leaching of metals from Zn hydrometallurgical solid wastes

There many pieces of research on the use of H_2SO_4 in the extraction of valuable metals such as Zn, Cu, Ni, Co, Cd, Ga, In, and Ge from Zn hydrometallurgical wastes (Behnajady and Moghaddam, 2017a; Fattahi et al., 2016; Kul and Topkaya, 2008; Kumar Sahu et al., 2020; Li et al., 2017; Q. Li et al., 2013; Liu et al., 2019; Raghavan et al., 1998b; Rao et al., 2019; Ruşen et al., 2008a; Rüşen and Topçu, 2018; Safarzadeh et al., 2009b, 2009c; Sethurajan et al., 2016b, 2017b; Wang and Zhou, 2002; Xin et al., 2013) owing to (1) it being selective toward the dissolution of Pb, Ca, Ba and Ag, and (2) its low price and availability because it is produced from SO_2 gas which is in most cases a byproduct of roasting of sulfide minerals (King et al., 2013; Kiss et al., 2010).

Zinc

Zinc is the fourth highest consumed metal whose use span from steel galvanizing, brass casting, bronze casting, manufacture of medicines, rubbers, and pigments (Daigo et al., 2014; Kaya et al., 2020). The forecast of Zn metal demand and consumption shows a steady increase while high-grade Zn geogenic ores continue to deplete (Backman, 2008; Daigo et al., 2014; Halada et al., 2008; Watari et al., 2020) (Fig. 3). It is for this reason that the extraction of Zn from wastes, particularly Zn

hydrometallurgical solid wastes, has gained momentum (Kaya et al., 2020). Major Zn minerals in Zn hydrometallurgical solid wastes include Zn_2SiO_2, $ZnFe_2O_4$, $ZnSO_4 \cdot xH_2O$ (x=2-7), Zn, ZnS, and ZnO whose abundance depend on the primary ore, stage at which they were generated, and process route used for Zn extraction (Fattahi et al., 2016; Raghavan et al., 1998c; Rao et al., 2019; Ruşen et al., 2008a; Safarzadeh et al., 2009b; Sethurajan et al., 2017b). The dissolution of Zn from some of these minerals in H_2SO_4 can be explained by Eqs. 2-40 to 2-43

$$Zn_2SiO_4 + 2H_2SO_4 = 2ZnSO_4 + H_4SiO_4 \quad (2\text{-}40)$$

$$ZnFe_2O_4 + 4H_2SO_4 = ZnSO_4 + Fe_2(SO_4)_3 + 4H_2O \quad (2\text{-}41)$$

$$ZnO + H_2SO_4 = ZnSO_4 + H_2O \quad (2\text{-}42)$$

$$Zn + H_2SO_4 + 1/2O_2 = ZnSO_4 + H_2O \quad (2\text{-}43)$$

The extraction of Zn from Zn_2SiO_4 mineral requires comparatively concentrated H_2SO_4 (Eq. 2-40) and produces undesirable H_4SiO_4 (silica gel) which negatively affects solid-liquid separation by filtration due to the formation of impermeable filter cake (Hua et al., 2002). Similarly, a high amount of H_2SO_4 and high temperature are required to dissolve $ZnFe_2O_4$. Alternatively, enhancement of Zn dissolution from $ZnFe_2O_4$ is achieved via reductive leaching using ZnS and SO_2 as reducing agents as shown in Eqs. 2-44 to 2-47 (Zhang et al., 2016). The essence of the addition of reducing agent is to enhance dissolution of $ZnFe_2O_4$ via reduction of Fe^{3+} (i.e., $Fe_2(SO)_3$ primary Fe product from $ZnFe_2O_4$ leaching) to Fe^{2+} (i.e., $FeSO_4$) hence chemical reaction depicted by Eq. 2-41 and Eq. 2-44 move to the right (forward) directions to satisfy the Le Chatelier's principle.

$$ZnFe_2O_4 + 4H_2SO_4 = ZnSO_4 + Fe_2(SO_4)_3 + 4H_2O \quad (2\text{-}44)$$

$$Fe_2(SO_4)_3 + ZnS = ZnSO_4 + FeSO_4 + S \quad (2\text{-}45)$$

$$SO_2 + H_2O = H_2SO_3 \quad (2\text{-}46)$$

$$ZnFe_2O_4 + H_2SO_4 + H_2SO_3 = ZnSO_4 + FeSO_4 + 4H_2O \quad (2\text{-}47)$$

The only drawback of extraction of Zn from $ZnFe_2O_4$ is the co-dissolution of Fe which makes the downstream purification process challenging and expensive.

Oxidative leaching shown in Eq. 2-43 is the conventional method to extract Zn from a purification filter cake (i.e., cementation product produced by the addition of Zn powder). However, this approach dissolves even the cemented noble metals. To achieve selective Zn leaching and avoid co-dissolution cemented noble metals from purification filter cake, galvanic leaching is usually applied (Stanojević et al., 2000). Freshly produced cementation product with unoxidized noble metals

cemented on the surface of Zn (i.e., galvanic cells) is put in fresh H_2SO_4 only Zn dissolves while enriching noble metals in the sponge (cementation product).

Copper

Copper is widely used in electrical and electronics equipment, construction, manufacturing of medicines among other uses. Most of the mined Zn ores contain copper as minor minerals and during Zn extraction, by hydrometallurgical processes, it is removed as an impurity during leachate purification together with other elements. Depending on primary Zn ores processed, Zn purification residues by cementation contain high amounts of Cu hence they are explored as a secondary resource (Kul and Topkaya, 2008; Li et al., 2018; Sethurajan et al., 2016b). The identified minerals of Cu in some of the zinc purification residues include Cu, Cu_2O, CuO, and $(CuCO_3)_6{\cdot}Cu(OH)_2$ (Li et al., 2018; Sethurajan et al., 2016b). Solubilization of Cu from these minerals in H_2SO_4 can be explained by Eq. 2-48 to 2-51.

$$Cu_2O + H_2SO_4 = CuSO_4 + Cu + H_2O \quad (2\text{-}48)$$

$$Cu_2O + 2H_2SO_4 + 1/2O_2 = 2CuSO_4 + 2H_2O \quad (2\text{-}49)$$

$$Cu + H_2SO_4 + 1/2O_2 = 2CuSO_4 + H_2O \quad (2\text{-}50)$$

$$((CuCO\_3\ )_6{\cdot}Cu(OH)_2 + 3H_2SO_4 = 3CuSO_4 + 2CO_2 + 4H_2O \quad (2\text{-}51)$$

Sethurajan and coworkers (Sethurajan et al., 2016b) investigated leaching of copper from Zn cementation purification residues obtained from Brazil using H_2SO_4 and its subsequent selective recovery as copper sulfide precipitates from polymetallic leachate. They reported that using 1 M H_2SO_4 at 40°C without the addition of oxidizing agent, pulp density of 20 g/L, and stirring speed 450 rpm, around 70% of the total copper was extracted. Dissolved copper was selectively precipitated (more than 95% of total dissolved Cu) as copper sulfide by the addition of Na_2S after adjusting pH to 1.5 while co-dissolved Zn and Cd remained in leachate. The addition of oxidizing agent, H_2O_2, during leaching of Zn purification residues in H_2SO_4 for Cu recovery was investigated by Li and coworkers (Li et al., 2018). They reported an extraction efficiency of around 95% at optimum conditions of 1.83 M H_2SO_4 at 80°C, liquid to solid ratio 3 mL/g, H_2O_2 excess coefficient of 7, and leaching for 3 h. The extracted Cu was recovered by cyclone electrowinning (purity >99.5% and current efficiency >97) without any purification of leachate.

Cobalt

Cobalt demand, as well as the price, have in the past three decades rapidly increased and it is forecasted the current demand will even quadruple in the next four decades because of its use in low-

carbon technologies like rechargeable batteries (i.e., batteries for smartphones, renewable energy storage, and computers and electric vehicles) and use in foundry and manufacturing of turbine blades for aircraft engines, magnets, catalysts, and pigments among others uses (Huang et al., 2020b; Watari et al., 2020). The soaring price of cobalt and the fact that 90% of global cobalt reserves are distributed in few countries (i.e., Democratic Republic of Congo, Australia, Cuba, Zambia, Russia, and New Caledonia) have led to it being listed among the global critical metals (Huang et al., 2020b; van den Brink et al., 2020). Zinc cementation purification residues that contain Co are now being investigated and considered as the secondary source of cobalt because Co content in these wastes is comparable to geogenic ores (Fattahi et al., 2016; Safarzadeh et al., 2011; Stanojević et al., 2000). The mineral characteristics of Co in Zn purification residues are not reported in literature perhaps due to the content being below the X-ray diffractometry (XRD) detection limit. Nonetheless, satisfactory extraction of Co from Zn purification residues has been reported using H_2SO_4 solution. Fattahi and coworkers (Fattahi et al., 2016), as well as Safarzadeh and coworkers (Safarzadeh et al., 2011), reported extraction of Co from zinc purification residues (cobalt purification cake) by reductive leaching using phenol (C_6H_5OH) and citric acid ($C_6H_8O_7$), respectively, as the reducing agent in H_2SO_4 solution. The studied cobalt purification cake was the special type because it was produced as the result of the addition of potassium permanganate to the Zn leachate to remove Co by oxidizing Co^{2+} to Co^{3+} which precipitated as either $Co(OH)_3$ or CoOOH. The reductive extraction mechanism of Co when either C_6H_5OH or $C_6H_8O_7$ is added in H_2SO_4 solution is depicted by Eq. 2-52 to 2-55.

$$18Co(OH)_3 + C_6H_8O_7 + 18H_2SO_4 = 18CoSO_4 + 49H_2O + 6CO_2 \quad (2\text{-}52)$$

$$18CoOOH + C_6H_8O_7 + 18H_2SO_4 = 18CoSO_4 + 31H_2O + 6CO_2 \quad (2\text{-}53)$$

$$2Co(OH)_3 + C_6H_5OH + 2H_2SO_4 = 2CoSO_4 + 5H_2O + C_6H_6O_2 \quad (2\text{-}54)$$

$$2CoOOH + C_6H_5OH + 2H_2SO_4 = 2CoSO_4 + 31H_2O + 3CO_2 \quad (2\text{-}55)$$

Safarzadeh et al. (2011) extracted 97% Co using 2 M H_2SO_4 at 85°C from Zn purification residues of particle size –75+53 µm, using 10% C_6H_5OH and stirring speed 600 rpm. Similarly, 96.4% Co was extracted when using 51.2% $C_6H_8O_7$ in 1 M H_2SO_4 at 85°C, S/L 0.02 g/mL, treatment time 60 min by Fattahi et al. (2016). Meanwhile, Stanojević and coworkers (Stanojević et al., 2000) studied enrichment of Co in cobalt purification filter cake via galvanic leaching in fresh H_2SO_4. Freshly purification cobalt cake was added in 150 g/L H_2SO_4 while controlling pH ≥ 3. Less noble metals (i.e., Zn and Cd) dissolved selectively thereby enriching Co in residues from around 1% to 12%.

Indium, gallium, and germanium

Indium, Ga, and Ge are among the critical metals in low-carbon technologies and key emerging technologies (i.e., electronic, health care, photoelectronic and computer, etc.,) (Licht et al., 2015). There are researches on the extraction of these metals from Zn hydrometallurgical solid wastes using H_2SO_4 as lixiviant (Fan et al., 2019; Koleini et al., 2010; Kul and Topkaya, 2008; Rao et al., 2019; Zhang et al., 2016).

Indium in the indium-bearing Zn plant leach residues generated from roast-leach-electrowinning process route is as the result its incorporation in refractory $ZnFe_2O_4$ mineral—the inevitable product at a roasting stage for sulfide concentrate containing Zn and Fe—by isomorphic substitution of Fe in the lattice. Therefore, dissolution of In in principle means dissolution of refractory $ZnFe_2O_4$, thus, reductive leaching and using concentrated H_2SO_4 are applied as previously discussed for Zn extraction from $ZnFe_2O_4$ (Fan et al., 2019; Koleini et al., 2010; Zhang et al., 2016). For example, Zhang and coworkers (Zhang et al., 2016) demonstrated that 94.8% In was extracted when 95% of theoretical ZnS was added to 150 g/L H_2SO_4 at 90°C and leaching for 4 h. When SO_2 gas partial pressure of 0.3 MPa was maintained in 65 g/L H_2SO_4 at 85°C for 120 min 93% of In was extracted.

Kul and Topkaya (2008) investigated the option of selective leaching and collective leaching Ge from Zn purification residues. For selective leaching of Ge, relatively low temperature and low H_2SO_4 concentration without the addition of oxidant was adopted. Using 100g/L H_2SO_4 at 40-60°C, solid to liquid ratio 1/4, and leaching for 30 min. around 78% Ge was extracted with low co-dissolution of other metals (i.e. Co, Ni, Fe, Cu, and Cd) from purification residues. For collective Ge recovery 92.7% and 100% of other metals dissolved when 150 g/L H_2SO_4 at 85°C with air purging and treatment time of 1 h. Two-stage extraction of Ga and Ge from Zn purification residues was investigated by Rao et al. (2019). Around 100% Ga and only <8% Ge were extracted using 2 M H_2SO_4 at 80°C, solid to liquid ratio 10 mL/g, and treatment time of 4. Low extraction of Ge in H_2SO_4 solution was attributed to high amounts of dissolved Si which formed Si-Ge gel hence Ge was extracted at the second stage using NaOH which dissolved the Si-Ge gel.

2.2.1.1.2. Hydrochloric acid and chloride leaching of metals from Zn hydrometallurgical solid wastes

Chloride solutions (i.e., neutral and acidified (HCl) chloride solutions) have been studied to extract Pb from Zn hydrometallurgical solid wastes in most cases after pretreatment by water washing or H_2SO_4 washing (Abo Atia and Spooren, 2020b; Behnajady et al., 2012; Fan et al., 2020; Farahmand

et al., 2009c; Guo et al., 2010; Marsden, 1961; Raghavan et al., 1998b; Ruşen et al., 2008b; Sinadinović et al., 1997; Srivastava et al., 2018; Turan et al., 2004; Wang et al., 2015; Xing et al., 2017; Ye et al., 2017; Zhang et al., 2019). The abundant Pb mineral in Zn hydrometallurgical solid wastes is $PbSO_4$. The mechanism of dissolution of Pb from $PbSO_4$ in chloride solution is based on the formation of Pb-chloride and as shown in Eqs. 2-56 to 2-59 (Farahmand et al., 2009c; Zhang et al., 2019).

$$PbSO_4 + Cl^- = PbCl^+ + SO_4^{2-} \quad (2\text{-}56)$$

$$PbCl^+ + Cl^- = PbCl_2 \quad (2\text{-}57)$$

$$PbCl_2 + Cl^- = PbCl_3^- \quad (2\text{-}58)$$

$$PbCl_3^- + Cl^- = PbCl_4^{2-} \quad (2\text{-}59)$$

Raghavan et al., (1998a) investigated acidified brine leaching of Pb and Ag from Zn leach residues that were obtained after pretreatment washing with H_2SO_4. They demonstrated that over 90% Pb and 80% Ag could be extracted from residues obtained after pretreatment washing with high H_2SO_4 (>100 g/L) and high temperature (80–85°C) when using 200 g/L NaCl, maintaining pH at 1.5–2 (adjusted using HCl), maintaining pulp density at 150 g/L and then leaching for 30 min. Extracted Pb and Ag in filtered leachate was recovered by cementation as Pb-Ag alloy when Al powder was added. A similar study was done by Farahmand et al. (2009c) who extracted around 89% Pb from Zn leach residues generated from NILZ plant in Iran using 300 g/L NaCl, pH 1, pulp density 25 g/L, stirring speed 400 rpm, and treatment time of 30 min. Recovery of Pb from the filtrate was conducted in a separate paper where cemented using Al was applied (Farahmand et al., 2009a).

Meanwhile, Zhang et al (2019) used NaCl-$CaCl_2$-$NaClO_3$ for their leaching of Pb and Ag from Zn leach residues from Yunnan China. Dissolved Ca^{2+} from $CaCl_2$ helped reduction of SO_4^{2-} by sequestering it as $CaSO_4$ precipitate hence enhancing the dissolution of Pb and Ag. Additionally, the oxidant, sodium chlorate ($NaClO_3$), was crucial in leaching Pb and Ag in sulfide minerals form. To obtain 98% Pb and 95% Ag recovery the following optimum conditions were applied 207.5 g/L NaCl, 12 g/L $NaClO_3$, 1.3 times the stoichiometric calculated $CaCl_2$, the temperature of 90°C 10 solid to liquid ratio 10:1 and leaching time of 1 h at stirring speed of 450 rpm. Behnajady and coworkers (Behnajady et al., 2012) considered acidification of brine solution using H_2SO_4 for leaching of Pb from Zn leach residues and capturing of SO_4^{2-} from $PbSO_4$ as well as H_2SO_4 as $CaSO_4$ precipitates by the addition of $Ca(OH)_2$. The main reason for using H_2SO_4 instead of HCl for brine acidification is because the former is more cost-effective than the latter. Although they could obtain 85.1% Pb extraction of Zn leach residues at optimum conditions (i.e., temperature 55°C and maintaining liquid

to solid ratio of 20, pH 3.5-4, and treatment for 1 h.), the required concentration of NaCl to attain that extraction efficiency required was 400 g/L which was relatively high.

2.4.2.2. Alkaline leaching and valuable metals recovery

The alternative to acid leaching of valuable metals from Zn hydrometallurgical wastes is alkaline leaching. When an alkaline solution is used as a lixiviant for recovery of valuable metals from Zn hydrometallurgical wastes only the amphoteric elements such as Zn, Pb, Al, Ge, and Sn are dissolved into solution. This dissolution selectivity of alkaline solutions for amphoteric compounds over nonamphoteric compounds and their elements (e.g., Fe, Cu, Ni, Cd, and Ca compounds that are arguably the abundant gangue in some Zn hydrometallurgical wastes and Zn oxide ores) has led to many kinds of research on the use of alkaline solutions for recovery of Pb and Zn from Zn hydrometallurgical solid wastes and oxide ores (Geng et al., 2020; Huang et al., 2020a; Ntumba Malenga et al., 2015; Şahin and Erdem, 2015; Santos et al., 2010; Seyed Ghasemi and Azizi, 2018; Xia and Pickles, 1999; Zhao and Stanforth, 2000). The dissolution mechanism of Pb and Zn in alkaline solution is based on the formation of Pb- and Zn-hydroxyl complexes as depicted by Eqs. 2-60 to 2-68 (Santos et al., 2010; Wang et al., 2009)

$$Zn^{2+} + OH^- = ZnOH^+ \quad (2\text{-}60)$$

$$ZnOH^+ + OH^- = Zn(OH)_2 \quad (2\text{-}61)$$

$$Zn(OH)_2 + OH^- = Zn(OH)_3^- \quad (2\text{-}62)$$

$$Zn(OH)_3^- + OH^- = Zn(OH)_4^{2-} \quad (2\text{-}63)$$

$$Pb^{2+} + OH^- = PbOH^+ \quad (2\text{-}64)$$

$$PbOH^+ + OH^- = Pb(OH)_2 \quad (2\text{-}65)$$

$$Pb(OH)_2 + OH^- = Pb(OH)_3^- \quad (2\text{-}66)$$

$$2Pb^{2+} + OH^- = Pb_2OH^{3+} \quad (2\text{-}67)$$

$$2Pb_2(OH)^{3+} + 2OH^- = Pb_4(OH)_4^{4+} \quad (2\text{-}68)$$

The only drawback of an alkaline solution as lixiviant (e.g., Caustic soda (NaOH)) for Pb and Zn, is the co-dissolution of Al compounds and Si compounds (Şahin and Erdem, 2015) which increases consumption of alkaline solution, increases the viscosity of the solution hence presenting downstream processing challenges.

Şahin and Erdem (2015) investigated the recovery of Pb from high lead-bearing zinc leach residues using caustic soda as the lixiviant. They reported extraction efficiencies of 99.6% Pb and 30% Zn from Zn pant leach residues of an initial grade of 19% Pb when optimum conditions of 11%

NaOH at the temperature of 100°C, liquid to solid ratio of 5, and treatment time of 1 h were applied. Furthermore, the said authors demonstrated that 99.85% of total dissolved Pb could be selectively recovered from co-dissolved elements by precipitation as PbS similar to the selective precipitation study by Youcai and Stanforth (2000). Another study by Huang and coworkers (Huang et al., 2020a) demonstrated the use of an alkaline solution to extract Zn from high Zn-bearing Zn purification residues. The extraction efficiency of around 96% Zn was obtained when Zn purification residues containing 51.3% Zn, 1.69% Pb, 0.78% Cg, and 0.18% Co were leached in 3M NaOH at temperature 40°C, L/S 20mg/L, and leaching time of 50 min.

The investigation by Rao and coworkers (Rao et al., 2019) showed that Ge could not be dissolved using H_2SO_4 solution from Zn purification residues and this was attributed to co-dissolution of Si which formed Si-Ge gel and precipitated as oxides. Therefore, dissolution of Si-Ge gel and the formed Si-Ge-O precipitates were vital for bringing Ge into a solution and this was achieved by alkaline leaching. The Ge and Pb enriched residues were leached using 1M NaOH at 80°C, S/L at 20 mL/g, and leaching time 4 h to obtain leaching efficiencies of Ge and Pb at 90% and 33%, respectively.

2.4.3. Pyrometallurgical route for valuable metals extraction from zinc hydrometallurgy solid wastes

Pyrometallurgical treatment of Zn hydrometallurgical solid wastes for recovery of valuable as well as critical metals and production of inert wastes has been investigated by many researchers and some of the processes developed have been commercialized (Di Maria and Van Acker, 2018b; Hoang et al., 2009; Min et al., 2016b; Mombelli et al., 2019, 2018; Rämä et al., 2018; Salminen et al., 2020; Tang et al., 2019, 2018; Verscheure et al., 2007a, 2007b; Zhang et al., 2020; Zhu et al., 2018a). For example, Waelz kiln, top submerged lance furnace (Ausmelt), plasma arc furnace, and submerged arc furnace among others have been commercialized.

During pyrometallurgical treatment of Zn hydrometallurgical solid wastes, many compounds get decomposed (Eqs. 2-69 to 2-77), sulfation (Eqs. 2-78 to 2-85), and some metal oxide undergo carbothermic reduction under reducing environment (low O_2 partial pressure) (Eqs. 2-85 to 2-108) as shown by simplified chemical reactions summarized in Table 2-2 (Lin et al., 2017; Tang et al., 2018; Zhu et al., 2018a). Reduced metals may volatilize, melted into matte, or lost to non-hazardous slag. Volatile metals and metalloids in Zn hydrometallurgical solid wastes include Zn, Pb, Ag, Cd, In, As, and Ge while non-volatile metals and compounds include Fe, Cu, Ni, Co, Cr, and Mn.

Table 2-2. The pyrometallurgical reaction during thermal decomposition and carbothermic reduction

Chemical reaction	$\Delta G_T^\theta - T(kJ/mol)$	Eq.	Classification
$CaSO_4 \cdot xH_2O = CaSO_4 + xH_2O$	-	2-69	Thermal decomposition (dihydroxylation and desulfation reaction)
$CaSO_4 = CaO + SO_{3(g)}$	-	2-70	
$PbSO_4 = PbO + SO_{3(g)}$	-	2-71	
$ZnSO_4 \cdot xH_2O = ZnSO_4 + xH_2O_{(g)}$	-	2-72	
$ZnSO_4 = ZnO + SO_{3(g)}$	-	2-73	
$FeOOH = Fe_2O_3 + H_2O_{(g)}$	-	2-74	
$MFe_3(SO_4)_2(OH)_6 = MFe(SO_4)_2 + Fe_2O_3 + 3H_2O_{(g)}$	-	2-75	
$MFe(SO_4)_2 = MSO_4 + Fe_2O_3 + 3SO_{3(g)}$	-	2-76	
$ZnFe_2O_{4(s)} + CO_{(s)} = ZnO_{(g)} + 2FeO_{(s)} + CO_{2(g)}$	-	2-77	
$3(NH_4)_2SO_4 = 4NH_3 + N_2 + 3SO_2 + 6H_2O$	-	2-78	Sulfation roasting
$Fe_2(SO_4)_3 = Fe_2O_3 + 3SO_2$	-	2-79	
$S + O_2 = SO_2$	-	2-80	
$ZnFe_2O_4 + SO_3 = ZnSO_4 + Fe_2O_3$	-	2-81	
$ZnFe_2O_4 + 4SO_2 + 2O_2 = ZnSO_4 + Fe_2(SO_4)_3$	-	2-82	
$ZnSiO_2 + SO_3 = ZnSO_4 + SiO_2$	-	2-83	
$Pb/Zn/Cu/CdO + SO_3 = Pb/Zn/Cu/CdSO_4$	-	2-84	
$Pb/Zn/Cu/CdS + 2O_2 = Pb/Zn/Cu/CdSO_4$	-	2-85	
$ZnFe_2O_{4(s)} + 2C_{(s)} = Zn_{(g)} + 2FeO_{(s)} + 2CO_{(g)}$	–0.49T + 411.1	2-86	Carbothermic reduction
$ZnFe_2O_{4(s)} + 2CO_{(g)} = Zn_{(g)} + 2FeO_{(s)} + 2CO_{2(g)}$	–0.14T + 164.1	2-87	
$ZnFe_2O_{4(s)} + 4C_{(s)} = Zn_{(g)} + 2Fe_{(s)} + 4CO_{(g)}$	–0.804T + 856.0	2-88	
$ZnFe_2O_{4(s)} + 4CO_{(s)} = Zn_{(g)} + 2Fe_{(s)} + 4CO_{2(g)}$	–0.109T + 174.3	2-89	
$ZnSO_{4(s)} + 2C_{(s)} = Zn_{(g)} + SO_{2(g)} + 2CO_{(g)}$	–0.62T + 397.7	2-90	
$ZnSO_{4(s)} + 2CO_{(g)} = Zn_{(g)} + SO_{2(g)} + 2CO_{2(g)}$	–0.27T + 150.7	2-91	
$ZnSO_{4(s)} + 2CuO_{(s)} + 6C = Zn_{(g)} + C_2S_{(s)} + 6CO_{2(g)}$	–1.18T + 330.3	2-92	
$ZnSO_{4(s)} + 2CuO_{(s)} + 6CO = Zn_{(g)} + C_2S_{(s)} + 6CO_{(g)}$	–0.13T – 410.4	2-93	
$ZnO_{(s)} + C_{(s)} = Zn_{(g)} + CO_{(g)}$	–0.293T + 362.9	2-94	

$ZnO_{(s)} + CO_{(g)} = Zn_{(g)} + CO_{2g)}$	–0.120T + 191.8	2-95	Carbothermic reduction
$PbSO_{4(s)} + 2C_{(s)} = Pb_{(g)} + SO_{2(g)} + 2CO_{(g)}$	–0.62T + 408.1	2-96	
$PbSO_{4(s)} + 2CO_{(g)} = Pb_{(g)} + SO_{2(g)} + 2CO_{2(g)}$	–0.27T + 161.1	2-97	
$PbSO_{4(s)} + 2CuO_{(s)} + 6C = Pb_{(g)} + C_2S_{(s)} + 6CO_{2(g)}$	–1.18T + 340.7	2-98	
$PbSO_{4(s)} + 2CuO_{(s)} + 6CO = Pb_{(g)} + C_2S_{(s)} + 6CO_{(g)}$	–0.13T – 400.4	2-99	
$PbO_{(s)} + C_{(s)} = Pb_{(l)} + CO_{(g)}$	–0.170T + 98.1	2-100	
$PbO_{(s)} + CO_{(g)} = Pb_{(g)} + CO_{2g)}$	–0.0.014T – 62.1	2-101	
$3Fe_2O_{4(s)} + CO_{(g)} = 2Fe_3O_{4(s)} + CO_{2(g)}$	–0.048T – 38.6	2-102	
$Fe_3O_{4(s)} + CO_{(g)} = 3FeO_{(s)} + CO_{2(g)}$	–0.028T – 26.2	2-103	
$FeO_{(s)} + CO_{(g)} = Fe_{(s)} + CO_{2(g)}$	0.028T – 19.3	2-104	
$CdO_{(s)} + CO_{(g)} = Cd_{(g)} + CO_{2(g)}$	–0.288T + 252.0	2-105	
$In_2O_{3(s)} + CO_{(s)} = In_2O_{(g)} + CO_{2(g)}$	-	2-106	
$Ga_2O_{3(s)} + 3CO_{(g)} = 2Ga_{(l)} + CO_{2(g)}$	-	2-107	
$C + CO_{2(s)} = CO_{(g)}$	-0.175T + 171.1	2-108	

Wang and coworkers (Wang et al., 2013) investigated the top-blown reductive fuming of Pb, Zn, and Ag from the mixture of Zn plant leach residues and Pb-Ag cementation purification residues. They reported fuming efficiency of around 97.2% Zn, 98.1% Pb, and 82% Ag, respectively, when optimum conditions CaO/SiO_2 =0.71, C/feed ratio 24, reduction time 50 min. and reduction temperature 1300°C were applied. Instead of top-blown fuming, Zhang et al., (2020) used the bottom blown furnace to fume Pb and Zn from Zn plant leach residues. The advantage of using a bottom-blown furnace over a top-blown furnace to fume Pb and Zn is an enhancement of mixing of reactants hence resulting in improved reaction kinetics. The study by Zhang et al., (2020) demonstrated that at optimum conditions (reduction temperature 1200°C, coal addition 35%, CaO/SiO_2 0.6, and reduction time 70 min.) 90% Pb and 94% Zn can be fumed from Zn leaching residues.

Zhu et al., (2018a) treated jarosite by pyrometallurgy processes via three major stages to recover Fe, Zn, In, Ga and S. The first stage, preliminary roasting (dihydroxylation and desulfation roasting), at 1200°C was conducted aiming at removing absorbed and crystallization water as well as to desulfurize Jarosite. The preliminary roasting was necessary to obtain flue gas with high amounts of SO_x for H_2SO_4 manufacturing. The second stage was the reductive roasting at 1200°C where 99%

Zn and 85% In were reduced from their oxides, volatilize, and then collected as oxides in flue dust. In the final stage, the reduced residues from the previous stage were subjected to carbothermic smelted at 1500°C to obtain non-hazardous slag and matte composed of Fe and Ga at a recovery rate of 93% and 90%, respectively.

A similar study was conducted by Mombelli and coworkers (Mombelli et al., 2018) who investigated the production of cast iron by reducing smelting of jarosite in an Arc Transferred Plasma (ATP) reactor. Firstly, jarosite was roasted at 1000°C to drive off adsorbed and crystallized water as well as to decompose sulfate minerals. The calcined jarosite contained mostly hematite was then suitable for carbothermic reduction in ATP at 1600-1700°C with the addition of metallurgical coke and limestone (flux). The produced cast iron was believed to be used for steel making while the inert slag to be used in civil engineering construction works. In another follow-up study by the same authors (Mombelli et al., 2019) it was demonstrated that blast furnace sludges (as the cheap source of C for reduction reaction) can be used instead of metallurgical coke to produce cast iron and inert slag. They reported that blast furnace sludge of 15% equivalent C and 5% CaO on jarosite mass could be used to profitably produce cast iron and inert glass slag.

The disadvantages of treating Zn hydrometallurgical solid wastes by pyrometallurgical are the release of toxic gases and greenhouse gasses that need gas cleaning facility and sequestration, respectively. Besides, using pyrometallurgical processes solely for metal recovery from Zn hydrometallurgical solid wastes is not economical because some of these wastes contain lean valuable metals hence high amount of energy is wasted heating gangue minerals.

2.4.4. A combination of pyro- and hydrometallurgical processes for valuable metals recovery from Zn hydrometallurgical solid wastes

Recovery of metals from Zn hydrometallurgical solid wastes solely by hydrometallurgical processes has limitations because minerals such as Zn ferrite, Zn silicate, and jarosite can only dissolve in very aggressive lixiviants. Even when the dissolution of Zn and other metals is achieved, the downstream processes should deal with the complex process for the removal of co-dissolved Fe and Si among other undesirable elements/metals before electrowinning, hence increasing the operating costs. On the other hand, applying pyrometallurgical processes consumes high amounts of energy because high temperature (i.e., >1300°C) is required to heat huge amounts of gangue minerals to volatilize/fume valuable metals that are just the fraction of the total amounts of Zn hydrometallurgical solid wastes. Therefore, processes have been developed that employ pyrometallurgical methods as the pretreatment at relatively low temperature before subjecting the pretreated materials to hydrometallurgical

processes using relatively low concentrated acids or water as lixiviant. The purpose of pretreatment by pyrometallurgical processes (mostly roasting) is the decomposition and transformation of valuable metals bearing minerals to water or low concentrated acid-soluble minerals. Pyrometallurgical pretreatment for Zn hydrometallurgical solid wastes are categorized into three (1) sulfation roasting, (2) reduction roasting, and (3) alkaline roasting.

2.4.4.1. Sulfation roasting and leaching of Zn hydrometallurgical solid wastes

Sulfation pretreatment is done so that Zn ferrite and jarosite are decomposed to their sulfates and metal oxides (e.g., CuO, ZnO, CdO) are converted to their sulfate minerals which are soluble in water as well as weak acids (Eqs. 2-78 to 2-85) (Hu et al., 2015; Jiang et al., 2017; Li et al., 2015; Liu et al., 2017; Zhang et al., 2011). The use of water or low concentrated acid enriches Fe in the produced residues with the potential to be used as feed in ferrous industries. Sulfur, ferric sulfate, ammonium sulfate, and sulfuric acid have been used to blend or form a paste with Zn hydrometallurgical solid wastes before roasting (Hu et al., 2015; Jiang et al., 2017; Li et al., 2015; Liu et al., 2017; Zhang et al., 2011). The source of heat for roasting is usually by electric means in either a furnace or microwave. The advantages of the latter are that (1) selective and rapid heating is achieved, (2) it is easy and quick to start and stop, and (3) it is easy to control with a high level of safety (Liu et al., 2017).

Zhang et al., (Zhang et al., 2011) investigated the use of sulfur in sulfation roasting of Zn ferrite in Zn leach residues and water leaching of roasting products. Dissolution of Zn in water leaching increased with increasing the roasting temperature and amounts of S added. However, results obtained showed that when the roasting temperature was beyond 250°C dissolutions of Zn in water decreased drastically and this was attributed to the formation of Zn oxysulfate which is slightly insoluble in water. They reported optimum conditions to be 1.2 times theoretical S amounts, 2 h roasting at 250°C, and to obtain 80% solubilization of Zn in the water at room temperature using the liquid to solid ratio 4 and leaching time of 30 min.

Meanwhile, Hu et al., (Hu et al., 2015) and Jiang et al., (Jiang et al., 2017) used ferric sulfate and mixed it with Zn plant leach residues, and heated it in a furnace at different temperature before applying water leaching of the roasted products. Hu et al. reported Zn leaching efficiency of around 91% and minimum Fe leaching rate of around 0.2%, when the ferric sulfate/Zn plant leach residues ratio was 0.05, roasting temperature at 640°C for 30 min and room temperature leaching for 20 min. For the same materials, Jiang et al. analyzed Mn, Cu, and Cd apart from Zn and they reported leaching efficiency of 93.3% Mn, 99.3% Cu, and 91.4% Cd.

Ammonium sulfate was used by Li and coworkers (Li et al., 2015) in sulfation roasting of Zn plant leach residues. Selective and high leaching efficiency of Zn of around 92.6% and low leaching efficiency of Fe of around 2% was obtained when the blend of ammonium sulfate/Zn ferrite was roasted at 650°C for 1 h and leaching in water. This enriched Fe in the produced residues after water leaching to over 45% suitable for the iron making process.

Instead of using the furnace for sulfation roasting, Liu et al., (Liu et al., 2017) investigated the use of a microwave to heat jarosite paste made after mixing with concentrated H_2SO_4. Although the leaching efficiency of Zn from roasted paste using water was high (80.7%), selectivity towards Fe was low because 89.4% Fe co-dissolved. Unselective dissolution of Zn was expected because conditions applied, that is, the use of concentrated H_2SO_4 to make paste and water leaching of roasted paste at high temperature was as aggressive as hot H_2SO_4 leaching (Sethurajan et al., 2017b).

2.4.4.2. Reduction roasting and leaching of Zn hydrometallurgical solid wastes

Reduction roasting is done as a pretreatment to produce acid-soluble minerals in Zn hydrometallurgical solid wastes. In particular reduction decomposition of $ZnFe_2O_4$ is done to obtain ZnO and Fe_3O_4. This is carried out in a similar manner as reduction fuming of volatile metals as previously discussed. The difference is the required critical control of temperature (relatively lower temperature) and $CO/(CO + CO_2)$ ratio to selectively decompose and reduce $ZnFe_2O_4$ to ZnO and Fe_3O_4 while avoiding the formation of FeO, metallic Fe as well as zero-valent Zn. FeO dissolves during acid leaching which increases the burden of leachate purification and at the same time, it is a loss to the recovery of Fe that is produced as feed for ferrous metallurgy after magnetic concentrator. Meanwhile, Zn is lost to a gas phase when ZnO is reduced to zero-valent Zn. At a high $CO/(CO + CO_2)$ ratio (i.e., >0.3) and high amounts of C, more FeO and Zn are produced and the converse is true when $CO/(CO + CO_2)$ ratio (i.e., ≤ 3) and amounts of C are very low. Additionally, high temperature positively affects the $CO/(CO + CO_2)$ ratio via the Boudouard reaction which results in an undesirable reduction of Fe_3O_4 to FeO (Li et al., 2012; Peng et al., 2015).

Li and coworkers (Li et al., 2012) investigated the recovery of Fe from Zn leach residues by firstly apply selective reduction roasting with carbon then magnetic separation to recover formed magnetite, and finally H_2SO_4 acid leaching of magnetic tailings to extract Zn. They demonstrated that 86.4% Zn and 68.4% Fe could be recovered when 4% carbon is used in reduction roasting at 750°C for 1 h. However, 13% of the total Fe dissolved during acid leaching, and this was attributed to the production of FeO during roasting as the result of high $CO/(CO + CO_2)$ as noted by Peng et al.,

(2015) who compared the mineral phases for Zn ferrite-carbon and Zn ferrite-carbon monoxide reduction roasting systems.

Meanwhile, Yan et al., (2014) used CO gas instead of carbon in their reduction roasting of Zn leach residues. The optimum reduction roasting was determined to be 750°C and roasting for 1.5 h while maintaining $CO/(CO + CO_2)$ ratio at 0.3. When the roasting product was leached in 90 g/L H_2SO_4 solution at 35°C and for 1 h, 61.4% Zn was extracted while 80.9% Fe was recovered from acid leach residues by magnetic separation.

2.5. Summary

Zinc hydrometallurgical solid wastes pose environmental threats because they contain toxic heavy metals. However, they are currently explored as a secondary resource of valuable as well as critical metals. Reprocessing/reclaiming these wastes by various techniques to recover valuable and critical metals indirectly solves the environmental threats posed by them. Although concentration techniques of valuable metals by froth flotation is applied so that less energy and chemical are used during extraction processes, recovery of valuable mineral to concentrate is low and need vigorous control of parameters (pH and activators dosage) to narrow range which makes the commercial implementation of froth flotation challenging.

Pyrometallurgical processes have extraction efficiency of valuable and critical metals as high as 99%, however, they are not economical especially for Zn hydrometallurgical solid wastes that contain lean valuable and critical metals. Besides, the produced toxic gas and greenhouse gases during pyrometallurgical operation need cleaning and sequestration.

Hydrometallurgical processes, on the other hand, are relatively less energy-intensive and produce solid residues as well as gases that may cause less or no secondary environmental pollution. All the studied hydrometallurgical processes follow the conventional sequence of (1) leaching, (2) solid-liquid separation, and (3) finally recovery of dissolved metals from leachates. Although hydrometallurgical processes that follow the conventional sequence achieve the intended purpose of toxic heavy metal removal or valuable and critical metals recovery from Zn wastes, there are two serious drawbacks. Firstly, at the leaching stage, highly concentrated lixiviants are required to extract the target metal(s) (Farahmand et al., 2009c; Guo et al., 2010). Secondly, resultant leaching residues contain a heavy metal-rich residual solution due to difficulties and inherently incomplete solid-liquid separation partly exacerbated by silica gel formation and the presence of very fine particles in Zn residues wastes (Bodas, 1996; He et al., 2011). To remove residual solutions from generated solid

residues after solid-liquid separation, extensive washing or stabilization before disposal should be carried out, requiring complex treatment processes that increase operating costs.

This study proposed coupled extraction-cementation (CEC) hydrometallurgical processes for Zn hydrometallurgical wastes. For CEC hydrometallurgical process, extracted metals are captured/sequestered by cementation before solid-liquid separation hence eliminates the need for extensive resultant residues washing carried out to remove the residual heavy metal-rich solution. Additionally, a low concentrated solution is used to achieve high removal/recovery as the solution would not be saturated with dissolved metals.

References

Abkhoshk, E., Jorjani, E., Al-Harahsheh, M.S., Rashchi, F., Naazeri, M., 2014. Review of the hydrometallurgical processing of non-sulfide zinc ores. Hydrometallurgy 149, 153–167. https://doi.org/10.1016/j.hydromet.2014.08.001.

Abo Atia, T., Spooren, J., 2020a. Microwave assisted alkaline roasting-water leaching for the valorisation of goethite sludge from zinc refining process. Hydrometallurgy 191, 105235. https://doi.org/10.1016/j.hydromet.2019.105235.

Abo Atia, T., Spooren, J., 2020b. Microwave assisted chloride leaching of zinc plant residues. Journal of Hazardous Materials 398, 122814. https://doi.org/10.1016/j.jhazmat.2020.122814.

Anju, M., Banerjee, D.K., 2011. Associations of cadmium, zinc, and lead in soils from a lead and zinc mining area as studied by single and sequential extractions. Environ Monit Assess 176, 67–85. https://doi.org/10.1007/s10661-010-1567-4.

Asokan, P., Saxena, M., Asolekar, S.R., 2010. Recycling hazardous jarosite waste using coal combustion residues. Materials Characterization 61, 1342–1355. https://doi.org/10.1016/j.matchar.2010.09.005.

Asokan, P., Saxena, M., Asolekar, S.R., 2006. Hazardous jarosite use in developing non-hazardous product for engineering application. Journal of Hazardous Materials 137, 1589–1599. https://doi.org/10.1016/j.jhazmat.2006.04.054.

Backman, C.-M., 2008. Global supply and demand of metals in the future. J Toxicol Environ Health A 71, 1244–1253. https://doi.org/10.1080/15287390802209582.

Balarini, J.C., Polli, L. de O., Miranda, T.L.S., Castro, R.M.Z. de, Salum, A., 2008. Importance of roasted sulphide concentrates characterization in the hydrometallurgical extraction of zinc. Minerals Engineering, Selected papers from Bio and Hydrometallurgy ’07, Falmouth, UK, May 2007 21, 100–110. https://doi.org/10.1016/j.mineng.2007.10.002.

Bataillard, P., Cambier, P., Picot, C., 2003. Short-term transformations of lead and cadmium compounds in soil after contamination. European Journal of Soil Science 54, 365–376. https://doi.org/10.1046/j.1365-2389.2003.00527.x.

Behnajady, B., Moghaddam, J., 2017a. Selective leaching of zinc from hazardous As-bearing zinc plant purification filter cake. Chemical Engineering Research and Design 117, 564–574. https://doi.org/10.1016/j.cherd.2016.11.019.

Behnajady, B., Moghaddam, J., 2017b. Selective leaching of zinc from hazardous As-bearing zinc plant purification filter cake. Chemical Engineering Research and Design 117, 564–574. https://doi.org/10.1016/j.cherd.2016.11.019.

Behnajady, B., Moghaddam, J., Behnajady, M.A., Rashchi, F., 2012. Determination of the Optimum Conditions for the Leaching of Lead from Zinc Plant Residues in NaCl–H2SO4–Ca(OH)2 Media by the Taguchi Method. Ind. Eng. Chem. Res. 51, 3887–3894. https://doi.org/10.1021/ie202571x.

Bevandić, S., Blannin, R., Vander Auwera, J., Delmelle, N., Caterina, D., Nguyen, F., Muchez, P.,

2021. Geochemical and Mineralogical Characterisation of Historic Zn–Pb Mine Waste, Plombières, East Belgium. Minerals 11, 28. https://doi.org/10.3390/min11010028.

Bodas, M.G., 1996. Hydrometallurgical treatment of zinc silicate ore from Thailand. Hydrometallurgy 40, 37–49. https://doi.org/10.1016/0304-386X(94)00076-F.

Boyanov, B., Peltekov, A., Petkova, V., 2014. Thermal behavior of zinc sulfide concentrates with different iron content at oxidative roasting. Thermochimica Acta 586, 9–16. https://doi.org/10.1016/j.tca.2014.04.005.

Boyanov, B.S., Konareva, V.V., Kolev, N.K., 2004. Purification of zinc sulfate solutions from cobalt and nickel through activated cementation. Hydrometallurgy 73, 163–168. https://doi.org/10.1016/j.hydromet.2003.09.002.

Çoruh, S., Elevli, S., Ergun, O.N., Demir, G., 2013. Assessment of leaching characteristics of heavy metals from industrial leach waste. International Journal of Mineral Processing 123, 165–171. https://doi.org/10.1016/j.minpro.2013.06.005.

Çoruh, S., Ergun, O.N., 2010. Use of fly ash, phosphogypsum and red mud as a liner material for the disposal of hazardous zinc leach residue waste. Journal of Hazardous Materials 173, 468–473. https://doi.org/10.1016/j.jhazmat.2009.08.108.

Daigo, I., Osako, S., Adachi, Y., Matsuno, Y., 2014. Time-series analysis of global zinc demand associated with steel. Resources, Conservation and Recycling 82, 35–40. https://doi.org/10.1016/j.resconrec.2013.10.013.

DASHTI, A., RASHCHI, F., 2005. Estimation of Reagent Consumption in Lead Flotation of a Zinc Leach Residue. Canadian Metallurgical Quarterly 44, 483–488. https://doi.org/10.1179/cmq.2005.44.4.483.

Demır, G., Çoruh, S., Ergun, O.N., 2008. Leaching behavior and immobilization of heavy metals in zinc leach residue before and after thermal treatment. Environmental Progress 27, 479–486. https://doi.org/10.1002/ep.10302.

Di Maria, A., Van Acker, K., 2018a. Turning Industrial Residues into Resources: An Environmental Impact Assessment of Goethite Valorization. Engineering 4, 421–429. https://doi.org/10.1016/j.eng.2018.05.008.

Di Maria, A., Van Acker, K., 2018b. Turning Industrial Residues into Resources: An Environmental Impact Assessment of Goethite Valorization. Engineering 4, 421–429. https://doi.org/10.1016/j.eng.2018.05.008.

Dutrizac, J.E., 1984. The Behavior of Impurities during Jarosite Precipitation, in: Bautista, R.G. (Ed.), Hydrometallurgical Process Fundamentals, NATO Conference Series. Springer US, Boston, MA, pp. 125–169. https://doi.org/10.1007/978-1-4899-2274-8_6.

Elizondo-Álvarez, M.A., Uribe-Salas, A., Nava-Alonso, F., 2020. Flotation studies of galena (PbS), cerussite (PbCO3) and anglesite (PbSO4) with hydroxamic acids as collectors. Minerals Engineering 155, 106456. https://doi.org/10.1016/j.mineng.2020.106456.

Erdem, M., Özverdi, A., 2011. Environmental risk assessment and stabilization/solidification of zinc

extraction residue: II. Stabilization/solidification. Hydrometallurgy 105, 270–276. https://doi.org/10.1016/j.hydromet.2010.10.014.

Fan, Y., Liu, Y., Niu, L., Jing, T., Zhang, W., Zhang, T., 2019. Reductive leaching of indium-bearing zinc ferrite in sulfuric acid using sulfur dioxide as a reductant. Hydrometallurgy 186, 192–199. https://doi.org/10.1016/j.hydromet.2019.04.020.

Fan, Y., Liu, Y., Niu, L., Zhang, W., Zhang, T., 2020. Leaching of silver from silver-bearing residue by a choline chloride aqueous solution and the sustained deposition of silver on copper. Hydrometallurgy 197, 105454. https://doi.org/10.1016/j.hydromet.2020.105454.

Farahmand, F., Moradkhani, D., Sadegh Safarzadeh, M., Rashchi, F., 2009a. Optimization and kinetics of the cementation of lead with aluminum powder. Hydrometallurgy 98, 81–85. https://doi.org/10.1016/j.hydromet.2009.04.001.

Farahmand, F., Moradkhani, D., Safarzadeh, M.S., Rashchi, F., 2009b. Brine leaching of lead-bearing zinc plant residues: Process optimization using orthogonal array design methodology. Hydrometallurgy 95, 316–324. https://doi.org/10.1016/j.hydromet.2008.07.012.

Farahmand, F., Moradkhani, D., Safarzadeh, M.S., Rashchi, F., 2009c. Brine leaching of lead-bearing zinc plant residues: Process optimization using orthogonal array design methodology. Hydrometallurgy 95, 316–324. https://doi.org/10.1016/j.hydromet.2008.07.012.

Fattahi, A., Rashchi, F., Abkhoshk, E., 2016. Reductive leaching of zinc, cobalt and manganese from zinc plant residue. Hydrometallurgy 161, 185–192. https://doi.org/10.1016/j.hydromet.2016.02.003.

Forbes, E.A., Posner, A.M., Quirk, J.P., 1976. THE SPECIFIC ADSORPTION OF DIVALENT Cd, Co, Cu, Pb, AND Zn ON GOETHITE. Journal of Soil Science 27, 154–166. https://doi.org/10.1111/j.1365-2389.1976.tb01986.x.

Fritz, J.J., 1985. Thermodynamic properties of chloro-complexes of silver chloride in aqueous solution. J Solution Chem 14, 865–879. https://doi.org/10.1007/BF00646296.

Gallagher, N.P., Lei, K.P.V., 1989. Recovery of Lead and Silver from Plumbojarosite by Hydrothermal Sulfidation and Chloride Leaching. U.S. Department of the Interior, Bureau of Mines.

Geng, Y., Han, G., Huang, Yukun, Ma, Z., Huang, Yanfang, Peng, W., 2020. Separation and Recovery of Zinc and Cobalt from Zinc Plant Residue by Alkali Leaching, in: Chen, X., Zhong, Y., Zhang, L., Howarter, J.A., Baba, A.A., Wang, C., Sun, Z., Zhang, M., Olivetti, E., Luo, A., Powell, A. (Eds.), Energy Technology 2020: Recycling, Carbon Dioxide Management, and Other Technologies, The Minerals, Metals & Materials Series. Springer International Publishing, Cham, pp. 397–404. https://doi.org/10.1007/978-3-030-36830-2_38.

Glover, L.J., Eick, M.J., Brady, P.V., 2002. Desorption Kinetics of Cadmium2+ and Lead2+ from Goethite. Soil Science Society of America Journal 66, 797–804. https://doi.org/10.2136/sssaj2002.7970.

Guo, Z., Pan, F., Xiao, X., Zhang, L., Jiang, K., 2010. Optimization of brine leaching of metals from hydrometallurgical residue. Transactions of Nonferrous Metals Society of China 20, 2000–2005. https://doi.org/10.1016/S1003-6326(09)60408-8.

Gutiérrez, M., Mickus, K., Camacho, L.M., 2016. Abandoned PbZn mining wastes and their mobility as proxy to toxicity: A review. Science of The Total Environment 565, 392–400. https://doi.org/10.1016/j.scitotenv.2016.04.143.

Halada, K., Shimada, M., Ijima, K., 2008. Forecasting of the Consumption of Metals up to 2050. Materials Transactions 49, 402–410. https://doi.org/10.2320/matertrans.ML200704.

Han, H., Sun, W., Hu, Y., Jia, B., Tang, H., 2014a. Anglesite and silver recovery from jarosite residues through roasting and sulfidization-flotation in zinc hydrometallurgy. Journal of Hazardous Materials 278, 49–54. https://doi.org/10.1016/j.jhazmat.2014.05.091.

Han, H., Sun, W., Hu, Y., Tang, H., 2014b. The application of zinc calcine as a neutralizing agent for the goethite process in zinc hydrometallurgy. Hydrometallurgy 147–148, 120–126. https://doi.org/10.1016/j.hydromet.2014.05.005.

He, S., Wang, J., Yan, J., 2011. Pressure leaching of synthetic zinc silicate in sulfuric acid medium. Hydrometallurgy 108, 171–176. https://doi.org/10.1016/j.hydromet.2011.04.004.

Hoang, J., Reuter, M.A., Matusewicz, R., Hughes, S., Piret, N., 2009. Top submerged lance direct zinc smelting. Minerals Engineering, Special Issue featuring papers on Zinc Processing 22, 742–751. https://doi.org/10.1016/j.mineng.2008.12.014.

Hornn, V., Ito, M., Shimada, H., Tabelin, C.B., Jeon, S., Park, I., Hiroyoshi, N., 2020. Agglomeration–Flotation of Finely Ground Chalcopyrite Using Emulsified Oil Stabilized by Emulsifiers: Implications for Porphyry Copper Ore Flotation. Metals 10, 912. https://doi.org/10.3390/met10070912.

Hu, M., Peng, B., Chai, L., Li, Y., Peng, N., Yuan, Y., Chen, D., 2015. High-Zinc Recovery from Residues by Sulfate Roasting and Water Leaching. JOM 67, 2005–2012. https://doi.org/10.1007/s11837-015-1483-8.

Hua, Y., Lin, Z., Yan, Z., 2002. Application of microwave irradiation to quick leach of zinc silicate ore. Minerals Engineering 15, 451–456. https://doi.org/10.1016/S0892-6875(02)00050-X.

Huang, Y., Geng, Y., Han, G., Cao, Y., Peng, W., Zhu, X., Zhang, T., Dou, Z., 2020a. A perspective of stepwise utilization of hazardous zinc plant purification residue based on selective alkaline leaching of zinc. Journal of Hazardous Materials 389, 122090. https://doi.org/10.1016/j.jhazmat.2020.122090.

Huang, Y., Zhang, Z., Cao, Y., Han, G., Peng, W., Zhu, X., Zhang, T., Dou, Z., 2020b. Overview of cobalt resources and comprehensive analysis of cobalt recovery from zinc plant purification residue-a review. Hydrometallurgy 193, 105327. https://doi.org/10.1016/j.hydromet.2020.105327.

Jha, M.K., Kumar, V., Singh, R.J., 2001. Review of hydrometallurgical recovery of zinc from industrial wastes. Resources, Conservation and Recycling 33, 1–22. https://doi.org/10.1016/S0921-3449(00)00095-1.

Jiang, G., Peng, B., Liang, Y., Chai, L., Wang, Q., Li, Q., Hu, M., 2017. Recovery of valuable metals from zinc leaching residue by sulfate roasting and water leaching. Transactions of Nonferrous Metals Society of China 27, 1180–1187. https://doi.org/10.1016/S1003-6326(17)60138-9.

Ju, S., Zhang, L., Peng, J., Shi, Z., Guo, S., Liu, B., Wang, Y., 2013. Thermodynamics of leaching

roasted jarosite residue from zinc hydrometallurgy in NH4Cl system. Transactions of Nonferrous Metals Society of China 23, 1179–1183. https://doi.org/10.1016/S1003-6326(13)62581-9.

Ju, S., Zhang, Yifei, Zhang, Yi, Xue, P., Wang, Y., 2011a. Clean hydrometallurgical route to recover zinc, silver, lead, copper, cadmium and iron from hazardous jarosite residues produced during zinc hydrometallurgy. Journal of Hazardous Materials 192, 554–558. https://doi.org/10.1016/j.jhazmat.2011.05.049.

Ju, S., Zhang, Yifei, Zhang, Yi, Xue, P., Wang, Y., 2011b. Clean hydrometallurgical route to recover zinc, silver, lead, copper, cadmium and iron from hazardous jarosite residues produced during zinc hydrometallurgy. Journal of Hazardous Materials 192, 554–558. https://doi.org/10.1016/j.jhazmat.2011.05.049.

Karbassi, S., Nasrabadi, T., Shahriari, T., 2016. Metallic pollution of soil in the vicinity of National Iranian Lead and Zinc (NILZ) Company. Environ Earth Sci 75, 1433. https://doi.org/10.1007/s12665-016-6244-7.

Kaya, M., Hussaini, S., Kursunoglu, S., 2020. Critical review on secondary zinc resources and their recycling technologies. Hydrometallurgy 195, 105362. https://doi.org/10.1016/j.hydromet.2020.105362.

Ke, Y., Chai, L.-Y., Min, X.-B., Tang, C.-J., Chen, J., Wang, Y., Liang, Y.-J., 2014. Sulfidation of heavy-metal-containing neutralization sludge using zinc leaching residue as the sulfur source for metal recovery and stabilization. Minerals Engineering 61, 105–112. https://doi.org/10.1016/j.mineng.2014.03.022.

Ke, Y., Peng, N., Xue, K., Min, X., Chai, L., Pan, Q., Liang, Y., Xiao, R., Wang, Y., Tang, C., Liu, H., 2018. Sulfidation behavior and mechanism of zinc silicate roasted with pyrite. Applied Surface Science 435, 1011–1019. https://doi.org/10.1016/j.apsusc.2017.11.202.

Kerolli–Mustafa, M., Fajković, H., Rončević, S., Ćurković, L., 2015. Assessment of metal risks from different depths of jarosite tailing waste of Trepça Zinc Industry, Kosovo based on BCR procedure. Journal of Geochemical Exploration 148, 161–168. https://doi.org/10.1016/j.gexplo.2014.09.001
Khosravirad, M.M., Bakhtiari, F., Ghader, S., Abkhoshk, E., 2020a. An improved process methodology for extracting cobalt from zinc plant residues. Hydrometallurgy 191, 105163. https://doi.org/10.1016/j.hydromet.2019.105163.

Khosravirad, M.M., Bakhtiari, F., Ghader, S., Abkhoshk, E., 2020b. An improved process methodology for extracting cobalt from zinc plant residues. Hydrometallurgy 191, 105163. https://doi.org/10.1016/j.hydromet.2019.105163.

Kim, J.Y., Rosato, L., Stanley, R.W., 1991. Silver recovery from zinc plant residues by flotation. Mining, Metallurgy & Exploration 8, 43–47. https://doi.org/10.1007/BF03402930.

King, M., Moats, M., Davenport, W.G., 2013. Sulfuric Acid Manufacture: Analysis, Control and Optimization. Newnes.

Kiss, A.A., Bildea, C.S., Grievink, J., 2010. Dynamic modeling and process optimization of an industrial sulfuric acid plant. Chemical Engineering Journal 158, 241–249. https://doi.org/10.1016/j.cej.2010.01.023.

Koleini, S.M.J., Mehrpouya, H., Saberyan, K., Abdolahi, M., 2010. Extraction of indium from zinc plant residues. Minerals Engineering 23, 51–53. https://doi.org/10.1016/j.mineng.2009.09.007.

Kříbek, B., Nyambe, I., Majer, V., Knésl, I., Mihaljevič, M., Ettler, V., Vaněk, A., Penížek, V., Sracek, O., 2019. Soil contamination near the Kabwe Pb-Zn smelter in Zambia: Environmental impacts and remediation measures proposal. Journal of Geochemical Exploration 197, 159–173. https://doi.org/10.1016/j.gexplo.2018.11.018.

Kul, M., Topkaya, Y., 2008. Recovery of germanium and other valuable metals from zinc plant residues. Hydrometallurgy 92, 87–94. https://doi.org/10.1016/j.hydromet.2007.11.004.

Kumar, P.B.A.Nanda., Dushenkov, Viatcheslav., Motto, Harry., Raskin, Ilya., 1995. Phytoextraction: The Use of Plants To Remove Heavy Metals from Soils. Environ. Sci. Technol. 29, 1232–1238. https://doi.org/10.1021/es00005a014.

Kumar Sahu, S., Kargar Razi, M., Beuscher, M., Chagnes, A., 2020. Recovery of Metal Values from Ni-Cd Cake Waste Residue of an Iranian Zinc Plant by Hydrometallurgical Route. Metals 10, 655. https://doi.org/10.3390/met10050655.

Leteinturier, B., Laroche, J., Matera, J., Malaisse, F., 2001. Reclamation of lead / zinc processing wastes at Kabwe, Zambia : a phytogeochemical approach. South African Journal of Science 97, 624–627.

Li, B., Wang, X., Wei, Y., Wang, H., Barati, M., 2018. Extraction of copper from copper and cadmium residues of zinc hydrometallurgy by oxidation acid leaching and cyclone electrowinning. Minerals Engineering 128, 247–253. https://doi.org/10.1016/j.mineng.2018.09.007.

Li, M., Peng, B., Chai, L., Peng, N., Xie, X., Yan, H., 2013. Technological mineralogy and environmental activity of zinc leaching residue from zinc hydrometallurgical process. Transactions of Nonferrous Metals Society of China 23, 1480–1488. https://doi.org/10.1016/S1003-6326(13)62620-5.

Li, M., Peng, B., Chai, L., Peng, N., Yan, H., Hou, D., 2012. Recovery of iron from zinc leaching residue by selective reduction roasting with carbon. Journal of Hazardous Materials 237–238, 323–330. https://doi.org/10.1016/j.jhazmat.2012.08.052.

Li, M., Zheng, S., Liu, B., Du, H., Dreisinger, D.B., Tafaghodi, L., Zhang, Y., 2017. The leaching kinetics of cadmium from hazardous Cu-Cd zinc plant residues. Waste Management 65, 128–138. https://doi.org/10.1016/j.wasman.2017.03.039.

Li, Q., Zhang, B., Min, X., Shen, W., 2013. Acid leaching kinetics of zinc plant purification residue. Transactions of Nonferrous Metals Society of China 23, 2786–2791. https://doi.org/10.1016/S1003-6326(13)62798-3.

Li, Y., Liu, H., Peng, B., Min, X., Hu, M., Peng, N., Yuang, Y., Lei, J., 2015. Study on separating of zinc and iron from zinc leaching residues by roasting with ammonium sulphate. Hydrometallurgy 158, 42–48. https://doi.org/10.1016/j.hydromet.2015.10.004.

Liang, Y.-J., Chai, L.-Y., Liu, H., Min, X.-B., Mahmood, Q., Zhang, H.-J., Ke, Y., 2012a. Hydrothermal sulfidation of zinc-containing neutralization sludge for zinc recovery and stabilization. Minerals Engineering 25, 14–19. https://doi.org/10.1016/j.mineng.2011.09.014.

Liang, Y.-J., Chai, L.-Y., Min, X.-B., Tang, C.-J., Zhang, H.-J., Ke, Y., Xie, X.-D., 2012b. Hydrothermal sulfidation and floatation treatment of heavy-metal-containing sludge for recovery and stabilization. Journal of Hazardous Materials 217–218, 307–314. https://doi.org/10.1016/j.jhazmat.2012.03.025.

Licht, C., Peiró, L.T., Villalba, G., 2015. Global Substance Flow Analysis of Gallium, Germanium, and Indium: Quantification of Extraction, Uses, and Dissipative Losses within their Anthropogenic Cycles. Journal of Industrial Ecology 19, 890–903. https://doi.org/10.1111/jiec.12287.

Lin, X., Peng, Z., Yan, J., Li, Z., Hwang, J.-Y., Zhang, Y., Li, G., Jiang, T., 2017. Pyrometallurgical recycling of electric arc furnace dust. Journal of Cleaner Production 149, 1079–1100. https://doi.org/10.1016/j.jclepro.2017.02.128.

Liu, C., Ju, S.H., Zhang, L.B., Srinivasakannan, C., Peng, J.H., Le, T.Q.X., Guo, Z.Y., 2017. Recovery of valuable metals from jarosite by sulphuric acid roasting using microwave and water leaching. Canadian Metallurgical Quarterly 56, 1–9. https://doi.org/10.1080/00084433.2016.1242972.

Liu, F., Wang, J., Peng, C., Liu, Z., Wilson, B.P., Lundström, M., 2019. Recovery and separation of silver and mercury from hazardous zinc refinery residues produced by zinc oxygen pressure leaching. Hydrometallurgy 185, 38–45. https://doi.org/10.1016/j.hydromet.2019.01.017.

Liu, H., Chen, T., Frost, R.L., 2014. An overview of the role of goethite surfaces in the environment. Chemosphere 103, 1–11. https://doi.org/10.1016/j.chemosphere.2013.11.065.

Liu, R., Liu, D., Li, J., Liu, S., Liu, Z., Gao, L., Jia, X., Ao, S., 2020. Improved understanding of the sulfidization mechanism in cerussite flotation: An XPS, ToF-SIMS and FESEM investigation. Colloids and Surfaces A: Physicochemical and Engineering Aspects 595, 124508. https://doi.org/10.1016/j.colsurfa.2020.124508.

Lorestani, B., Yousefi, N., Cheraghi, M., Farmany, A., 2013. Phytoextraction and phytostabilization potential of plants grown in the vicinity of heavy metal-contaminated soils: a case study at an industrial town site. Environ Monit Assess 185, 10217–10223. https://doi.org/10.1007/s10661-013-3326-9.

Lu, D., Jin, Z., Shi, L., Tu, G., Xie, F., Asselin, E., 2014. A novel separation process for detoxifying cadmium-containing residues from zinc purification plants. Minerals Engineering 64, 1–6. https://doi.org/10.1016/j.mineng.2014.03.026.

Marion, C., Jordens, A., Li, R., Rudolph, M., Waters, K.E., 2017. An evaluation of hydroxamate collectors for malachite flotation. Separation and Purification Technology 183, 258–269. https://doi.org/10.1016/j.seppur.2017.02.056.

Marsden, D.D., 1961. Recovery of lead from zinc plant residues by brine leaching and electrodeposition. Journal of the Southern African Institute of Mining and Metallurgy 61, 522–534.

Martínez-Sánchez, M.J., Solan-Marín, A.M., Hidalgo, A.M., Pérez-Sirvent, C., 2019. Characterization and mobilization of toxic metals from electrolytic zinc waste. Chemosphere 233, 414–421. https://doi.org/10.1016/j.chemosphere.2019.05.257.

Matinde, E., Simate, G.S., Ndlovu, S., 2018. Mining and metallurgical wastes: a review of recycling

and re-use practices. Journal of the Southern African Institute of Mining and Metallurgy 118, 825–844. https://doi.org/10.17159/2411-9717/2018/v118n8a5.

Milby, T.H., Baselt, R.C., 1999. Hydrogen sulfide poisoning: Clarification of some controversial issues. American Journal of Industrial Medicine 35, 192–195. https://doi.org/10.1002/(SICI)1097-0274(199902)35:2<192::AID-AJIM11>3.0.CO;2-C.

Min, X., Jiang, G., Wang, Y., Zhou, B., Xue, K., Ke, Y., Xu, Q., Wang, J., Ren, H., 2020. Sulfidation roasting of zinc leaching residue with pyrite for recovery of zinc and iron. J. Cent. South Univ. 27, 1186–1196. https://doi.org/10.1007/s11771-020-4359-1.

Min, X., Xie, X., Chai, L., Liang, Y., Li, M., Ke, Y., 2013. Environmental availability and ecological risk assessment of heavy metals in zinc leaching residue. Transactions of Nonferrous Metals Society of China 23, 208–218. https://doi.org/10.1016/S1003-6326(13)62448-6.

Min, X., Zhou, B., Ke, Y., Chai, L., Xue, K., Zhang, C., Zhao, Z., Shen, C., 2016a. Sulfidation behavior of ZnFe2O4 roasted with pyrite: Sulfur inducing and sulfur-oxygen interface exchange mechanism. Applied Surface Science 371, 67–73. https://doi.org/10.1016/j.apsusc.2016.02.229.

Min, X., Zhou, B., Ke, Y., Chai, L., Xue, K., Zhang, C., Zhao, Z., Shen, C., 2016b. Sulfidation behavior of ZnFe2O4 roasted with pyrite: Sulfur inducing and sulfur-oxygen interface exchange mechanism. Applied Surface Science 371, 67–73. https://doi.org/10.1016/j.apsusc.2016.02.229.

Mombelli, D., Mapelli, C., Barella, S., Gruttadauria, A., Spada, E., 2019. Jarosite wastes reduction through blast furnace sludges for cast iron production. Journal of Environmental Chemical Engineering 7, 102966. https://doi.org/10.1016/j.jece.2019.102966.

Mombelli, D., Mapelli, C., Di Cecca, C., Barella, S., Gruttadauria, A., Ragona, M., Pisu, M., Viola, A., 2018. Characterization of cast iron and slag produced by jarosite sludges reduction via Arc Transferred Plasma (ATP) reactor. Journal of Environmental Chemical Engineering 6, 773–783. https://doi.org/10.1016/j.jece.2018.01.006.

Mwandira, W., Nakashima, K., Kawasaki, S., Ito, M., Sato, T., Igarashi, T., Chirwa, M., Banda, K., Nyambe, I., Nakayama, S., Nakata, H., Ishizuka, M., 2019. Solidification of sand by Pb(II)-tolerant bacteria for capping mine waste to control metallic dust: Case of the abandoned Kabwe Mine, Zambia. Chemosphere 228, 17–25. https://doi.org/10.1016/j.chemosphere.2019.04.107.

Nagaraj, D.R., Farinato, R.S., 2016. Evolution of flotation chemistry and chemicals: A century of innovations and the lingering challenges. Minerals Engineering, Special Issue: Froth Flotation 96–97, 2–14. https://doi.org/10.1016/j.mineng.2016.06.019.

Needleman, H., 2004. Lead Poisoning. Annual Review of Medicine 55, 209–222. https://doi.org/10.1146/annurev.med.55.091902.103653.

Ng, K.S., Head, I., Premier, G.C., Scott, K., Yu, E., Lloyd, J., Sadhukhan, J., 2016. A multilevel sustainability analysis of zinc recovery from wastes. Resources, Conservation and Recycling 113, 88–105. https://doi.org/10.1016/j.resconrec.2016.05.013.

Ntumba Malenga, E., Mulaba-Bafubiandi, A.F., Nheta, W., 2015. Alkaline leaching of nickel bearing ammonium jarosite precipitate using KOH, NaOH and NH4OH in the presence of EDTA and Na2S. Hydrometallurgy 155, 69–78. https://doi.org/10.1016/j.hydromet.2015.04.004.

Nusen, S., Yottawee, N., Cheng, C.Y., Chairuangsri, T., 2015. Characterisation of zinc plant, cold-purification filter cake and leaching of indium by aqueous sulphuric acid solution.

Oyedele, D.J., Obioh, I.B., Adejumo, J.A., Oluwole, A.F., Aina, P.O., Asubiojo, O.I., 1995. Lead contamination of soils and vegetation in the vicinity of a lead smelter in Nigeria. Science of The Total Environment 172, 189–195. https://doi.org/10.1016/0048-9697(95)04810-3.

Özverdİ, A., Erdem, M., 2010. Environmental risk assessment and stabilization/solidification of zinc extraction residue: I. Environmental risk assessment. Hydrometallurgy 100, 103–109. https://doi.org/10.1016/j.hydromet.2009.10.011.

Palden, T., Onghena, B., Regadío, M., Binnemans, K., 2019a. Methanesulfonic acid: a sustainable acidic solvent for recovering metals from the jarosite residue of the zinc industry. Green Chemistry 21, 5394–5404. https://doi.org/10.1039/C9GC02238D.

Palden, T., Regadío, M., Onghena, B., Binnemans, K., 2019b. Selective Metal Recovery from Jarosite Residue by Leaching with Acid-Equilibrated Ionic Liquids and Precipitation-Stripping. ACS Sustainable Chem. Eng. 7, 4239–4246. https://doi.org/10.1021/acssuschemeng.8b05938.

Pappu, A., Saxena, M., Asolekar, S.R., 2006. Jarosite characteristics and its utilisation potentials. Science of The Total Environment 359, 232–243. https://doi.org/10.1016/j.scitotenv.2005.04.024.

Park, I., Hong, S., Jeon, S., Ito, M., Hiroyoshi, N., 2020. A Review of Recent Advances in Depression Techniques for Flotation Separation of Cu–Mo Sulfides in Porphyry Copper Deposits. Metals 10, 1269. https://doi.org/10.3390/met10091269.

Pelino, M., Cantalini, C., Abbruzzese, C., Plescia, P., 1996. Treatment and recycling of goethite waste arising from the hydrometallurgy of zinc. Hydrometallurgy 40, 25–35. https://doi.org/10.1016/0304-386X(95)00004-Z.

Peng, B., Peng, N., Min, X.-B., Liu, H., Li, Y., Chen, D., Xue, K., 2015. Separation of Zinc from High Iron-Bearing Zinc Calcines by Reductive Roasting and Leaching. JOM 67, 1988–1996. https://doi.org/10.1007/s11837-015-1476-7.

Puigdomenech, I., 2010. Make equilibrium diagrams using sophisticated algorithms (MEDUSA), inorganic chemistry.

Rafati Rahimzadeh, Mehrdad, Rafati Rahimzadeh, Mehravar, Kazemi, S., Moghadamnia, A., 2017. Cadmium toxicity and treatment: An update. Caspian J Intern Med 8, 135–145. https://doi.org/10.22088/cjim.8.3.135.

Raghavan, R., Mohanan, P.K., Patnaik, S.C., 1998a. Innovative processing technique to produce zinc concentrate from zinc leach residue with simultaneous recovery of lead and silver. Hydrometallurgy 48, 225–237. https://doi.org/10.1016/S0304-386X(97)00082-0.

Raghavan, R., Mohanan, P.K., Patnaik, S.C., 1998b. Innovative processing technique to produce zinc concentrate from zinc leach residue with simultaneous recovery of lead and silver. Hydrometallurgy 48, 225–237. https://doi.org/10.1016/S0304-386X(97)00082-0.

Raghavan, R., Mohanan, P.K., Patnaik, S.C., 1998c. Innovative processing technique to produce zinc

concentrate from zinc leach residue with simultaneous recovery of lead and silver. Hydrometallurgy 48, 225–237. https://doi.org/10.1016/S0304-386X(97)00082-0.

Rämä, M., Nurmi, S., Jokilaakso, A., Klemettinen, L., Taskinen, P., Salminen, J., 2018. Thermal Processing of Jarosite Leach Residue for a Safe Disposable Slag and Valuable Metals Recovery. Metals 8, 744. https://doi.org/10.3390/met8100744.

Rao, B.P., Rao, K.H., 2005. Distribution of In3+ ions in indium-substituted Ni–Zn–Ti ferrites. Journal of Magnetism and Magnetic Materials 292, 44–48. https://doi.org/10.1016/j.jmmm.2004.10.093.

Rao, S., Wang, D., Liu, Z., Zhang, K., Cao, H., Tao, J., 2019. Selective extraction of zinc, gallium, and germanium from zinc refinery residue using two stage acid and alkaline leaching. Hydrometallurgy 183, 38–44. https://doi.org/10.1016/j.hydromet.2018.11.007.

Rashchi, F., Dashti, A., Arabpour-Yazdi, M., Abdizadeh, H., 2005. Anglesite flotation: a study for lead recovery from zinc leach residue. Minerals Engineering, Reagents '04 18, 205–212. https://doi.org/10.1016/j.mineng.2004.10.014.

Rodríguez, L., Ruiz, E., Alonso-Azcárate, J., Rincón, J., 2009. Heavy metal distribution and chemical speciation in tailings and soils around a Pb–Zn mine in Spain. Journal of Environmental Management 90, 1106–1116. https://doi.org/10.1016/j.jenvman.2008.04.007.

Rodriguez, N.R., Machiels, L., Onghena, B., Spooren, J., Binnemans, K., 2020. Selective recovery of zinc from goethite residue in the zinc industry using deep-eutectic solvents. RSC Adv. 10, 7328–7335. https://doi.org/10.1039/D0RA00277A.

Romero, M., Rincón, J.Ma., 1997. Microstructural characterization of a goethite waste from zinc hydrometallurgical process. Materials Letters 31, 67–73. https://doi.org/10.1016/S0167-577X(96)00235-2.

Roshanfar, M., Khanlarian, M., Rashchi, F., Motesharezadeh, B., 2020. Phyto-extraction of zinc, lead, nickel, and cadmium from a zinc leach residue. Journal of Cleaner Production 266, 121539. https://doi.org/10.1016/j.jclepro.2020.121539.

Ruşen, A., Sunkar, A.S., Topkaya, Y.A., 2008a. Zinc and lead extraction from Çinkur leach residues by using hydrometallurgical method. Hydrometallurgy 93, 45–50. https://doi.org/10.1016/j.hydromet.2008.02.018.

Ruşen, A., Sunkar, A.S., Topkaya, Y.A., 2008b. Zinc and lead extraction from Çinkur leach residues by using hydrometallurgical method. Hydrometallurgy 93, 45–50. https://doi.org/10.1016/j.hydromet.2008.02.018.

Rüşen, A., Topçu, M.A., 2018. Investigation of zinc extraction from different leach residues by acid leaching. Int. J. Environ. Sci. Technol. 15, 69–80. https://doi.org/10.1007/s13762-017-1365-4.

Safarzadeh, M.S., Dhawan, N., Birinci, M., Moradkhani, D., 2011. Reductive leaching of cobalt from zinc plant purification residues. Hydrometallurgy 106, 51–57. https://doi.org/10.1016/j.hydromet.2010.11.017.

Safarzadeh, M.S., Moradkhani, D., Ashtari, P., 2009a. Recovery of zinc from Cd–Ni zinc plant residues. Hydrometallurgy 97, 67–72. https://doi.org/10.1016/j.hydromet.2009.01.003.

Safarzadeh, M.S., Moradkhani, D., Ashtari, P., 2009b. Recovery of zinc from Cd–Ni zinc plant residues. Hydrometallurgy 97, 67–72. https://doi.org/10.1016/j.hydromet.2009.01.003.

Safarzadeh, M.S., Moradkhani, D., Ojaghi-Ilkhchi, M., 2009c. Kinetics of sulfuric acid leaching of cadmium from Cd–Ni zinc plant residues. Journal of Hazardous Materials 163, 880–890. https://doi.org/10.1016/j.jhazmat.2008.07.082.

Şahin, M., Erdem, M., 2015. Cleaning of high lead-bearing zinc leaching residue by recovery of lead with alkaline leaching. Hydrometallurgy 153, 170–178. https://doi.org/10.1016/j.hydromet.2015.03.003.

Salminen, J., Nyberg, J., Imris, M., Heegaard, B.M., 2020. Smelting Jarosite and Sulphur Residue in a Plasma Furnace, in: Siegmund, A., Alam, S., Grogan, J., Kerney, U., Shibata, E. (Eds.), PbZn 2020: 9th International Symposium on Lead and Zinc Processing, The Minerals, Metals & Materials Series. Springer International Publishing, Cham, pp. 391–403. https://doi.org/10.1007/978-3-030-37070-1_34.

Santos, F.M.F., Pina, P.S., Porcaro, R., Oliveira, V.A., Silva, C.A., Leão, V.A., 2010. The kinetics of zinc silicate leaching in sodium hydroxide. Hydrometallurgy 102, 43–49. https://doi.org/10.1016/j.hydromet.2010.01.010.

Schaider, L.A., Senn, D.B., Brabander, D.J., McCarthy, K.D., Shine, J.P., 2007. Characterization of Zinc, Lead, and Cadmium in Mine Waste: Implications for Transport, Exposure, and Bioavailability. Environ. Sci. Technol. 41, 4164–4171. https://doi.org/10.1021/es0626943.

Sethurajan, M., Huguenot, D., Jain, R., Lens, P.N.L., Horn, H.A., Figueiredo, L.H.A., van Hullebusch, E.D., 2017a. Leaching and selective zinc recovery from acidic leachates of zinc metallurgical leach residues. Journal of Hazardous Materials, Selected papers presented at the 4th International Conference on Research Frontiers in Chalcogen Cycle Science and Technology, Delft, The Netherlands, May 28 - May 29, 2015 324, 71–82. https://doi.org/10.1016/j.jhazmat.2016.01.028.

Sethurajan, M., Huguenot, D., Lens, P.N.L., Horn, H.A., Figueiredo, L.H.A., van Hullebusch, E.D., 2016a. Fractionation and leachability of heavy metals from aged and recent Zn metallurgical leach residues from the Três Marias zinc plant (Minas Gerais, Brazil). Environ Sci Pollut Res 23, 7504–7516. https://doi.org/10.1007/s11356-015-6014-1.

Sethurajan, M., Huguenot, D., Lens, P.N.L., Horn, H.A., Figueiredo, L.H.A., van Hullebusch, E.D., 2016b. Leaching and selective copper recovery from acidic leachates of Três Marias zinc plant (MG, Brazil) metallurgical purification residues. Journal of Environmental Management 177, 26–35. https://doi.org/10.1016/j.jenvman.2016.03.041.

Seyed Ghasemi, S.M., Azizi, A., 2018. Alkaline leaching of lead and zinc by sodium hydroxide: kinetics modeling. Journal of Materials Research and Technology 7, 118–125. https://doi.org/10.1016/j.jmrt.2017.03.005.

Sinadinović, D., Kamberović, Ž., Šutić, A., 1997. Leaching kinetics of lead from lead (II) sulphate in aqueous calcium chloride and magnesium chloride solutions. Hydrometallurgy 47, 137–147. https://doi.org/10.1016/S0304-386X(97)00041-8.

Smedley, P.L., Kinniburgh, D.G., 2002. A review of the source, behaviour and distribution of arsenic

in natural waters. Applied Geochemistry 17, 517–568. https://doi.org/10.1016/S0883-2927(02)00018-5

Srivastava, A., Srivastava, P.C., 1990. Adsorption-desorption behaviour of zinc(II) at iron(III) hydroxide-aqueous solution interface as influenced by pH and temperature. Environmental Pollution 68, 171–180. https://doi.org/10.1016/0269-7491(90)90020-D.

Srivastava, R.R., Lee, Jae-chun, Nguyen, T.T., Kim, M., Kang, J., 2018. Hydrometallurgical Extraction of Lead in Brine Solution from a TSL Processed Zinc Plant Residue, in: Davis, B.R., Moats, M.S., Wang, S., Gregurek, D., Kapusta, J., Battle, T.P., Schlesinger, M.E., Alvear Flores, G.R., Jak, E., Goodall, G., Free, M.L., Asselin, E., Chagnes, A., Dreisinger, D., Jeffrey, M., Lee, Jaeheon, Miller, G., Petersen, J., Ciminelli, V.S.T., Xu, Q., Molnar, R., Adams, J., Liu, W., Verbaan, N., Goode, J., London, I.M., Azimi, G., Forstner, A., Kappes, R., Bhambhani, T. (Eds.), Extraction 2018, The Minerals, Metals & Materials Series. Springer International Publishing, Cham, pp. 1205–1212. https://doi.org/10.1007/978-3-319-95022-8_97.

Stanojević, D., Nikolić, B., Todorović, M., 2000. Evaluation of cobalt from cobaltic waste products from the production of electrolytic zinc and cadmium. Hydrometallurgy 54, 151–160. https://doi.org/10.1016/S0304-386X(99)00062-6.

Tabelin, C.B., Dallas, J., Casanova, S., Pelech, T., Bournival, G., Saydam, S., Canbulat, I., 2021. Towards a low-carbon society: A review of lithium resource availability, challenges and innovations in mining, extraction and recycling, and future perspectives. Minerals Engineering 163, 106743. https://doi.org/10.1016/j.mineng.2020.106743.

Tabelin, C.B., Igarashi, T., Villacorte-Tabelin, M., Park, I., Opiso, E.M., Ito, M., Hiroyoshi, N., 2018. Arsenic, selenium, boron, lead, cadmium, copper, and zinc in naturally contaminated rocks: A review of their sources, modes of enrichment, mechanisms of release, and mitigation strategies. Science of The Total Environment 645, 1522–1553. https://doi.org/10.1016/j.scitotenv.2018.07.103.

Tang, L., Tang, C., Xiao, J., Zeng, P., Tang, M., 2018. A cleaner process for valuable metals recovery from hydrometallurgical zinc residue. Journal of Cleaner Production 201, 764–773. https://doi.org/10.1016/j.jclepro.2018.08.096.

Tangviroon, P., Noto, K., Igarashi, T., Kawashima, T., Ito, M., Sato, T., Mufalo, W., Chirwa, M., Nyambe, I., Nakata, H., Nakayama, S., Ishizuka, M., 2020. Immobilization of Lead and Zinc Leached from Mining Residual Materials in Kabwe, Zambia: Possibility of Chemical Immobilization by Dolomite, Calcined Dolomite, and Magnesium Oxide. Minerals 10, 763. https://doi.org/10.3390/min10090763.

Turan, M.D., Altundoğan, H.S., Tümen, F., 2004. Recovery of zinc and lead from zinc plant residue. Hydrometallurgy 75, 169–176. https://doi.org/10.1016/j.hydromet.2004.07.008.

van den Brink, S., Kleijn, R., Sprecher, B., Tukker, A., 2020. Identifying supply risks by mapping the cobalt supply chain. Resources, Conservation and Recycling 156, 104743. https://doi.org/10.1016/j.resconrec.2020.104743.

Verscheure, K., Van Camp, M., Blanpain, B., Wollants, P., Hayes, P., Jak, E., 2007a. Continuous Fuming of Zinc-Bearing Residues: Part I. Model Development. Metall Mater Trans B 38, 13–20. https://doi.org/10.1007/s11663-006-9009-y.
.

Verscheure, K., Van Camp, M., Blanpain, B., Wollants, P., Hayes, P., Jak, E., 2007b. Continuous Fuming of Zinc-Bearing Residues: Part II. The Submerged-Plasma Zinc-Fuming Process. Metall Mater Trans B 38, 21–33. https://doi.org/10.1007/s11663-006-9010-5.

Wang, L., Mu, W., Shen, H., Liu, S., Zhai, Y., 2015. Leaching of lead from zinc leach residue in acidic calcium chloride aqueous solution. Int J Miner Metall Mater 22, 460–466. https://doi.org/10.1007/s12613-015-1094-y.

.

Wang, X.Q., Xie, K.Q., Ma, W.H., Yang, M.Y., Zeng, P., Cao, Y.C., 2013. Recovery of zinc and other valuable metals from zinc leach residue by top blowing fuming method. Mineral Processing and Extractive Metallurgy 122, 174–178. https://doi.org/10.1179/1743285513Y.0000000045.

.

Wang, Y., Chai, L., Chang, H., Peng, X., Shu, Y., 2009. Equilibrium of hydroxyl complex ions in Pb2+-H2O system. Transactions of Nonferrous Metals Society of China 19, 458–462. https://doi.org/10.1016/S1003-6326(08)60295-2.

Wang, Y., Zhou, C., 2002. Hydrometallurgical process for recovery of cobalt from zinc plant residue. Hydrometallurgy 63, 225–234. https://doi.org/10.1016/S0304-386X(01)00213-4.

Wani, A.L., Ara, A., Usmani, J.A., 2015. Lead toxicity: a review. Interdiscip Toxicol 8, 55–64. https://doi.org/10.1515/intox-2015-0009.

Wardell, M.P., Davidson, C.F., 1987. Acid Leaching Extraction of Ga and Ge. JOM 39, 39–41. https://doi.org/10.1007/BF03258061.

Watari, T., Nansai, K., Nakajima, K., 2020. Review of critical metal dynamics to 2050 for 48 elements. Resources, Conservation and Recycling 155, 104669. https://doi.org/10.1016/j.resconrec.2019.104669.

Wills, B.A., Finch, J., 2015. Wills' Mineral Processing Technology: An Introduction to the Practical Aspects of Ore Treatment and Mineral Recovery. Butterworth-Heinemann.

Wu, D., Ma, W., Mao, Y., Deng, J., Wen, S., 2017. Enhanced sulfidation xanthate flotation of malachite using ammonium ions as activator. Scientific Reports 7, 2086. https://doi.org/10.1038/s41598-017-02136-x.

Wu, J., Zhao, X., Li, Z., Gu, X., 2020. Thermodynamic and kinetic coupling model of Cd(II) and Pb(II) adsorption and desorption on goethite. Science of The Total Environment 727, 138730. https://doi.org/10.1016/j.scitotenv.2020.138730.

Xia, D.K., Pickles, C.A., 1999. Kinetics of zinc ferrite leaching in caustic media in the deceleratory period. Minerals Engineering 12, 693–700. https://doi.org/10.1016/S0892-6875(99)00052-7.

Xin, W., Srinivasakannan, C., Xin-hui, D., Jin-hui, P., Da-jin, Y., shao-hua, J., 2013. Leaching kinetics of zinc residues augmented with ultrasound. Separation and Purification Technology 115, 66–72. https://doi.org/10.1016/j.seppur.2013.04.043.

Xing, P., Ma, B., Zeng, P., Wang, C., Wang, L., Zhang, Y., Chen, Y., Wang, S., Wang, Q., 2017. Deep cleaning of a metallurgical zinc leaching residue and recovery of valuable metals. Int J Miner Metall Mater 24, 1217–1227. https://doi.org/10.1007/s12613-017-1514-2.

Yabe, J., Nakayama, S.M.M., Ikenaka, Y., Yohannes, Y.B., Bortey-Sam, N., Oroszlany, B., Muzandu, K., Choongo, K., Kabalo, A.N., Ntapisha, J., Mweene, A., Umemura, T., Ishizuka, M., 2015. Lead poisoning in children from townships in the vicinity of a lead–zinc mine in Kabwe, Zambia. Chemosphere 119, 941–947. https://doi.org/10.1016/j.chemosphere.2014.09.028.

Yan, H., Chai, L., Peng, B., Li, M., Peng, N., Hou, D., 2014. A novel method to recover zinc and iron from zinc leaching residue. Minerals Engineering 55, 103–110. https://doi.org/10.1016/j.mineng.2013.09.015.

Yao, W., Li, M., Cui, R., Jiang, X., Jiang, H., Deng, X., Li, Y., Zhou, S., 2018. Flotation Behavior and Mechanism of Anglesite with Salicyl Hydroxamic Acid as Collector. JOM 70, 2813–2818. https://doi.org/10.1007/s11837-018-3149-9.

Yao, W., Li, M., Zhang, M., Cui, R., Jiang, H., Li, Y., Zhou, S., 2019. Lead Recovery from Zinc Leaching Residue by Flotation. JOM 71, 4588–4593. https://doi.org/10.1007/s11837-019-03526-4.

Ye, M., Li, G., Yan, P., Zheng, L., Sun, S., Huang, S., Li, H., Chen, Y., Yang, L., Huang, J., 2017. Production of lead concentrate from bioleached residue tailings by brine leaching followed by sulfide precipitation. Separation and Purification Technology 183, 366–372. https://doi.org/10.1016/j.seppur.2017.04.020.

Youcai, Z., Stanforth, R., 2000. Integrated hydrometallurgical process for production of zinc from electric arc furnace dust in alkaline medium. Journal of Hazardous Materials 80, 223–240. https://doi.org/10.1016/S0304-3894(00)00305-8.

Zhang, F., Wei, C., Deng, Z., Li, X., Li, C., Li, M., 2016. Reductive leaching of indium-bearing zinc residue in sulfuric acid using sphalerite concentrate as reductant. Hydrometallurgy 161, 102–106. https://doi.org/10.1016/j.hydromet.2016.01.029.

Zhang, X., Yang, L., Li, Y., Li, H., Wang, W., Ye, B., 2012. Impacts of lead/zinc mining and smelting on the environment and human health in China. Environ Monit Assess 184, 2261–2273. https://doi.org/10.1007/s10661-011-2115-6.

Zhang, Y., Jin, B., Song, Q., Chen, B., Wang, C., 2019. Leaching Behavior of Lead and Silver from Lead Sulfate Hazardous Residues in NaCl-CaCl2-NaClO3 Media. JOM 71, 2388–2395. https://doi.org/10.1007/s11837-019-03472-1.

Zhang, Y., Yu, X., Li, X., 2011. Zinc recovery from franklinite by sulphation roasting. Hydrometallurgy 109, 211–214. https://doi.org/10.1016/j.hydromet.2011.07.002

Zhang, Z., Li, W., Zhan, J., Li, G., Zhao, Z., Hwang, J.-Y., 2020. A Novel Technology for the Recovery of Zinc from the Zinc Leaching Residue by the Bottom-blown Reduction. Mineral Processing and Extractive Metallurgy Review 0, 1–8. https://doi.org/10.1080/08827508.2020.1793143.

Zhao, Y., Stanforth, R., 2000. Production of Zn powder by alkaline treatment of smithsonite Zn–Pb ores. Hydrometallurgy 56, 237–249. https://doi.org/10.1016/S0304-386X(00)00079-7.

.

Zheng, Y., Liu, W., Qin, W., Jiao, F., Han, J., Yang, K., Luo, H., 2015. Reduction of lead sulfate to lead sulfide with carbon monoxide. J. Cent. South Univ. 22, 2929–2935. https://doi.org/10.1007/s11771-015-2828-8.

Zhu, D., Yang, C., Pan, J., Guo, Z., Li, S., 2018a. New pyrometallurgical route for separation and recovery of Fe, Zn, In, Ga and S from jarosite residues. Journal of Cleaner Production 205, 781–788. https://doi.org/10.1016/j.jclepro.2018.09.152.

Zhu, D., Yang, C., Pan, J., Guo, Z., Li, S., 2018b. New pyrometallurgical route for separation and recovery of Fe, Zn, In, Ga and S from jarosite residues. Journal of Cleaner Production 205, 781–788. https://doi.org/10.1016/j.jclepro.2018.09.152.

CHAPTER 3: DETOXIFICATION OF ZINC PLANT LEACH RESIDUES BY REMOVAL OF LEAD USING COUPLED EXTRACTION-CEMENTATION AND MICRO-SCALE ZERO-VALENT IRON IN ACIDIFIED BRINE SOLUTION

3.1. Introduction

Lead pollutions of the air, water, and soil are among the three of the biggest environmental challenges in developing countries, particularly in several African countries (Eqani et al., 2016; Ngueta and Ndjaboue, 2013; Nweke and Sanders, 2009; Oyedele et al., 1995). For example, the Kabwe town—the capital of Central Province, Zambia—is one of the world's most Pb-polluted areas where the topsoil of residential areas has alarmingly high Pb content of over 2000 mg/kg (Kříbek et al., 2019; Tembo et al., 2006).

Several techniques such as immobilization of Pb by solidification/stabilization (Demır et al., 2008; Erdem and Özverdi, 2011; Mwandira et al., 2019), phytoextraction/phytostabilization (Kumar et al., 1995; Lorestani et al., 2013), and chemical extraction of Pb from ZPLRs (Farahmand et al., 2009; Ruşen et al., 2008; Turan et al., 2004) have been proposed as potential strategies to limit the Pb pollution problem from ZPLRs. Stabilization/solidification is, however, not a lasting detoxification approach for ZPLRs because Pb and other toxic heavy metals are only 'stored' and not permanently removed hence needs constant monitoring (Tiruta-Barna et al., 2004). Meanwhile, phytoextraction/phytostabilization of Pb, typically requires a very long time for detoxification and suffers from serious challenges in terms of plant growth (Cunningham and Berti, 2000). To date, solidification using bacteria and phytostabilization have been applied to stabilize Pb in ZPLRs in Kabwe (Leteinturier et al., 2001; Mwandira et al., 2019). Unfortunately, the long-term evaluation and monitoring of Pb stability after solidification have not been carried out while stunted plant growth during phytostabilization remains a critical problem.

In this chapter, an innovative approach to achieve the rapid and permanent detoxification of ZPLRs via coupled extraction-cementation (CEC) process—a process whereby Pb (most toxic metal) from the pulp is recovered/captured as soon as it is extracted during the leaching stage via cementation onto magnetic materials (micro-scale zero-valent iron (mZVI))—prior to solid-liquid separation is reported. This process is referred to as the Fe-based CEC process because mZVI is used as the reductant of extracted Pb^{2+}. Besides, using mZVI makes it easy for physical separation of reductively precipitated Pb on surface of mZVI from the leaching pulp using a magnet. Specific objectives of this chapter are as follows: (1) to characterize the chemical and mineralogical properties of ZPLRs, (2) to identify the solid-phase partitioning of Pb and asses toxicity of ZPLRs, (3) to remove Pb from ZPLRs

using the proposed technique, and (4) evaluate the Pb leachability of the regenerated residues after the Fe-based CEC process.

3.2. Materials and Methods

3.2.1. Materials

The ZPLRs samples were collected from the dump site and air-dried for 30 days in the laboratory. The samples contained compact and agglomerated particles hence they were lightly crushed with an agate mortar and pestle, then dry-sieved using stainless steel sieves to obtain –106 µm fraction. All chemicals (by Wako Pure Chemical Industries, Ltd., Japan) used in this chapter were of reagent grade and were used without further purification. To prepare the leaching solutions of different concentrations, given chemicals were dissolved or diluted using deionized (DI) water (18 MΩ·cm, Milli-Q® Integral Water Purification System, Merck Millipore, USA). To reductively precipitate dissolved Pb in leaching pulp, ultrapure micro-scale zero-valent iron (mZVI) (>99.9%, –150 µm, Wako Pure Chemical Industries, Ltd., Osaka, Japan) was used.

3.2.2. Methods

3.2.2.1. Elemental and mineralogical composition

The samples were analyzed for their elemental compositions by dry and wet methods using X-ray fluorescence spectroscopy (XRF) (EDXL 300, Rigaku Corporation, Japan) and inductively coupled plasma atomic emission spectroscopy (ICP-AES) (ICPE-9820, Shimadzu Corporation, Japan) (margin of error = ±2%), respectively. For XRF analysis, sample powder was analyzed in oxide mode. For wet method, 1 g of the sample was digested in 16 mL aqua regia (i.e., 12 mL of HCl (37%) and 4 mL HNO_3 (65%)) using a microwave-assisted acid digestion system (Ethos Advanced Microwave Lab station, Milestone Inc., USA). After digestion 1 M HNO_3 was added and then made up to 100 mL. The solution was filtered through 0.20 µm syringe-driven membrane filters (Sartoris AG, Gottingen, Germany) before analyzing the filtrates for Pb, Cu, Zn, Fe, and Ca using ICP-AES.

To analyze the mineralogical composition, samples were further ground to –53 µm before subjecting them to X-ray powder diffraction (XRD) equipped with a Cu-Kα radiation source (MultiFlex, Rigaku Corporation, Japan). The scan speed was 0.02º/s for the angle range of 5–70º/2θ.

3.2.2.1. Solid-phase fractionation of lead, zinc, and iron in zinc plant leach residues

Solid-phase fractionation of Pb, Zn, and Fe in ZPLRs was investigated by the sequential extraction procedure developed by Dold (Dold, 2003) for mine tailings. This was carried out to gain insights

into the fraction of Pb-bearing solid phases in ZPLRs amenable to non-oxidative acidic leaching. Table 3.1 summarizes the different lixiviants and experimental conditions applied at each extraction step including their target solid phases. In the first step, 3 g of ZPLRs was mixed with 120 mL of deionized water in a 300-mL Erlenmeyer flask agitated using a magnetic stirrer at 200 rpm for 4 h. After equilibration, solid-liquid separation was done by centrifugation of suspensions at 3000 rpm for 20 minutes. The supernatant was decanted and filtered through 0.20 µm syringe-driven membrane filters (Sartoris AG, Gottingen, Germany) and the filtrates were analyzed for Pb, as well as Zn and Fe by ICP-AES. The solid residues were washed with 20 mL water before subjecting it to the next extraction step. The same procedure was repeated for all the extraction steps except for the last one (5^{th} step). In the 5^{th} step, the residue was dissolved in aqua regia using a microwave-assisted acid digestion system prior to ICP-AES analysis.

3.2.2.2. Leachability and gastric bio-accessibility tests

To assess the mobility and bio-accessibility of Pb from ZPLRs before and after the coupled extraction-cementation procedure proposed in this study, the toxicity characteristics leaching procedure (TCLP) (U.S. EPA, 1991) and in vitro solubility and bioavailability research consortium gastric phase (SBRC-G) (U.S. EPA, 2007) leaching tests were carried out. For the TCLP, 1 g of untreated ZPLRs or treated ZPLRs was mixed with 20 mL of acetic acid solution (pH 2.89) in a centrifuge tube shaken at 30 rpm on a rotary tumbler for 18 h. After each batch leachability test, the leachate was filtered through 0.20 µm syringe-driven membrane filters and analyzed for Pb concentration using ICP-AES. To evaluate Pb solubilization in the gastric fluid of fasting human (bio-accessibility), 1 g of sample was added in a 300 mL Erlenmeyer flask containing 100 mL solution composed of 0.4 M glycine with pH of 1.5±0.05 (pH adjusted using concentrated reagent HCl acid). Each flask was tightly capped using a silicon stopper and lightly shaken at 40 rpm in a thermostat water bath maintained at 37±0.5 °C for 1 h. After each test, the leachate was filtered through 0.20 µm syringe-driven membrane filters and analyzed for Pb concentration using ICP-AES.

Table 3-1. Sequential extraction procedure, lixiviants, and target solid phases

Step	Target phase(s)	Extractant(s)	Extraction conditions
1	Water soluble	Distilled water: 120 mL	Stirring speed of 200 rpm, extraction time of 4 h, and temperature of 25 °C
2	Ion-exchangeable and carbonates	1M sodium acetate (pH 5): 120 mL	Stirring speed 200 rpm, extraction time 4 h, and temperature of 25 °C
3	Amorphous Fe-Mn oxyhydroxides/oxides	10.9 g/L (0.12 M) oxalic acid ＋16.1 g/L (0.13 M) ammonium oxalate: 120 mL	Stirring speed 200 rpm, extraction time 6 h, and temperature 25 °C. This was conducted in the dark.
4	Crystalline Fe oxyhydroxides/oxides	(a) 0.3 M trisodium citrate + 0.2 M sodium hydrogen carbonate 60 ml (b) Sodium dithionite: 3 g	Add (a) and heat to 85 °C using heated magnetic stirrer Add (b) and continual stirring at 200 rpm, while maintaining at temperature 85 °C. Repeat the same procedure until brownish color (iron minerals color) disappears
5	Residual (sulfides /organic and silicates)	Aqua regia: 16 mL	Heat to 220 °C for 20 min. and hold for 30 min. using microwave acid assisted digester

3.2.2.3. Lead removal from zinc plant leach residues by leaching in chloride solution

Batch experiments with and without coupled extraction-cementation treatment of ZPLRs were carried out using 200 mL Erlenmeyer flasks and the solution volume was fixed at 50 mL for all experiments. Solutions containing different concentrations of NaCl and HCl were added in the flasks and purged with N_2 gas for 10 minutes prior to samples addition. 2.5 g of ZPLRs (i.e. solid to liquid ratio 1:20) with and without mZVI were added in the flasks containing the leaching solutions. N_2 purging in the pulp after sample addition was carried out for 5 minutes before completely sealing the flasks with silicon stoppers and parafilm®. The flasks were then shaken in a thermostat water bath shaker maintained at 25±0.5 ºC at a shaking speed of 120 strokes/min and amplitude of 40 mm. After the predetermined time, the suspension was collected, filtered through 0.20 µm syringe-driven membrane filters, and analyzed for Pb and Zn concentration using ICP-AES. After the coupled extraction-cementation treatment of ZPLRs, magnetic Pb-loaded mZVI was recovered from the pulp using a handheld 0.6 T magnet. The magnetic fractions were then thoroughly washed with deionized water and dried in a vacuum drying oven at 40 ºC for 24 h. After drying, the magnetic fractions were digested using aqua regia in a microwave-assisted acid digester and the leachates were analyzed for Pb by ICP-AES. In addition, the magnetic fractions were analyzed by SEM-EDX (JSM-IT200, JEOL Ltd., Tokyo, Japan) and XPS (JPS-9200, JEOL Ltd., Tokyo, Japan). For the XPS analysis, a monochromatic Al Kα X-ray source operating at 140 W (voltage, 14kV; current, 10mA) was used to analyze the sample in a chamber maintained under ultrahigh vacuum conditions (~10^{-7} Pa). Narrow scan spectra of $Pb4f_{7/2}$, $Fe2p_{3/2}$, and O1s were obtained and calibrated using the binding energy of adventitious carbon (C1s) (285.0 eV) for charge correction. Deconvolution of the XPS spectra was done using XPSPEAK version 4.1 by applying an 80% Gaussian–20% Lorentzian peak model and a true Shirley background (Nesbitt and Muir, 1994; Park et al., 2020; Tabelin et al., 2020).

Lead removal efficiency from ZPLRs after treatment was calculated according to Eq. (3-1):

$$\text{Pb removal (\%)} = \frac{M_m * W_m + C_{sol} * V_{sol}}{M_s * W_s} \text{ x } 100 \qquad (3\text{-}1)$$

where M_s is the mass of ZPLRs (g), $M_m$is the mass of magnetic fraction (g), W_s is the weight percent of Pb in ZPLRs (%), W_m is the weight percent of Pb in magnetic fraction, C_{sol} is the Pb concentration in solution (g/L) and V_{sol} is the volume of leach solution (L). When ZPLRs were leached without the addition of mZVI, the Pb removal efficiency was calculated using the Eq. (3-2);

$$\text{Pb removal (\%)} = \frac{C_{sol} * V_{sol}}{M_s * W_s} \text{ x } 100 \qquad (3\text{-}2)$$

3.3. Results and discussion

3.3.1. Elemental and mineralogical compositions of the zinc plant leach residues

Elemental composition analyzed by ICP-AES after aqua regia digestion and XRF showed that the historic ZLR samples from Kabwe, Zambia contain high amounts of Pb (6.19 wt%), Zn (2.53 wt%), Fe (17.0 wt%), Ca (7.3 wt%) and SiO_2 (31.4 wt%) (Table 3.2). The ZPLRs also contain small amounts of Cu (0.21 wt %), V (0.72 wt %) and other elements. The XRD pattern shows that the ZLR samples are composed of gypsum ($CaSO_4{\cdot}2H_2O$), anglesite ($PbSO_4$), zinc sulfate dihydrate ($ZnSO_4{\cdot}2H_2O$), quartz (SiO_2), and goethite (FeOOH) as crystalline minerals (Fig.3-1). The particle size distribution of the ZPLRs showed that it mainly contains very fine-sized particles (4.6–31.3 µm) The average particle size (D_{50}) was around 9.6 µm indicating that solid-liquid separation of ZPLRs when treated by leaching would be challenging. Moreover, the very fine particle size of historic ZPLRs from Kabwe could be easily transported by wind from the mine waste dumpsite to residential areas.

Table 3-2. Chemical composition of zinc plant leach residues

Metal composition by ICP-AES analysis after Aqua Regia digestion		Elemental composition by XRF analysis	
Elements	%	Elements (as oxide)	%
Pb	6.19 ± 0.16	PbO	6.48 ± 0.07
Zn	2.53 ± 0.14	ZnO	3.28 ± 0.02
Fe	17.02 ± 0.61	Fe_2O_3	24.3 ± 0.1
Cu	0.21± 0.12	CuO	0.25 ± 0.01
Ca	7.3 ± 0.21	CaO	10.57 ± 0.15
		SiO_2	31.43± 0.35
		Al_2O_3	2.89 ± 0.05
		SO_3	18.17 ± 0.31
		V_2O_5	0.72 ± 0.01
		MnO	0.25 ± 0.01
		P_2O_5	0.54 ± 0.01
		ZrO_2	0.59 ± 0.01

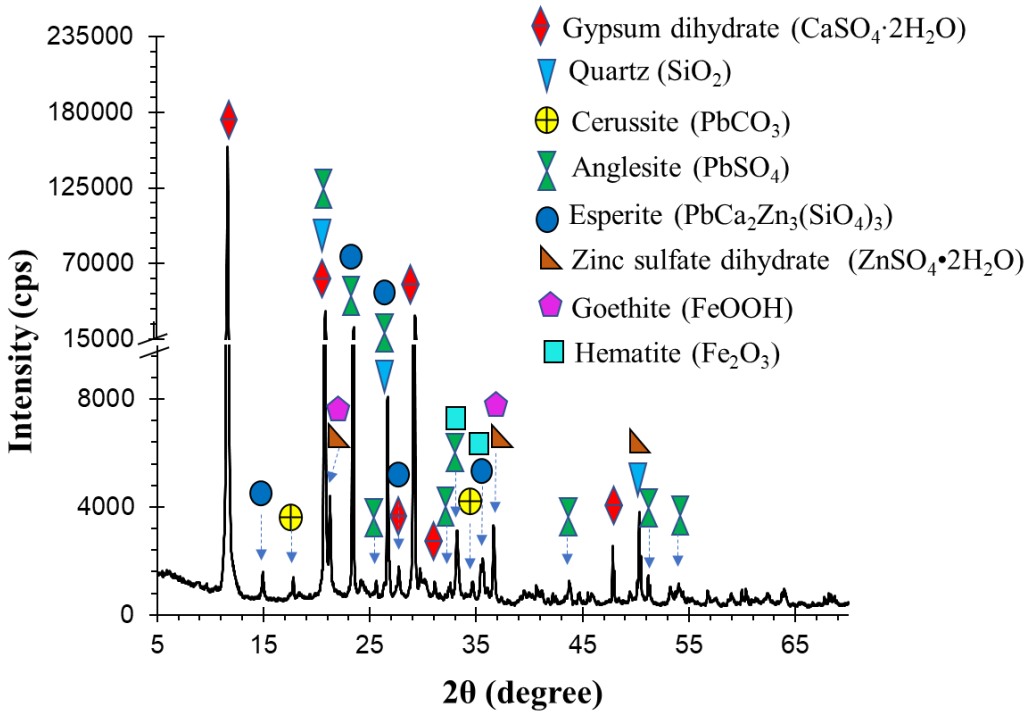

Fig. 3-1. XRD pattern of the zinc plant leach residues from Kabwe, Zambia.

3.3.1. Solid-phase fractionation of lead, zinc, and iron in zinc plant leach residues

Solid-phase fractionation of Pb as well Zn and Fe were carried out to understand the chemical forms and solid phase fraction amenable to non-oxidative acid leaching. Fig. 3-2 shows the solid-phase fractionation of Pb, Zn, and Fe in ZPLRs. Pb was mainly associated with three solid-phase fractions: 1.3% with water-soluble, 63.5% with exchangeable and carbonates, and 35.2% partitioned with the residual (in this study residual denotes Pb associated with sulfides/organic and silicates). The results indicate that high amounts of Pb (i.e. around 65% which is the summation of water, exchangeable, and carbonates fractions) can readily dissolve from the ZPLRs and pollute the environment under slightly acidic condition. High amounts of Pb associated with exchangeable and carbonates fractions in ZPLRs may be attributed to anglesite ($PbSO_4$) and cerussite ($PbCO_3$) that are slightly soluble in water and more soluble in acetate solution as the result of the formation of lead-acetate complexes (Giordano, 1989). The release of Pb from $PbSO_4$ in water is low but it increases with increasing aggressiveness of the solution. For example, in the previous research on the fractionation of Pb from reagent $PbSO_4$, it was found that Pb fractionated in high amounts at the carbonates stage with very

low amounts in preceding (water-soluble fraction) and succeeding (amorphous Fe/Mn-oxyhydroxides and crystalline Fe-oxides fractions) extraction stages (Leinz et al., 2000).

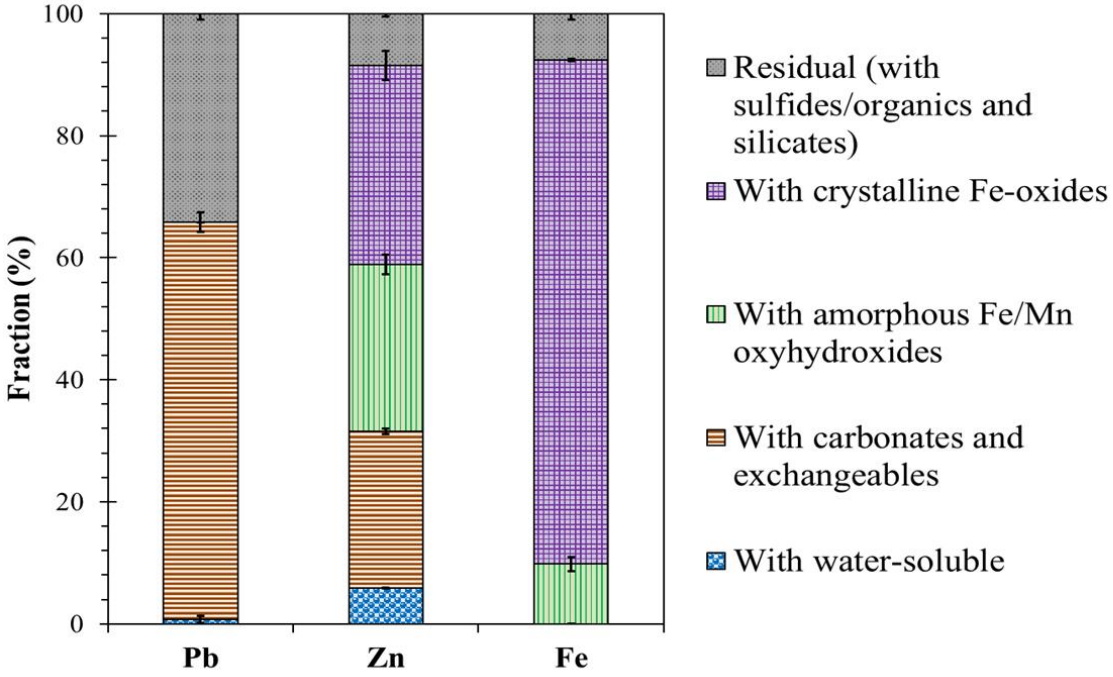

Fig. 3-2. Solid-phase fractionation of Pb, Zn, and Fe in zinc plant leach residues (ZPLRs)

Unlike Pb which was mainly partitioned in three of the five solid-phase fractions, Zn was distributed in all solid-phases in the following order: crystalline Fe-oxides > amorphous Fe/Mn oxyhydroxides ≈ carbonates > residual > water-soluble. High amounts of Zn associated with the reducible fraction (i.e., 27% at amorphous Fe/Mn oxyhydroxides and 33% crystalline Fe-oxides stages) have also been reported by Sethurajan et al. (2016), Iavazzo et al. (2012), and Anju and Banerjee (2011) in 30-year-old ZPLRs from Brazil, abandoned mine wastes from Morocco, and soil contaminated by mining activities of Pb and Zn in India, respectively. The possible reason for Zn association with reducible fractions can be due to isomorphic substitution of Fe or co-precipitation with Fe-oxyhydroxide (Herbert, 1996; Igarashi et al., 2020).

3.3.2. Leachability and gastric bio-accessibility of Pb from zinc plant leach residues

The leachability and gastric bio-accessibility of Pb from historic ZPLRs was evaluated by TCLP and SBRC-G. The amount of Pb leached from the ZPLRs using TCLP was around 12.9 mg/L which

exceeded the allowable threshold (i.e., 5 mg/L) by over 6 mg/L. Leached Zn by TCLP leachability test was also more than 18 fold of the allowable threshold (i.e., 473.5 mg/L against the threshold of 25 mg/L). Furthermore, the SBRC-G leaching results that around 12 300 mg/kg (19.8% of the total Pb) and 15 700 mg/kg (26% of the total Zn) Pb and Zn, respectively, could dissolve from ZLRs in gastric fluid especially for a fasting human being. The TCLP and SBRC-G leaching results indicate that Pb in ZPLRs is easily mobilized, which makes them potentially hazardous to the surrounding ecosystem and health of people living nearby.

3.3.3. Detoxification zinc plant leach residues by removal of Pb using the coupled extraction-cementation method

3.3.3.1. Effects of micro-scale zero valent iron addition

The concentration of dissolved Pb from ZPLRs (2.5 g) leached in a 50 mL solution composed of 5.13 M NaCl and 0.05 M HCl with and without addition 0.5 g mZVI (Fig. 3-3). In the absence of mZVI, the concentration of dissolved Pb increased rapidly with time, stabilizing at around 10.4 mM after 2 h. Considering the two Pb-bearing minerals —$PbSO_4$ and $PbCO_3$— that were detected in ZPLRs, Pb dissolution can be explained by the following chemical reactions (Eq. 3-3 to 3-7) (Farahmand et al., 2009; Sinadinović et al., 1997):

$$PbSO_4 + Cl^- = PbCl^+ + SO_4^{2-} \quad (3\text{-}3)$$

$$PbCO_3 + 2H^+ + Cl^- = PbCl^+ + H_2O + CO_2 \quad (3\text{-}4)$$

$$PbCl^+ + Cl^- = PbCl_2 \quad (3\text{-}5)$$

$$PbCl_2 + Cl^- = PbCl_3^- \quad (3\text{-}6)$$

$$PbCl_3^- + Cl^- = PbCl_4^{2-} \quad (3\text{-}7)$$

Chemical reaction depicted by Eq. 3-5 shows the formation of the sparingly soluble, $PbCl_2$, intermediate phase (solubility of $PbCl_2$ in water at 25ºC 0.99 g/L). The solubilization of $PbCl_{2(s)}$ can increase by either increasing the reaction temperature (Choi et al., 2019; Moon and Yoo, 2017) or increasing the chloride concentration to form soluble Pb-chloride complexes as depicted by Eq. 3-6 and Eq. 3-7 (Farahmand et al., 2009).

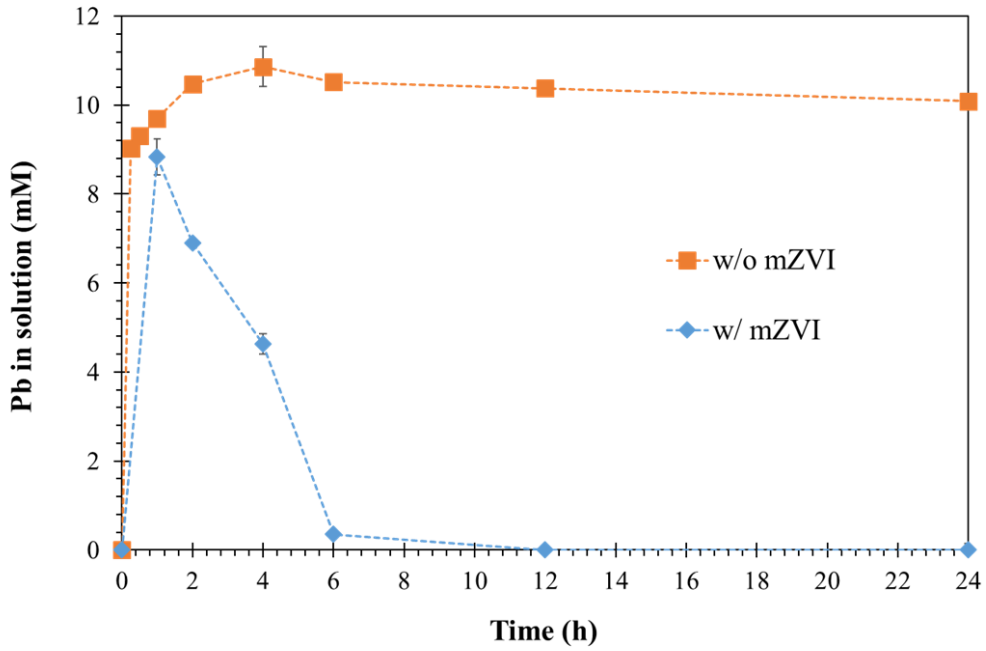

Fig. 3-3. The concentration of dissolved Pb from zinc plant leach residues (ZPLRs) as a function of time with and without micro-scale zero-valent iron (mZVI).

When mZVI was added during ZPLRs leaching, the concentration of dissolved Pb reached a maximum of around 8.8 mM after 1 h. After this, it decreased dramatically with time to around 0.35 and <1 x 10^{-6} mM (0.1 mg/L) after 6 and 12 h, respectively. The dissolved Pb concentration decreased after 1h suggesting that soluble Pb-Cl complexes were sequestered by mZVI, probably due to cementation (e.g., Eq. 3-8).

$$PbCl_4^{2-} + Fe = Pb^0 + Fe^{2+} + 4Cl^- \quad (3\text{-}8)$$

The magnetic fraction collected after 12 h of coupled extraction-cementation treatment of ZPLRs was analyzed by SEM-EDX. The SEM photomicrograph, EDX elemental maps, and EDX spectra showed Pb cemented on the surface of mZVI particles (Fig. 3-4). Further analysis of the magnetic fraction was carried out to identify the elemental forms of Pb observed on the surface of mZVI by XPS analysis. The XPS spectra of Pb 4f (i.e., Pb $4f_{7/2}$ and Pb $4f_{5/2}$), Fe $2p_{3/2}$, and O 1s are shown in Fig. 3-5 and the corresponding curve fitting parameters are summarized in Table 3-3. The Pb 4f spectrum (Fig. 3-5a) imply that Pb on mZVI was present in two valent forms: (1) as zero-valent lead (Pb^0) at binding energy 136.59 eV ($Pbf_{7/2}$) and 141.45 eV ($Pbf_{5/2}$) (Abdel-Samad and Watson, 1998; Pederson,

1982; Taylor, 1984), and (2) as divalent lead (Pb(II)) attributed to PbO at binding energy 138.50 eV ($Pbf_{7/2}$) and 143.32 eV ($Pbf_{5/2}$) (Abdel-Samad and Watson, 1998; Thomas and Tricker, 1975). The spectrum of Fe $2p_{3/2}$ (Fig. 3-5b) shows peaks of oxidized Fe at binding energies of 708.3 and 709.75 eV that are attributed to FeO while the peaks at binding energies at 711.1, 712.2, and 713.2 eV are attributed to goethite (α–FeOOH) (Grosvenor et al., 2004; Tabelin et al., 2019). The formation of PbO, FeO and α–FeOOH was also corroborated by the spectrum of O 1s (Fig. 3-5c), the deconvolution of which identified several peaks at different binding energies: (1) binding energies at 529.2 and 530.1 eV are attributed to lattice oxygen (O^{2-}), (2) binding energies at 531.3 and 532.3 eV are attributed to hydroxyl oxygen (OH^-), and (3) peak at binding energy at 533.4 eV is attributed to the adsorbed water ($\equiv H_2O$) (Grosvenor et al., 2004; Thomas and Tricker, 1975). Based on the XPS results, Pb recovered on mZVI was primarily because of the cementation of extracted Pb^{2+} on mZVI as Pb^0 (Eq. 3-8). Moreover, the presence of oxidation products of mZVI (FeO and α–FeOOH) and Pb^0 (PbO) could be attributed to the oxidation of mZVI and Pb^0 during the experiments, storage and drying because these two metals are known to readily react with oxygenated water and moist air (Taylor, 1984; Xi et al., 2010).

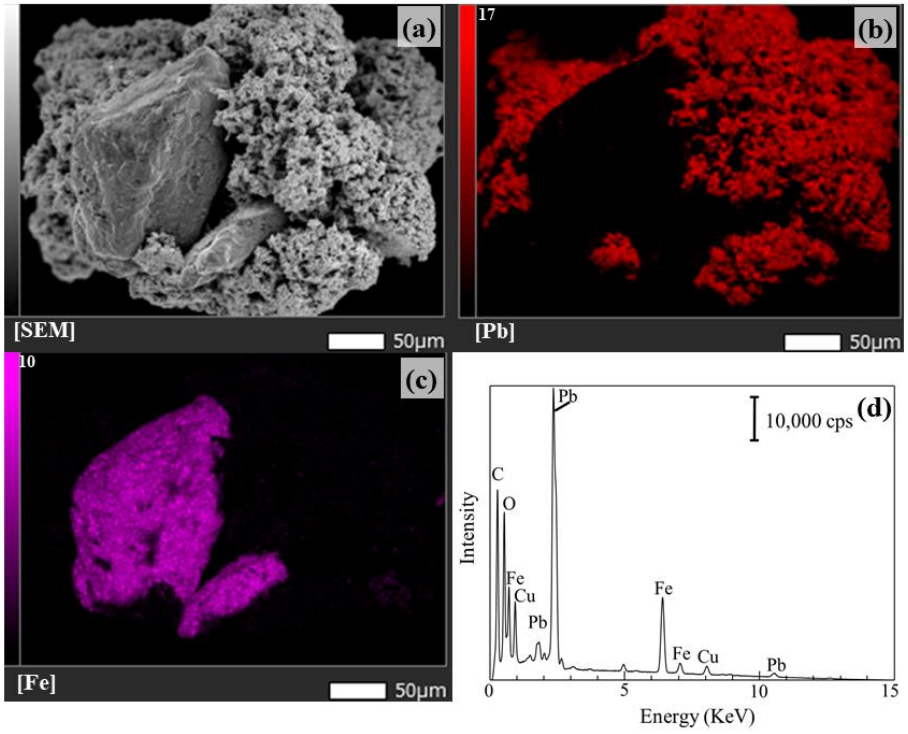

Fig. 3-4. SEM-EDX of the magnetic fraction obtained when mZVI was added during ZPLRs leaching for 12 h: (a) SEM microphotograph image, (b) EDX elemental mapping of Pb, (c) EDX elemental mapping of Fe, and (d) EDX spectra of the whole area.

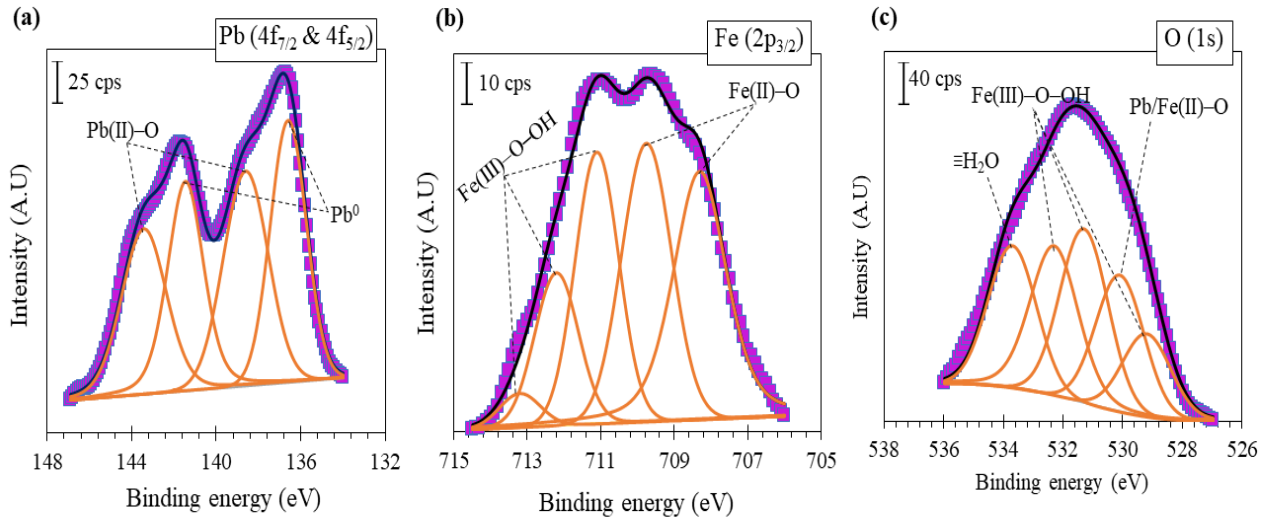

Fig. 3-5. XPS of the magnetic fraction obtained when mZVI was added during ZPLRs leaching for 12 h: (a) $Pb4f_{7/2\&5/2}$, (b) $Fe2p_{5/2}$, and (c) O1s. Data points are represented by squares, fitted results are referred to by the blue lines, and deconvoluted peaks are denoted by orange lines.

Table 3-3. XPS peak parameters and chemical state of Pb $4f_{7/2\&5/2}$, $Fe2p_{5/2}$, and O1s spectra.

Spectra Peak	Binding Energy (eV)		FWHM		Comments (chemical state)
	This study	Reference	This study	Reference	
Pb($4f_{7/2}$)	136.56	136.6[a]	2.01	-	Zero-valent lead (Pb^0)
Pb($4f_{5/2}$)	141.45	141.5[a]	2.01	-	Zero-valent lead (Pb^0)
Pb($4f_{7/2}$)	138.5	137.8[a]	2.5	-	Lead oxide (Pb(II)–O)
Pb($4f_{5/2}$)	143.32	142.7[a]	2.5	-	Lead oxide (Pb(II)–O)
Fe($2p_{3/2}$)	708.3	708.4[b]	1.65	1.4[b]	Iron oxide (Fe(II)–O)
Fe($2p_{3/2}$)	709.75	709.7[b]	1.65	1.6[b]	Iron oxide (Fe(II)–O)
Fe($2p_{3/2}$)	711.1	711.2[b]	1.4	1.2[b]	Iron hydroxide (α–Fe(III)–O–OH)
Fe($2p_{3/2}$)	712.2	712.1[b]	1.4	1.4[b]	Iron hydroxide (α–Fe(III)–O–OH)
Fe($2p_{3/2}$)	713.2	713.2[b]	1.4	1.4[b]	Iron hydroxide (α–Fe(III)–O–OH)
O(1s)	529.2	529.9[b]	1.9	-	Hydroxyl oxygen in Fe hydroxide (O^{2-}
O(1s)	530.1	530.0[c]	1.9	-	Lattice oxygen in Pb and Fe oxide (O^{2-}
O(1s)	531.3	531.2[e]	1.9	1.6[e]	Hydroxyl oxygen in Fe hydroxide (OH^-)
O(1s)	532.3	532.3[e]	1.9	1.6[e]	Hydroxyl oxygen in Fe hydroxide (OH^-)
O(1s)	533.7	533.2[e]	1.9	1.6[e]	Adsorbed water (≡H_2O)

[a](Pederson, 1982); [b](Grosvenor et al., 2004); [c](Ding and de Jong, 2007); [e](Park et al., 2020). Note "-" means "not reported"

The concentration of dissolved Zn when ZPLRs were leached with and without mZVI are shown in Fig. 3-6. Dissolved Zn from ZPLRs increased to around 10.5 mM after 15 min and then remained almost constant even after 24 h in the presence of mZVI. The results suggest that mZVI is ineffective in the recovery of dissolved Zn leached from ZPLRs via cementation, which is to be expected because dissolved Zn cementation onto mZVI is thermodynamically unfavorable because

Zn^{2+}/Zn (–0.763 V vs SHE) is more electronegative than Fe^{2+}/Fe (–0.44 V vs SHE)). To recover dissolved Zn in solution, techniques such as electrowinning (Kashida et al., 2017; Tuffrey et al., 1985) or precipitation (Sethurajan et al., 2017) may be applied. From this point forward, only the results and discussion of Pb removal are presented.

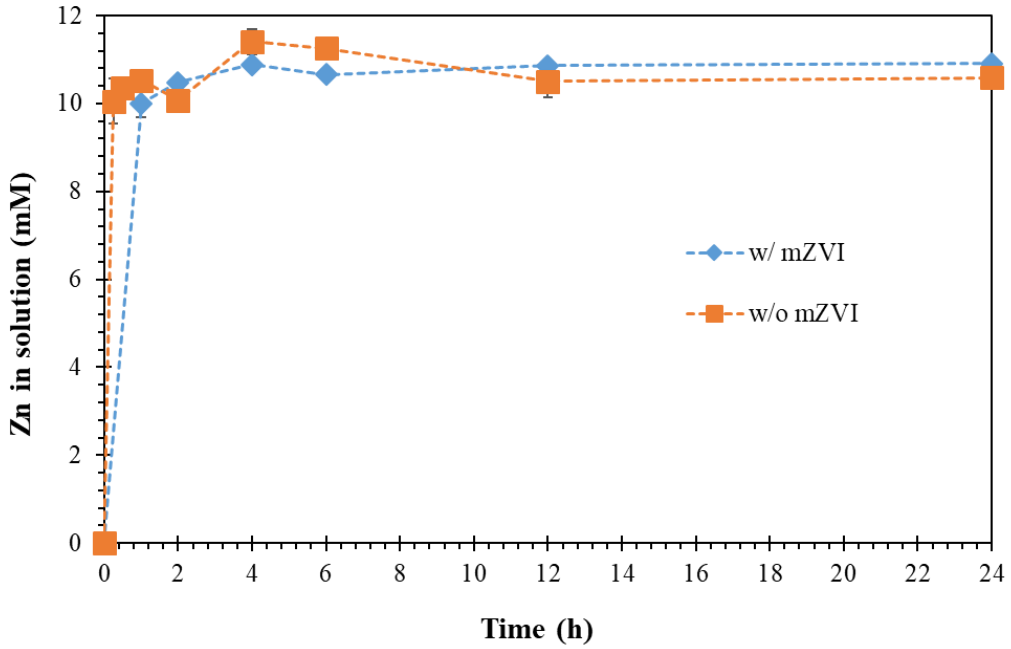

Fig. 3-6. Effects of time on concentration of dissolved Zn from 2.5 g ZLRs into leaching solution phase with and without addition of 0.5 g mZVI.

3.3.3.2. Effects of solution composition on lead distribution in solution, mZVI, and treated residues

The experimental conditions on the study of the effects of solution composition were based on our preliminary experimental results (results not shown) and previous results (Fig. 3-3), thus the solid-to-liquid ratio, mZVI dosage and treatment time were fixed at 1:20, 0.35 g and 12 h, respectively. During the coupled extraction-cementation treatment of ZPLRs, Pb was expected to distribute into three fractions: (1) extracted and cemented Pb on mZVI, (2), extracted Pb but remain in solution, and (3) unextracted Pb remaining in the residues.

Figure 3-7 shows the effects of solution composition (i.e., NaCl and HCl concentrations) on the distribution of Pb in the three defined fractions. The distribution of Pb to mZVI was independent of NaCl when HCl concentration in the system was 0.01 M or less (Fig. 3-7a and 3-7b). Pb recovered on mZVI fraction was around 28% of the total Pb in ZPLRs at 0.86 M (50g/L) NaCl solution and an insignificant increase was obtained even after increasing the NaCl concentration 6-fold to 5.13 M

(300g/L). At higher HCl concentrations (i.e., 0.05 M and 0.1 M), however, the partitioning of Pb to mZVI became more extensive as the NaCl concentration increased. Pb recovered by mZVI in 0.05 M and 0.1 M HCl increased from 32 to 65% and from 55% to 80% as the NaCl increased from 0.86 M to 5.13 M, respectively (Fig. 3.7c and 3.7d). The percentage of Pb remaining in the solution for almost all the solution compositions was almost zero except for 0.1 M HCl and 5.13 M NaCl solution composition as around 5% (0.2 mg/L) of Pb remained in solution. This means that almost all extracted Pb was cemented out of the leaching solution for almost all the solution compositions.

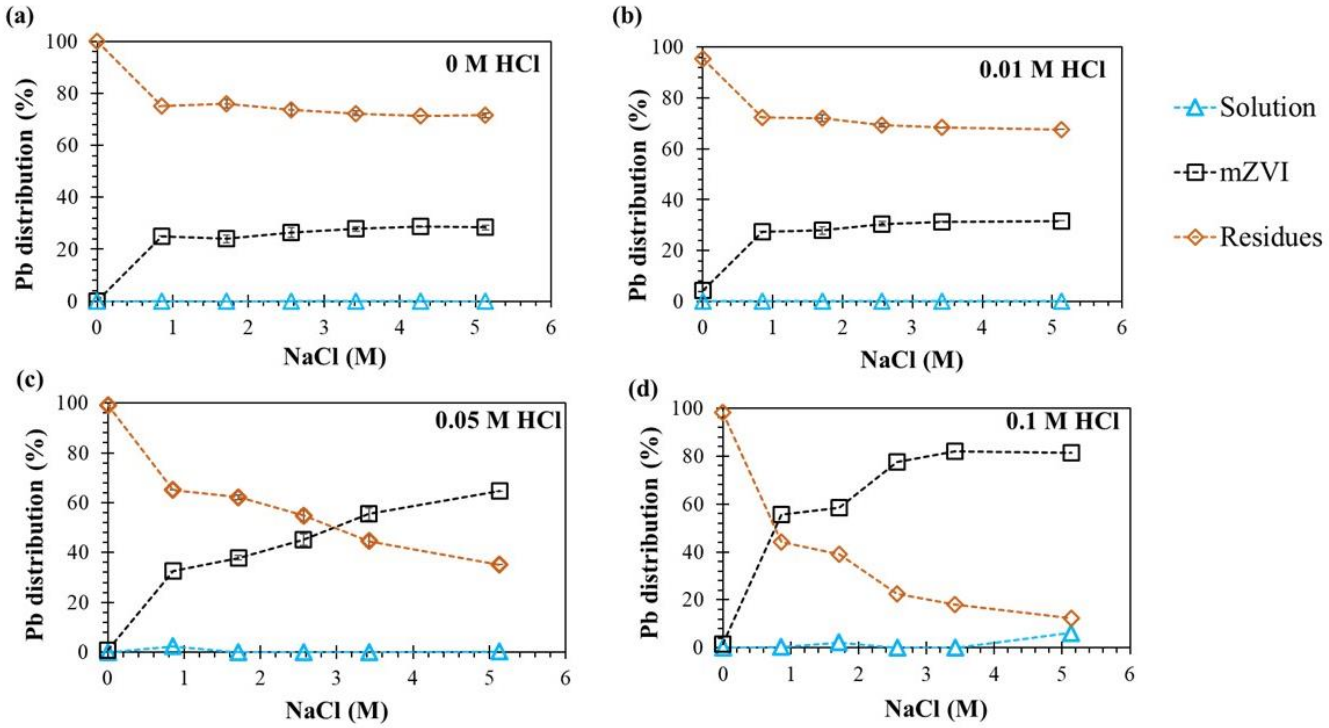

Figure 3-7. Effects of solution composition on distribution of Pb in three solution, mZVI and residues: (a) 0 M HCl and 0–5.13 M NaCl, (b) 0.01 M HCl and 0–5.13 M NaCl, (c) 0.05 M HCl and 0–5.13 M NaCl, and (d) 0.1 M HCl and 0–5.13 M NaCl.

The amounts of Pb removed from ZPLRs when leached with and without the addition of mZVI in different leaching solution compositions were compared. As defined in Eq. 3-2, Pb removal without mZVI addition during ZPLRs leaching is referred to as %Pb distributed in solution, whereas when mZVI was added Pb removal corresponds to the summation of %Pb distributed to the solution and mZVI (Eq. 3-1). Because Pb remaining in solution was almost 0% in the presence of mZVI, it is

reasonable to assume that Pb removal by mZVI is approximately equal to %Pb distributed to mZVI. When ZPLRs were leached without the addition of mZVI, Pb removal increased with increasing NaCl and HCl concentrations (Fig. 3-8a–c). However, the dependence of Pb removal from ZPLRs on NaCl concentration was insignificant when HCl was < 0.05 M (Fig. 3-8a&b). For example, for 0 and 0.01 M HCl increasing NaCl to 5.13 M removed Pb of around 16% and 32%, respectively. When HCl concentration was increased to 0.05 M and 0.1 M, Pb removal increased with increasing NaCl concentration (Fig. 3-8c&d). For the former case, the maximum Pb removal was around 70% at the highest NaCl concentration of 5.13 M while for the latter the removal was around 80% when NaCl concentration was 5.13 M.

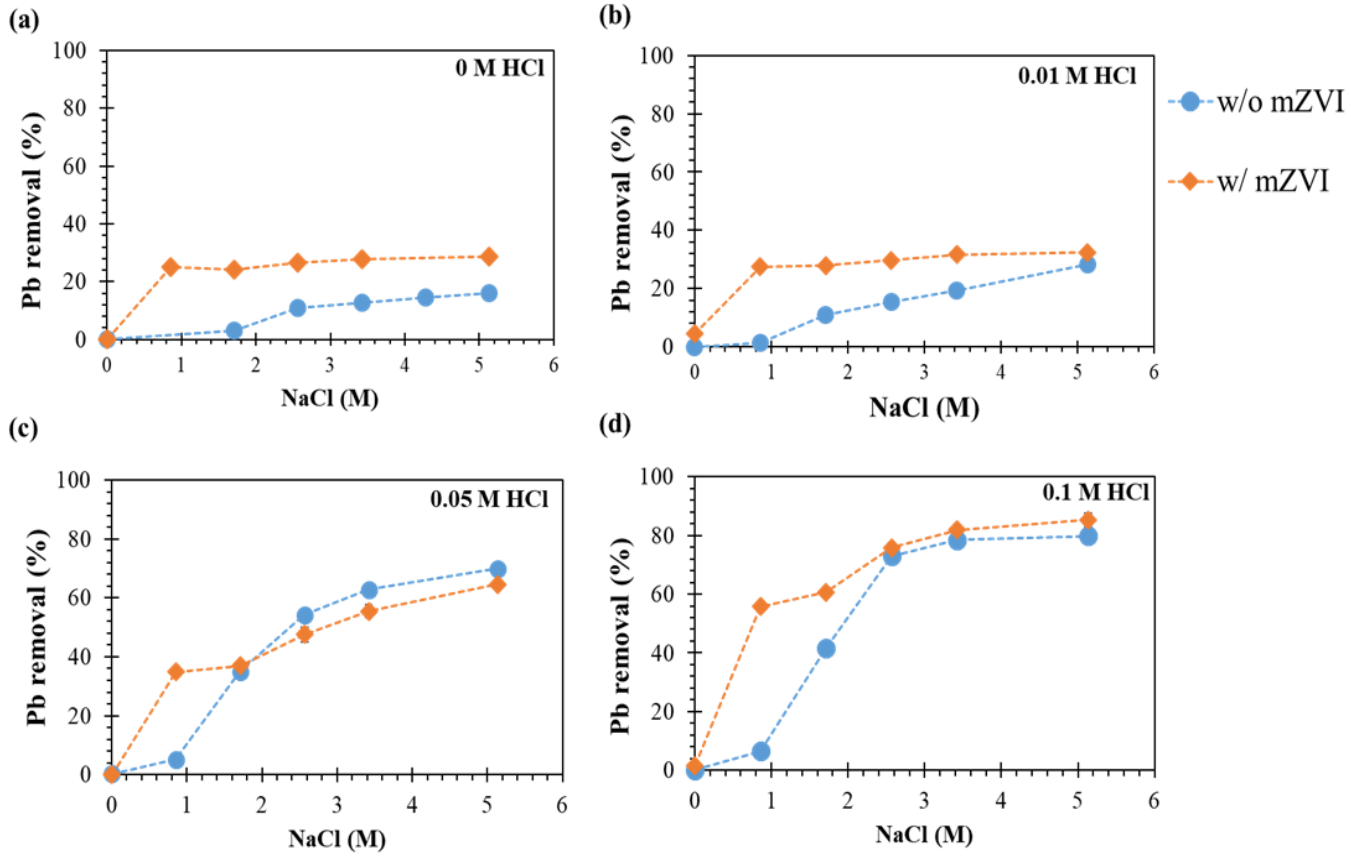

Fig. 3-8. Effects of solution composition on Pb removal from ZPLRs with and without addition of mZVI: (a) 0 M HCl and 0–5.13 M NaCl, (b) 0.01 M HCl and 0–5.13 M NaCl, (c) 0.05 M HCl and 0–5.13 M NaCl, and (d) 0.1 M HCl and 0–5.13 M NaCl.

The addition of mZVI during ZPLRs leaching (i.e., the coupled extraction-cementation technique) favored Pb removal at low NaCl concentrations (Fig. 3-8). For example, when NaCl concentration was fixed at 0.86 M and HCl concentrations were 0, 0.01, 0.05 and 0.1 M, Pb removal increased from 3 to 24%, 1.3 to 27.5%, 5.2 to 34.9%, and 6.5 to 55.8%, respectively. It is also noteworthy that the highest Pb removal obtained was around 80% of the total Pb in ZPLRs when HCl and NaCl concentrations were 0.1 M HCl and above 3.42 M, respectively. This was higher than the amount of Pb amenable to acid leaching as determined by sequential extraction (65%), which may be attributed to the dissolution of Pb associated with sulfide/organics. Chloride in acidic solutions typically enhances the non-oxidative dissolution of sulfide minerals (i.e. galena) (Awakura et al., 1980; Baba and Adekola, 2012).

The increase of Pb removal as NaCl concentration increased was attributed to the formation of soluble Pb-Cl complexes (i.e., $PbCl_3^-$ and $PbCl_4^{2-}$) as previous explained in chemical reactions in Eq. 3.5–3.7. Additionally, the concentration of sulfate (SO_4^{2-}) in the leaching system determines the required concentration of chloride (Cl^-) for chemical reaction represented by Eq. 3-3 to move forward to its completion. Furthermore, SO_4^{2-} and Cl^- concentration in the leaching system affect dissolved Pb^{2+} resulting from $PbCO_3$ leaching (depicted in Eq. 3-4) from precipitating as $PbSO_4$. In our leaching system, the source of SO_4^{2-} is not only $PbSO_4$ but also $CaSO_4{\cdot}2H_2O$ and $ZnSO_4{\cdot}2H_2O$, hence the need of high NaCl concentration to attain high Pb removal. Furthermore, proton (H^+) concentration (i.e., pH) also plays crucial role in release of Pb from both $PbSO_4$ and $PbCO_3$ minerals. Pb dissolution as function of H^+ concentration for the former mineral is indirect in the sense that it involves the speciation of SO_4^{2-}. At low pH SO_4^{2-} speciate as bisulfate (HSO_4^-) (Casas et al., 2000), meaning high H^+ concentration lowers the free SO_4^{2-} concentration in the leaching system that would hinder the chemical reaction depicted in Eq. 3-3 going in the forward direction (right direction), that is, promotes precipitation of $PbSO_4$.

Meanwhile, the enhancement of Pb removal from ZPLRs at low chloride (NaCl) concentration when mZVI was added during leaching can be attributed to shifting the equilibrium between the dissolved Pb (i.e., Pb^{2+} and $PbCl^+$) and sparingly soluble solid $PbCl_{2(s)}$ as well as Pb host minerals—$PbSO_4$ and $PbCO_3$. The addition of mZVI consumes Pb^{2+} and $PbCl^+$ by reductive precipitation (Eq. 3-8), so more $PbSO_4$(s) dissolves by the shift of equilibria in Eqs. 3-3 to 3-5. This could be one possible reason for the enhanced removal of Pb from ZPLRs when mZVI was added.

3.3.4. Leachability and gastric bio-accessibility of Pb from treated residues

The leachability (TCLP leaching test) and bio-accessibility (SBRC-G leaching test) of Pb from the residues after coupled extraction-cementation treatment (conditions: 5.13 M NaCl and 0.1 M HCl with addition of 0.35 g of mZVI) showed significant decrease from 12.9 mg/L (untreated ZPLRs) to 3.5 mg/L (below 5 mg/L which is the regulatory threshold (U.S. EPA, 1991)) and 12 300 (untreated ZPLRs) to 2840 mg/kg, respectively. These results suggest that detoxification of ZPLRs by removal of Pb using coupled extraction-cementation using mZVI is effective. The coupled extraction-cementation eliminated not only the need to extensively wash the generated residues to remove residual leaching solution but also the treatment of the contaminated solution after washing. Finally, the recovered Pb may be reprocessed for other applications.

3.4. Conclusions

This chapter investigated the detoxification of historic ZPLRs from Kabwe, Zambia by removing Pb using the coupled extraction-cementation method using mZVI in chloride media. Pb removal was investigated under different solution compositions and the detoxification efficacy of the method was evaluated using TCLP and SBRC-G. The findings are summarized as follows:

1) Concentration of Pb^{2+} in the leaching solution was <0.1 mg/L at the end of the treatment of ZPLRs by the coupled extraction-cementation method, so treated residues may not need extensive washing for the removal of a residual solution after solid-liquid separation.

2) Lead removal was low especially at low NaCl and HCl concentration (i.e. Pb removal 6.5% at 0.86 M NaCl and 0.1 M HCl) when ZPLRs were leached without the addition of mZVI, which could be attributed to the leaching solution reaching saturation with dissolved Pb^{2+}.

3) The coupled extraction-cementation method significantly enhanced Pb removal even at low NaCl and HCl concentration (i.e. Pb removal from 6.5 to 55.8% when mZVI was added at 0.86 M NaCl and 0.1 M HCl), which was ascribed to shifting of equilibrium between dissolved Pb (i.e., Pb^{2+} and $PbCl^{+}$) and the Pb host minerals (i.e., $PbSO_4$ and $PbCO_3$) as well as sparingly intermediate solid product $PbCl_2$(s).

4) Lead removal increased to around 80% when NaCl concentration was above 3.42 M in 0.1 M HCl solution.

5) Leachability of Pb from ZPLRs before and after treatment by the coupled extraction-cementation method drastically decreased from 12.9 to 3.5 mg/L, which was below the

regulatory threshold of 5 mg/L. Similarly, the bio-accessibility of Pb from the untreated and treated ZPLRs decreased from 12 300 to 2 840 mg/kg.

This chapter was based on a research paper published under the following details: -

Silwamba, M., Ito, M., Hiroyoshi, N., Tabelin, C.B., Fukushima, T., Park, I., Jeon, S., Igarashi, T., Sato, T., Nyambe, I., Chirwa, M., Banda, K., Nakata, H., Nakayama, S., Ishizuka, M., 2020a. Detoxification of lead-bearing zinc plant leach residues from Kabwe, Zambia by coupled extraction-cementation method. Journal of Environmental Chemical Engineering 8, 104197. https://doi.org/10.1016/j.jece.2020.104197.

References

Abdel-Samad, H., Watson, P.R., 1998. An XPS study of the adsorption of lead on goethite (α-FeOOH). Applied Surface Science 136, 46–54. https://doi.org/10.1016/S0169-4332(98)00337-7.

Anju, M., Banerjee, D.K., 2011. Associations of cadmium, zinc, and lead in soils from a lead and zinc mining area as studied by single and sequential extractions. Environ Monit Assess 176, 67–85. https://doi.org/10.1007/s10661-010-1567-4.

Awakura, Y., Kamei, S., Majima, H., 1980. A kinetic study of nonoxidative dissolution of galena in aqueous acid solution. MTB 11, 377–381. https://doi.org/10.1007/BF02676882.

Baba, A.A., Adekola, F.A., 2012. A study of dissolution kinetics of a Nigerian galena ore in hydrochloric acid. Journal of Saudi Chemical Society 16, 377–386. https://doi.org/10.1016/j.jscs.2011.02.005.

Casas, J.M., Alvarez, F., Cifuentes, L., 2000. Aqueous speciation of sulfuric acid–cupric sulfate solutions. Chemical Engineering Science 55, 6223–6234. https://doi.org/10.1016/S0009-2509(00)00421-8.

Choi, S., Yoo, K., Alorro, R.D., 2019. Hydrochloric acid leaching behavior of metals from non-magnetic fraction of Pb dross. Geosystem Engineering 22, 347–354. https://doi.org/10.1080/12269328.2019.1681301.

Cunningham, S.D., Berti, W.R., 2000. Phytoextraction and Phytostabilization: Technical, Economic, and Regulatory Considerations of the Soil–Lead Issue, in: Phytoremediation of Contaminated Soil and Water. Lewis Publishers, Boca Raton, pp. 359–379.

Demır, G., Çoruh, S., Ergun, O.N., 2008. Leaching behavior and immobilization of heavy metals in zinc leach residue before and after thermal treatment. Environmental Progress 27, 479–486. https://doi.org/10.1002/ep.10302.

Ding, M., de Jong, B.H.W.S., 2007. Chapter 30 Characterizing the surface chemistry of oxides with X-ray photoelectron spectroscopy: Assessment regarding surface oxygen valence charge and acid–base properties, in: Sarkar, D., Datta, R., Hannigan, R. (Eds.), Developments in Environmental Science, Concepts and Applications in Environmental Geochemistry. Elsevier, pp. 665–683. https://doi.org/10.1016/S1474-8177(07)05030-9.

Dold, B., 2003. Speciation of the most soluble phases in a sequential extraction procedure adapted for geochemical studies of copper sulfide mine waste. Journal of Geochemical Exploration 80, 55–68. https://doi.org/10.1016/S0375-6742(03)00182-1.

Eqani, S.A.M.A.S., Khalid, R., Bostan, N., Saqib, Z., Mohmand, J., Rehan, M., Ali, N., Katsoyiannis, I.A., Shen, H., 2016. Human lead (Pb) exposure via dust from different land use settings of Pakistan: A case study from two urban mountainous cities. Chemosphere 155, 259–265. https://doi.org/10.1016/j.chemosphere.2016.04.036.

Erdem, M., Özverdi, A., 2011. Environmental risk assessment and stabilization/solidification of zinc extraction residue: II. Stabilization/solidification. Hydrometallurgy 105, 270–276. https://doi.org/10.1016/j.hydromet.2010.10.014.

Farahmand, F., Moradkhani, D., Safarzadeh, M.S., Rashchi, F., 2009. Brine leaching of lead-bearing zinc plant residues: Process optimization using orthogonal array design methodology. Hydrometallurgy 95, 316–324. https://doi.org/10.1016/j.hydromet.2008.07.012.

Giordano, T.H., 1989. Anglesite (PbSO4) solubility in acetate solutions: The determination of stability constants for lead acetate complexes to 85°C. Geochimica et Cosmochimica Acta 53, 359–366. https://doi.org/10.1016/0016-7037(89)90387-6.

Grosvenor, A.P., Kobe, B.A., Biesinger, M.C., McIntyre, N.S., 2004. Investigation of multiplet splitting of Fe 2p XPS spectra and bonding in iron compounds. Surface and Interface Analysis 36, 1564–1574. https://doi.org/10.1002/sia.1984.

Herbert, R.B., 1996. Metal retention by iron oxide precipitation from acidic ground water in Dalarna, Sweden. Applied Geochemistry, Environmental Geochemistry 11, 229–235. https://doi.org/10.1016/0883-2927(95)00070-4.

Iavazzo, P., Adamo, P., Boni, M., Hillier, S., Zampella, M., 2012. Mineralogy and chemical forms of lead and zinc in abandoned mine wastes and soils: An example from Morocco. Journal of Geochemical Exploration, Reclamation of Mining Site Soils 113, 56–67. https://doi.org/10.1016/j.gexplo.2011.06.001.

Igarashi, T., Herrera, P.S., Uchiyama, H., Miyamae, H., Iyatomi, N., Hashimoto, K., Tabelin, C.B., 2020. The two-step neutralization ferrite-formation process for sustainable acid mine drainage treatment: Removal of copper, zinc and arsenic, and the influence of coexisting ions on ferritization. Science of The Total Environment 715, 136877. https://doi.org/10.1016/j.scitotenv.2020.136877.

Kashida, K., Oue, S., Nakano, H., 2017. Effect of Chloride Ions in Electrowinning Solutions on Zinc Deposition Behavior and Crystal Texture. Mater. Trans. 58, 1418–1426. https://doi.org/10.2320/matertrans.M-M2017827.

Kumar, P.B.A.Nanda., Dushenkov, Viatcheslav., Motto, Harry., Raskin, Ilya., 1995. Phytoextraction: The Use of Plants To Remove Heavy Metals from Soils. Environ. Sci. Technol. 29, 1232–1238. https://doi.org/10.1021/es00005a014.

Leinz, R.W., Sutley, S.J., Desborough, G.A., Briggs, P.H., 2000. An Investigation of the Partitioning of Metals in Mine Wastes Using Sequential Extractions, in: Proceedings from the Fifth International Conference on Acid Rock Drainage. Society for Mining, Metallurgy, and Exploration, Colorado USA, pp. 1489–1499.

Leteinturier, B., Laroche, J., Matera, J., Malaisse, F., 2001. Reclamation of lead / zinc processing wastes at Kabwe, Zambia : a phytogeochemical approach. South African Journal of Science 97, 624–627.

Lorestani, B., Yousefi, N., Cheraghi, M., Farmany, A., 2013. Phytoextraction and phytostabilization potential of plants grown in the vicinity of heavy metal-contaminated soils: a case study at an industrial town site. Environ Monit Assess 185, 10217–10223. https://doi.org/10.1007/s10661-013-3326-9.

Moon, G., Yoo, K., 2017. Separation of Cu, Sn, Pb from photovoltaic ribbon by hydrochloric acid leaching with stannic ion followed by solvent extraction. Hydrometallurgy 171, 123–127. https://doi.org/10.1016/j.hydromet.2017.05.003.

Mwandira, W., Nakashima, K., Kawasaki, S., Ito, M., Sato, T., Igarashi, T., Chirwa, M., Banda, K., Nyambe, I., Nakayama, S., Nakata, H., Ishizuka, M., 2019. Solidification of sand by Pb(II)-tolerant bacteria for capping mine waste to control metallic dust: Case of the abandoned Kabwe Mine, Zambia. Chemosphere 228, 17–25. https://doi.org/10.1016/j.chemosphere.2019.04.107.

Nesbitt, H.W., Muir, I.J., 1994. X-ray photoelectron spectroscopic study of a pristine pyrite surface reacted with water vapour and air. Geochimica et Cosmochimica Acta 58, 4667–4679. https://doi.org/10.1016/0016-7037(94)90199-6.

Ngueta, G., Ndjaboue, R., 2013. Blood lead concentrations in sub-Saharan African children below 6 years: systematic review. Tropical Medicine & International Health 18, 1283–1291. https://doi.org/10.1111/tmi.12179.

Nweke, O.C., Sanders, W.H., 2009. Modern environmental health hazards: a public health issue of increasing significance in Africa. Environ. Health Perspect. 117, 863–870. https://doi.org/10.1289/ehp.0800126.

Oyedele, D.J., Obioh, I.B., Adejumo, J.A., Oluwole, A.F., Aina, P.O., Asubiojo, O.I., 1995. Lead contamination of soils and vegetation in the vicinity of a lead smelter in Nigeria. Science of The Total Environment 172, 189–195. https://doi.org/10.1016/0048-9697(95)04810-3.

Park, I., Tabelin, C.B., Seno, K., Jeon, S., Inano, H., Ito, M., Hiroyoshi, N., 2020. Carrier-microencapsulation of arsenopyrite using Al-catecholate complex: nature of oxidation products, effects on anodic and cathodic reactions, and coating stability under simulated weathering conditions. Heliyon 6, e03189. https://doi.org/10.1016/j.heliyon.2020.e03189.

Pederson, L.R., 1982. Two-dimensional chemical-state plot for lead using XPS. Journal of Electron Spectroscopy and Related Phenomena 28, 203–209. https://doi.org/10.1016/0368-2048(82)85043-3.

Ruşen, A., Sunkar, A.S., Topkaya, Y.A., 2008. Zinc and lead extraction from Çinkur leach residues by using hydrometallurgical method. Hydrometallurgy 93, 45–50. https://doi.org/10.1016/j.hydromet.2008.02.018.

Sethurajan, M., Huguenot, D., Jain, R., Lens, P.N.L., Horn, H.A., Figueiredo, L.H.A., van Hullebusch, E.D., 2017. Leaching and selective zinc recovery from acidic leachates of zinc metallurgical leach residues. Journal of Hazardous Materials, Selected papers presented at the 4th International Conference on Research Frontiers in Chalcogen Cycle Science and Technology, Delft, The Netherlands, May 28 - May 29, 2015 324, 71–82. https://doi.org/10.1016/j.jhazmat.2016.01.028.

Sethurajan, M., Huguenot, D., Lens, P.N.L., Horn, H.A., Figueiredo, L.H.A., van Hullebusch, E.D., 2016. Fractionation and leachability of heavy metals from aged and recent Zn metallurgical leach residues from the Três Marias zinc plant (Minas Gerais, Brazil). Environ Sci Pollut Res 23, 7504–7516. https://doi.org/10.1007/s11356-015-6014-1.

Sinadinović, D., Kamberović, Ž., Šutić, A., 1997. Leaching kinetics of lead from lead (II) sulphate in aqueous calcium chloride and magnesium chloride solutions. Hydrometallurgy 47, 137–147. https://doi.org/10.1016/S0304-386X(97)00041-8.

Tabelin, C.B., Corpuz, R.D., Igarashi, T., Villacorte-Tabelin, M., Alorro, R.D., Yoo, K., Raval, S., Ito, M., Hiroyoshi, N., 2020. Acid mine drainage formation and arsenic mobility under

strongly acidic conditions: Importance of soluble phases, iron oxyhydroxides/oxides and nature of oxidation layer on pyrite. Journal of Hazardous Materials 399, 122844. https://doi.org/10.1016/j.jhazmat.2020.122844.

Tabelin, C.B., Corpuz, R.D., Igarashi, T., Villacorte-Tabelin, M., Ito, M., Hiroyoshi, N., 2019. Hematite-catalysed scorodite formation as a novel arsenic immobilisation strategy under ambient conditions. Chemosphere 233, 946–953. https://doi.org/10.1016/j.chemosphere.2019.06.020.

Taylor, J.A., 1984. An x-ray photoelectron and electron energy loss study of the oxidation of lead. Journal of Vacuum Science & Technology A 2, 771–774. https://doi.org/10.1116/1.572569.

Tembo, B.D., Sichilongo, K., Cernak, J., 2006. Distribution of copper, lead, cadmium and zinc concentrations in soils around Kabwe town in Zambia. Chemosphere 63, 497–501. https://doi.org/10.1016/j.chemosphere.2005.08.002.

Thomas, J. m, Tricker, M.J., 1975. Electronic structure of the oxides of lead. Part 2.-An XPS Study of Bulk Rhombic PbO, Tetragonal PbO, β-PbO2 and Pb304. J. Chem. Soc., Faraday Trans. 2 71, 313–328. https://doi.org/10.1039/F29757100313.

Tiruta-Barna, L., Imyim, A., Barna, R., 2004. Long-term prediction of the leaching behavior of pollutants from solidified wastes. Advances in Environmental Research 8, 697–711. https://doi.org/10.1016/S1093-0191(03)00042-X.

Tuffrey, N.E., Jiricny, V., Evans, J.W., 1985. Fluidized bed electrowinning of zinc from chloride electrolytes. Hydrometallurgy 15, 33–54. https://doi.org/10.1016/0304-386X(85)90065-9.

Turan, M.D., Altundoğan, H.S., Tümen, F., 2004. Recovery of zinc and lead from zinc plant residue. Hydrometallurgy 75, 169–176. https://doi.org/10.1016/j.hydromet.2004.07.008.

U.S. EPA, 2007. Estimation of relative bioaccessibility of lead in soil and soil-like materials using in vivo and in vitro methods.

U.S. EPA, 1991. Toxicity Characteristic Leaching Procedure (TCLP), test method 1311- TCLP.

Xi, Y., Mallavarapu, M., Naidu, R., 2010. Reduction and adsorption of Pb2+ in aqueous solution by nano-zero-valent iron—A SEM, TEM and XPS study. Materials Research Bulletin 45, 1361–1367. https://doi.org/10.1016/j.materresbull.2010.06.046.

CHAPTER 4: INVESTIGATING SELECTIVE AGGLOMERATION OF ZERO VALENT LEAD AND ZINC METALS IN SOLUTION

4.1. Introduction

Fine particle size enlargement by agglomeration can either be desirable or undesirable depending on the unit operation and process in chemical and metallurgical engineering (Pietsch, 1997). For size separation, agglomeration of very fine particles may be desirable if it is selective for particular very fine particles over other fine particles (Jansen and Glastonbury, 1968). For example, very fine (microsize) lead (Pb) and Zn metal particles are nonmagnetic, and they cannot be physically separated from other nonmagnetic fine particles or pulp unless they are selectively agglomerated.

The selective agglomeration of Pb and Zn from other fine solid particles has many separation applications by size among which is the coupled extraction-cementation (CEC) process where the cementation agent used is nonferromagnetic such as aluminum (Al) metal. Chapter 3 reported on the Fe-based CEC process and cemented Pb was harvested from the leaching pulp by magnetic separation. Low redox potential metal such as Al can be used in the CEC process to cement both Pb and Zn provided the cementation product agglomerate. The above necessitated an investigation of selective agglomeration of Pb and Zn before applying it to ZPLRs. Therefore the objectives of this chapter are to (1) evaluate conditions necessary for agglomeration of microscale size Pb and Zn and (2) examine selective agglomeration of these metals from other fine particles (e.g., quartz fine particle) for potential application in removal of Pb and Zn from ZPLRs using Al as the cementation agent in the CEC process (i.e., Al-based CEC).

4.2. Materials and methods

4.2.1. Materials

Lead (–75 µm), Zn (–45 µm), and Al (–45 µm) metal powder (>99%, Wako Pure Chemical Industries, Ltd., Osaka, Japan) were used without purification and pretreatment. Quartz (Wako Pure Chemical Industries, Ltd., Osaka, Japan) were ground using a disc mill (RS100, Retsch Inc., Haan, Germany) to –53 µm. Reagent grade HCl and NaCl (Wako Pure Chemical Industries, Ltd., Osaka, Japan) were used without further purification. To prepare stock solutions of given concentration and composition for agglomeration experiments, chemicals were dissolved or diluted using deionized (DI) water (18 MΩ·cm, Milli-Q® Integral Water Purification System, Merck Millipore, USA).

4.2.2. Methods

Batch agglomeration experiments of fine Pb, Zn, and Al metal powder were conducted using a constant 50 mL working volume of solution in a 200-mL Erlenmeyer flask. Different solution compositions of the proton (H^+) were prepared from HCl-NaCl. A given solution composition was poured into a flask and the solution was nitrogen gas (N_2) purged for 10 minutes to remove dissolved oxygen. Given metal powder of 0.15 g was then added and the flask was sealed with a silicon stopper after another 5 minutes N_2 purging. This was then shaken in a thermostatic water bath shaker for 2 h at shaking speed 120 stroke/minute, shaking amplitude 4 cm, and water bath maintained at temperature 25°C. The resultant solution after each shaking experiment was analyzed by inductively coupled plasma atomic emission spectroscopy (ICP-AES) (ICPE-9820, Shimadzu Corporation, Kyoto, Japan) while the solids were characterized by the scanning electron microscopy equipped with energy-dispersive X-ray spectroscopy (SEM-EDX) (JSM-IT200, JEOL Ltd., Tokyo, Japan).

4.3. Results and discussion

4.3.1. Agglomeration of fine metal powder in chloride solution

Preliminary experiments were carried out to check if Pb, Zn, and Al metal powder could agglomerate when shaken in 0.1 M HCl. The pictorial images shown in Fig. 4-1 revealed that only Pb metal powder (Fig.4-1a) agglomerated to millimeter/centimeter size.

Further experiments were carried on the agglomeration of Pb metal powder in chloride solution by varying H^+ concentration (using HCl) while maintaining the Cl^- concentration (using NaCl) and analyzed dissolved Pb^{2+} in a solution using ICP-EAS. Fig. 4-2 shows that dissolved concentration of Pb into solution as the function of H^+ for each solution type and selected pictorial images of Pb metal powder after agglomeration experiments. Concentration of dissolved Pb^{2+} from Pb metal powder was 12 mg/L in a solution composition of 0 M H^+ and 1M Cl^- (neutral 1 M NaCl). It then increased to around 406 mg/L for 0.005 M H^+ and 1M Cl^- and did not change greatly with the increase of H^+ concentration. Dissolution of Pb from Pb metal powder in acidified chloride solution can be described by chemical reactions depicted by Eq. 4-1 (dissolution of Pb by reduction of the proton) and Eq. 4-2 (dissolution of oxide film on the surface of Pb metal).

$$Pb + xHCl = PbCl_x^{(2-x)} + \frac{x}{2}H_2 \quad (4\text{-}1)$$

$$PbO + 2H^+ + xCl^- = PbCl_x^{(2-x)} + H_2O \quad (4\text{-}2)$$

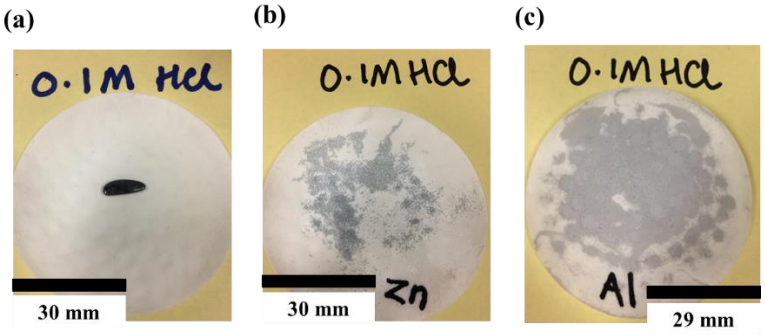

Fig. 4-1. Pictorial image of (a) Pb, (b) Zn and (c) Al metal after agglomeration experiment in 0.1 M HCl solution

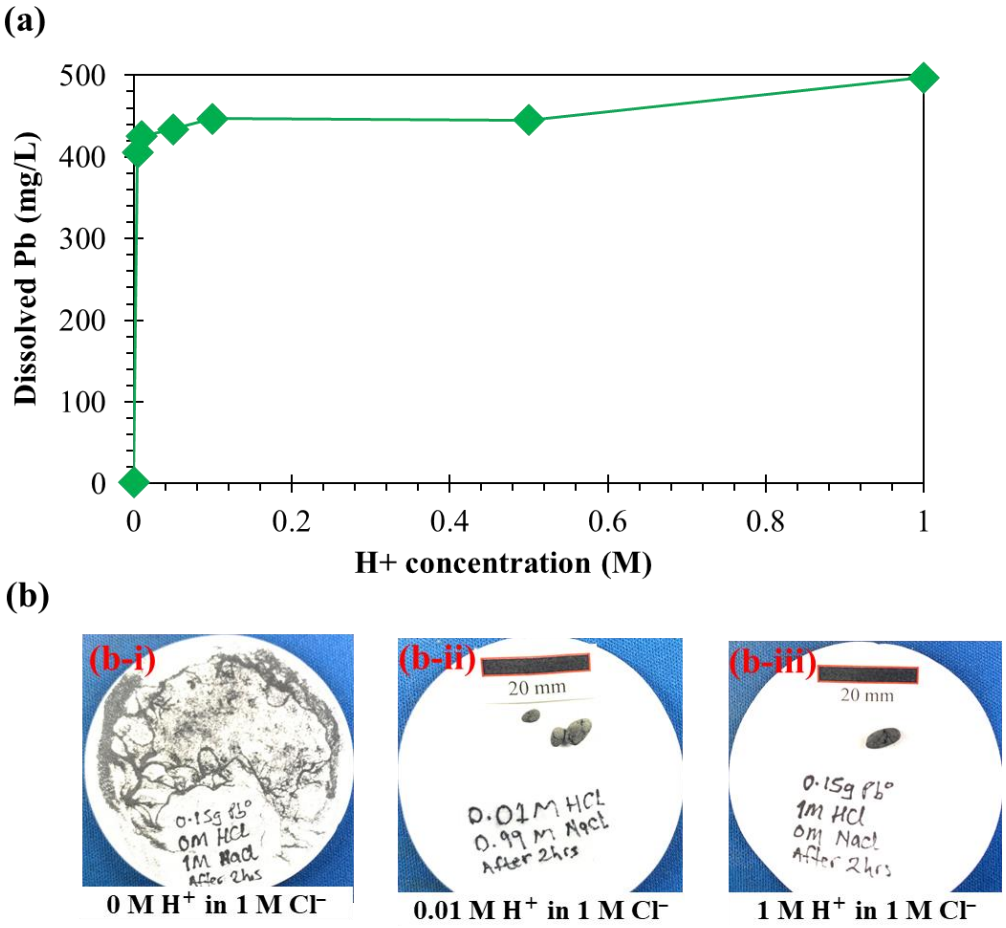

Fig. 4-2. (a) dissolved amounts Pb as function H^+ concentration and (b) selected pictorial images of Pb metal after agglomeration experiment in (b-i) 0 M H^+ and 1M Cl^- , (b-ii) 0.01 M H^+ and 1M Cl^-, and (b-iii) 1 M H^+ and 1M Cl^-.

From the pictorial images (Fig. 4-2b) it was shown that Pb agglomeration did not occur in 0 M H^+ and 1M Cl^- solution but occurred when H^+ was added in chloride solution. The results showed the dependence of agglomeration of fine Pb metal particles on solution composition and Pb dissolution from Pb metal powder.

The obtained Pb metal particle(s) after the agglomeration experiment were further characterized by SEM. Fig. 4-3 shows that agglomerated particles in acidified chloride solution was as the result of small fine particles being connected by a plate-shaped like connector. The change of morphology of Pb particles obtained after shaking in 0 M H^+ and 1M Cl^- shows only precipitate of rod-shaped like particles (Fig. 4-4 b).

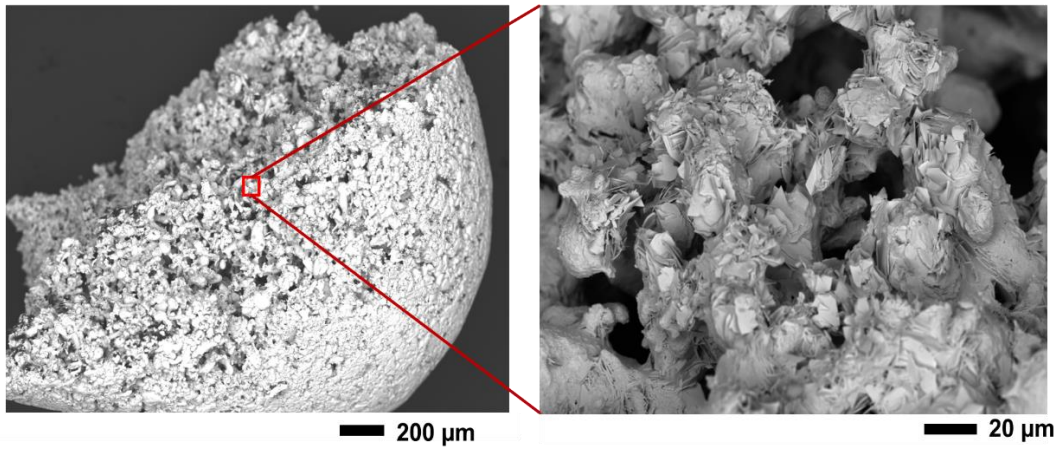

Figure 4-3. SEM-EDX of solid particles obtained when Pb metal powder treated in 0.01 M H^+ and 1M Cl^-

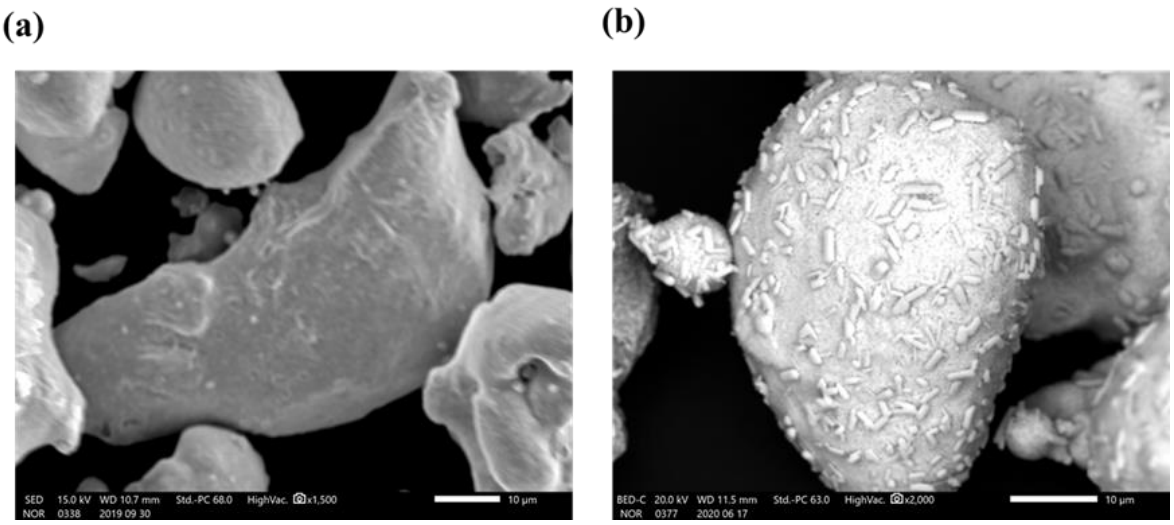

Fig. 4-4. SEM analysis of (a) untreated Pb metal powder and (b) Pb metal obtained after agglomeration experiment in 0.01 M H^+ and 1M Cl^- solution.

To get insight into the morphology of particle connections to form an agglomerate, a cross-section polisher (CP) (JEOL Ltd., Tokyo, Japan) working under a controlled atmosphere (O_2 < 1 ppm, H_2O < 1 ppm) using argon of agglomerated particles was conducted. The polished sample was analyzed by SEM-EDX. Figure 4-5 clearly shows the connection of particles by the plate-shaped connectors. Further analysis was done using Auger Spectroscopy ((JEOL Ltd., Tokyo, Japan) to ascertain the valence form of the connector. The mineral/valence form of the connector was 61.5% Pb^0 and 38.5% PbO (Fig. 4-6).

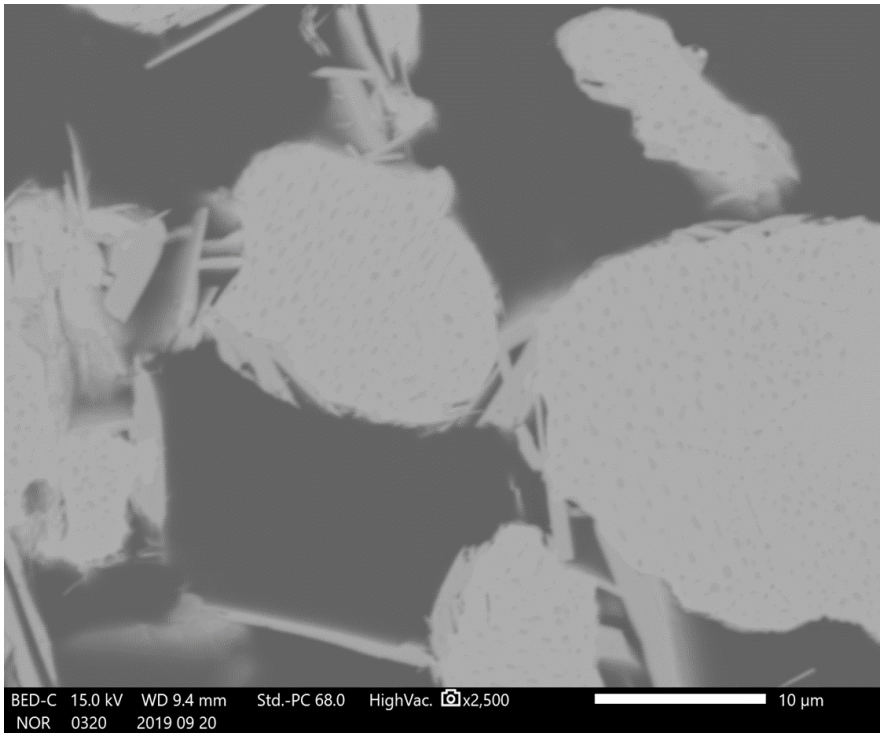

Fig. 4-5. SEM microphotograph after cross-section polisher of agglomerated Pb particles

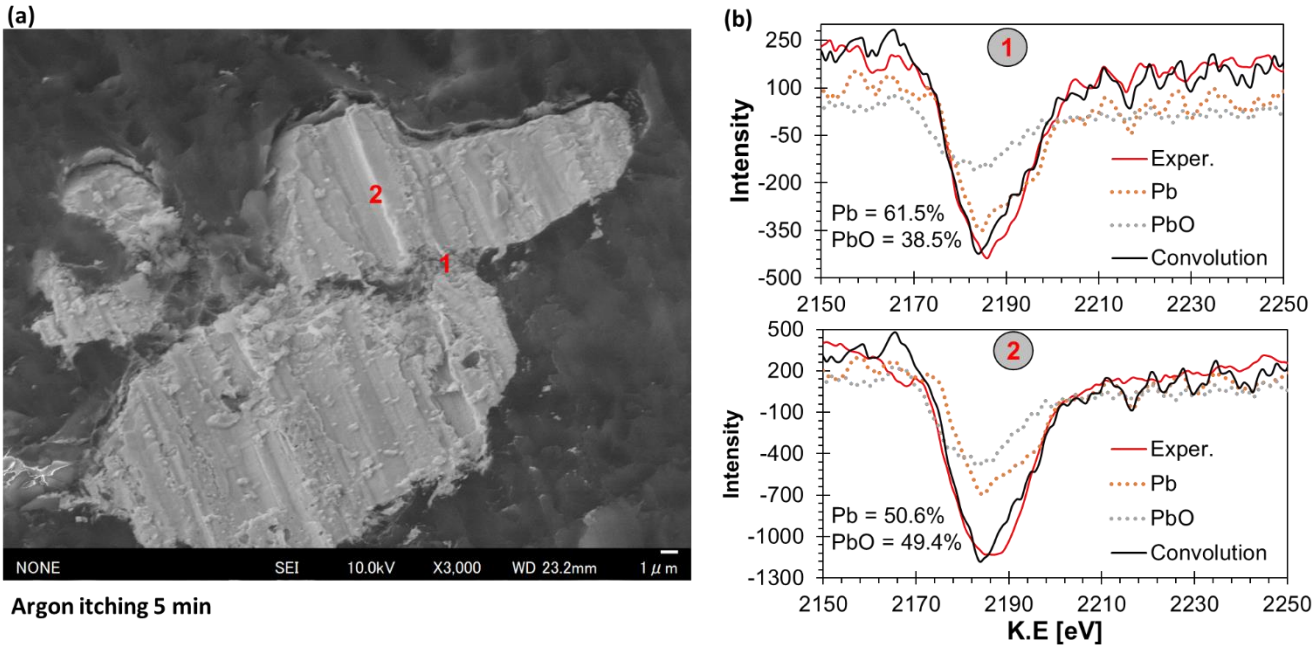

Fig. 4-6. (a) Auger Spectroscopy microphotograph and (b) peak fitting of Pb using Pb^0 and PbO of agglomerated Pb particles

From the above results, it was observed that agglomeration of Pb metal powder in chloride solution occurred when (1) sufficient H^+ was added to the solution and (2) dissolution Pb from Pb metal powder occurs. Under atmospheric conditions and in water metal surfaces are covered by the oxide film layers (Khaledi et al., 2019; Mori et al., 2013). For ductile metals, the oxide film layers formed are mostly hard and brittle. If these oxides are removed and two metal particles are brought into contact under pressure, particles deform and join by the formation of the metallurgical bond ('solid-state welding'). For soft metals such as Pb whose crystallization occurs even at 25°C (room temperature), the required pressure for metallurgical bond formation is minimal (Hotta et al., 2007; Khaledi et al., 2019). Thus, a possible reason why Pb agglomeration occurred in acidified chloride solution capable of removing oxide layer (Eq. 4-2) could be the formation of the metallurgical bond when particles collided in a flask.

4.3.2. Selective agglomeration of fine Pb metal from other fine particles and separation by sieving

Selectively agglomeration fine Pb particles and subsequent separation of agglomerated particles by size was investigated by mixing Pb metal powder, Al powder (the equivalent of $Al/Pb^{2+} = 2$ for cementation of dissolved Pb), and fine ground quartz (-75µm). Different amounts (3, 9, 18, and 24 g) of quartz were mixed with 0.15 g Pb metal powder in a solution composition of 0.01 M HCl and 1 M NaCl. Separation of agglomerated Pb metal powders was achieved by screening using stainless steel sieve of aperture size 150 µm. For material balance, agglomerated particles were digested in Aqua Regia and analyzed Pb content using ICP-EAS. Figure 4-7 shows selective agglomeration of fine Pb metal particles is possible, and that the pulp density (i.e., solid/liquid ratio) does not affect selective agglomeration. Around 98% (meaning dissolved Pb was reductively precipitated and agglomerate with added Pb metal powder) of Pb metal powder was selectively agglomerated and could be separated effectively from quartz even in a high mass ratio of quartz to Pb metal as 24 g to 0.15 g. This presents a possible means of physico-chemical separation of fine Pb metal particles from other fine solids. Additionally, it implies that Al-based CEC could be applied to ZPLRs because cemented and agglomerated Pb could be separated from the leaching pulp by sieving.

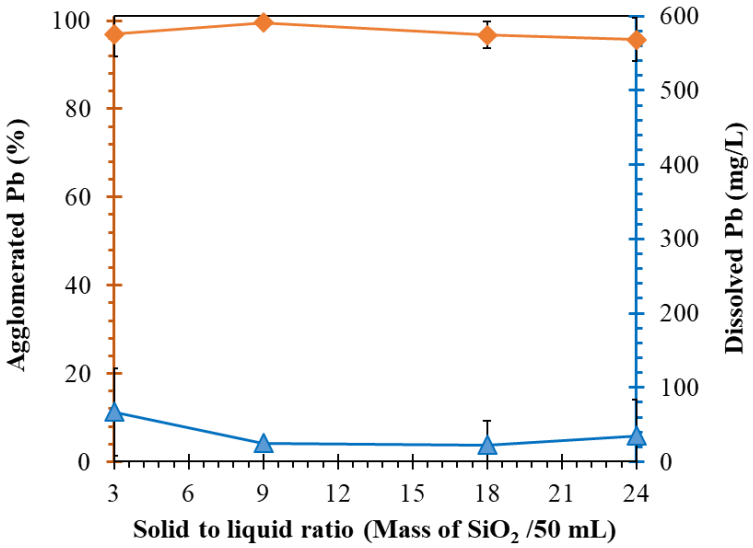

Fig. 4-7. Effects of solid (quartz) to the liquid ratio on selective agglomeration and amounts agglomerated Pb metal powder in 0.01 M H_2SO_4 and 1 M NaCl solution after 2 h.

4.4. Conclusions

This chapter investigated selective agglomeration of Pb, Zn, and Al in acidified chloride solution. This was necessary to evaluate the applicability of the Al-based CEC process for ZPLRs because the hypothesized cementation product (Pb-Zn-Al) cannot be separated physically from the leaching pulp using the magnet. The following is the summary of the findings:

1. For three metals (i.e., Pb, Zn, and Al) that were investigated, only fine Pb metal powder agglomerated.
2. Agglomeration of fine Pb metal particles only occurred in acidified chloride solution that dissolved around 405 mg/L of Pb. This agglomeration was attributed to the metallurgical bond formation (“solid-state cold welding’) due to the collision of oxide film-free Pb particles.
3. Fine Pb metal particles were selectively agglomerated from other fine quartz particles and separated by sieving. Around 98% of Pb metal powder could be separated effectively from quartz as high mass ratio of quartz to Pb metal as 24 g to 0.15 g. This presents a possible means of physico-chemical separation of fine Pb metal particles from other fine solids. Additionally, it implies that Al-based CEC could be applied to ZPLRs because cemented and agglomerated Pb could be separated from the leaching pulp by sieving.

References

Hotta, S., Matsumoto, K., Murakami, T., Narushima, T., Ouchi, C., 2007. Dynamic and Static Restoration Behaviors of Pure Lead and Tin in the Ambient Temperature Range. Materials Transactions 48, 2665–2673. https://doi.org/10.2320/matertrans.MRA2007078.

Jansen, M.L., Glastonbury, J.R., 1968. The size separation of particles by screening. Powder Technology 1, 334–343. https://doi.org/10.1016/0032-5910(68)80016-6.

Khaledi, K., Rezaei, S., Wulfinghoff, S., Reese, S., 2019. Modeling of joining by plastic deformation using a bonding interface finite element. International Journal of Solids and Structures 160, 68–79. https://doi.org/10.1016/j.ijsolstr.2018.10.014.

Mori, K., Bay, N., Fratini, L., Micari, F., Tekkaya, A.E., 2013. Joining by plastic deformation. CIRP Annals 62, 673–694. https://doi.org/10.1016/j.cirp.2013.05.004.

Parthasarathy, P., Virkar, A.V., 2013. Electrochemical Ostwald ripening of Pt and Ag catalysts supported on carbon. Journal of Power Sources 234, 82–90. https://doi.org/10.1016/j.jpowsour.2013.01.115.

Pietsch, W., 1997. Size Enlargement by Agglomeration, in: Fayed, M.E., Otten, L. (Eds.), Handbook of Powder Science & Technology. Springer US, Boston, MA, pp. 202–377. https://doi.org/10.1007/978-1-4615-6373-0_6.

Tang, L., Li, X., Cammarata, R.C., Friesen, C., Sieradzki, K., 2010. Electrochemical Stability of Elemental Metal Nanoparticles. J. Am. Chem. Soc. 132, 11722–11726. https://doi.org/10.1021/ja104421t.

Virkar, A.V., Zhou, Y., 2007. Mechanism of Catalyst Degradation in Proton Exchange Membrane Fuel Cells. J. Electrochem. Soc. 154, B540. https://doi.org/10.1149/1.2722563

CHAPTER 5: DETOXIFICATION OF ZINC PLANT LEACH RESIDUES BY REMOVAL OF LEAD AND ZINC USING COUPLED EXTRACTION-CEMENTATION AND ZERO-VALENT ALUMINIUM IN ACIDIFIED BRINE SOLUTION

5.1. Introduction

With the rapid depletion of high-grade ores, ZPLRs are now considered as secondary resources because they still contain substantial amounts of residual Zn, copper (Cu), lead (Pb), and iron (Fe) (Guo et al., 2010; Ru et al., 2015; Ruşen et al., 2008; Sethurajan et al., 2017). From an environmental point-of-view, ZPLRs are considered hazardous wastes because they contain hazardous heavy metals like Pb, Cu, and Zn. Lead, for example, is extremely toxic to babies and children and is known to cause various disorders of the reproductive organs, central nervous system, and kidneys (Needleman, 2004; Tabelin et al., 2014, 2012). Therefore, the reprocessing of ZPLRs for metal removal/recovery could address both environmental and resource concerns associated with these waste materials.

In Chapter 3, coupled extraction-cementation process was investigated as means of achieving rapid and permanent detoxification of ZPLRs by removal of Pb using micro-scale zero-valent iron (mZVI) in an acidified brine solution. Only extracted Pb was simultaneously sequestered by mZVI via cementation and was separated from the pulp magnetic concentration leaving extracted Zn in solution. Although Pb could be sequestered by cementation using mZVI, it took more than 12 h to reduce the amount of dissolved Pb to less than 0.01 mg/L. Secondly, a highly concentrated NaCl solution was used because low NaCl concentration could not give satisfactory Pb removal results even with the addition of mZVI. Finally, extracted Zn was not cemented onto mZVI and remained in solution because it is thermodynamically unfavorable as mZVI has a higher standard redox potential (i.e., $Fe/Fe^{2+} = -0.44$ vs SHE) than Zn (i.e., $Zn/Zn^{2+} = -0.763$V vs SHE).

In this chapter, the removal of both Pb and Zn from ZPLRs by coupled extraction-cementation processes using micro-scale zero-valent aluminum (ZVAl) in acidified brine solution is reported. Extracted Pb and Zn are both hypothesized to be cemented by ZVAl due to the fact that ZVAl is less noble (i.e., $Al/Al^{3+} = -1.66$ V vs SHE) than Pb and Zn (i.e., $Pb/Pb^{2+} = -0.126$ vs SHE and $Zn/Zn^{2+} = -0.763$V vs SHE).

5.2. Materials and methods

5.2.1. Materials

Chemical characterization mineralogical composition of ZPLRs were as reported in Chapter 3. Analysis of the particle size distribution of lightly pulverized ZPLRs was analyzed using Laser diffraction (Microtrac® MT3300SX, Nikkiso Co., Ltd., Japan). The size range of particles in ZPLRs was 1-10 µm with a medium size (D_{50}) of around 9.6 µm (Fig. 5-1a).

Reagent grade NaCl and HCl (Wako Pure Chemical Industries, Ltd., Japan) were used to prepare the leaching solutions of different concentrations by dissolution and dilution using deionized (DI) water (18 MΩ·cm, Milli-Q® Integral Water Purification System, Merck Millipore, USA). To simultaneously precipitate reductively (cement) the dissolved Pb^{2+} and Zn^{2+} in leaching pulp, ultra-pure ZVAl powder (>99.99%, +50 –150 µm, Wako Pure Chemical Industries, Ltd., Japan) was used (the median particle size (D_{50}) of ZVAl was 126.8 µm Fig 5-1b). Stainless steel sieve with 150 µm aperture size was used to separate cemented and agglomerated Pb and Zn from the leaching pulp. The sieve size was selected by taking into consideration of the particle size ranges of both ZPLRs and ZVAl. In other words, this sieve could only retain cemented and agglomerated particles while passing particles of unreacted ZVAl and particles of undissolved minerals particles of ZPLRs.

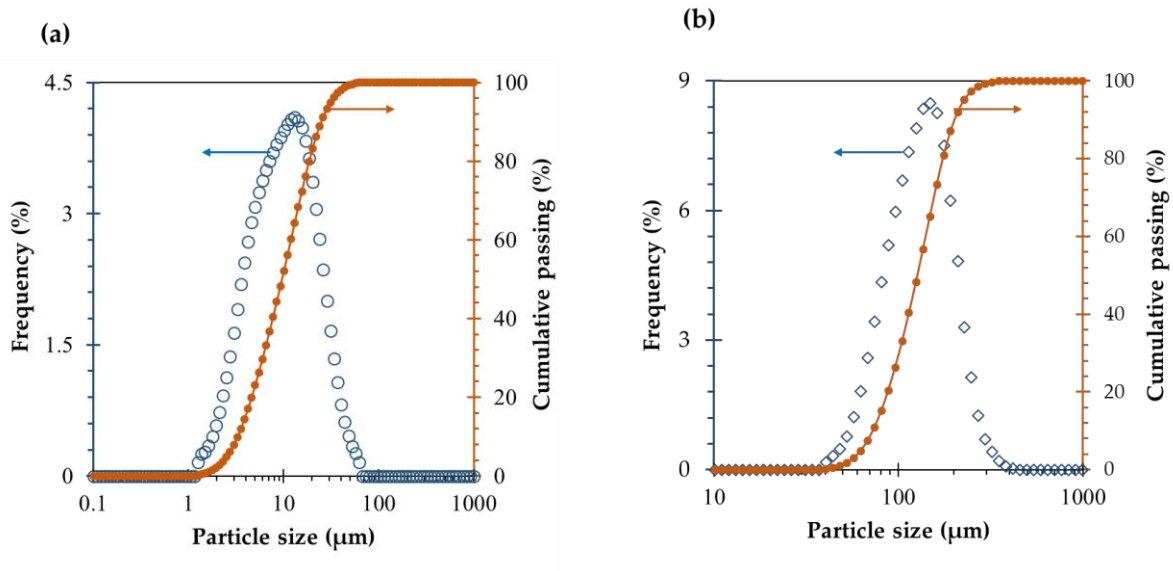

Fig. 5-1. The particle size distribution of (a) zinc plant leach residues and (b) zero-valent aluminum.

5.2.2. Methods

5.2.2.1. Leaching-cementation experiments in chloride solution

Batch leaching experiments for the extraction of Pb and Zn from ZPLRs with and without ZVAl additions were conducted using a 200-mL Erlenmeyer flask. The volume of the leaching solution was at 50 mL for all experiments. Concentrations of NaCl (0–3 M) were varied and acidified with different HCl concentrations (0–0.1 M) to obtain the required leaching solutions. Fifty milliliters (50 mL) of leaching solution of a given concentration was initially poured in an Erlenmeyer flask and nitrogen (N_2) was purged for 10 minutes to remove dissolved oxygen (DO). Nitrogen gas (N_2) purging was again carried out for 2 minutes after the addition of 2.5 g ZPLRs with and without 0.1 g ZVAl were added before sealing the flask using silicon stoppers and parafilm®. The flask was then shaken at 4 cm amplitude and 120 min^{-1} shaking frequency in a water-bath shaker maintained at 25 °C for a predetermined length of time. At the end of the predetermined shaking time, the leaching pulp was carefully collected, and solid-liquid separation was carried out by filtering the collected leaching pulp using a syringe-driven membrane filter (pore size of 0.20 µm). The filtrate was then analyzed for dissolved Pb and Zn using ICP-AES. In the case where ZVAl was added during ZPLR leaching, additional steps—the separation of cemented and agglomerated product from the leaching pulp by screening using a sieve of aperture size 150 µm—were carried out. The +150 µm particles (cemented and agglomerated) were thoroughly washed with deionized (DI) water before drying in a vacuum oven at 40 °C for 24 h. Dried +150 µm were then digested in aqua regia using a microwave-assisted acid digestion system and the leachate was analyzed for Pb and Zn using ICP-EAS. Furthermore, the +150 µm particles obtained were examined by both XRD and SEM-EDX (JSM-IT200, JEOL Ltd., Japan). All the experimental tests were carried out twice and the average is what is reported here.

The Pb and Zn removal ($R_{Pb,Zn}$) from ZPLRs without and with ZVAl were quantified using Eqs. 5-1 and 5-2, respectively.

$$R_{Pb,Zn} = \frac{V * C_{Pb,Zn}}{W_S * M_s} * 100 \quad (5\text{-}1)$$

$$R_{Pb,Zn} = \frac{(V * C_{Pb,Zn}) + (W_{cg} * M_{cg})}{W_S * M_s} * 100 \quad (5\text{-}2)$$

where $C_{Pb,Zn}$ is the concentration (g/L) of Pb and Zn, V is the volume (L) of leaching solution, W_S is the weight percent (%) of either Pb and Zn, M_s is the mass (g) of leached ZPLRs, M_{cg} is the mass (g) of cemented and agglomerated particles, and W_{cg} is the weight percent (%) of cemented and

agglomerated particles calculated based on the digested fraction of M_{cg} in aqua regia and analysis of the solution by ICP-AES.

5.2.2.2. Leachability of lead and zinc from regenerated residues after coupled extraction-cementation

To evaluate the leachability of Pb and Zn from ZPLRs before and residues after coupled extraction-cementation, leachability experiments were conducted according to the toxicity characteristic leaching procedure (TCLP) (U.S. EPA, 1991). For TCLP, 1 g of vacuum-dried treated and untreated residues were equilibrated with 20 mL of acetic acid solution (pH 2.89) in a centrifuge tube shaken at 30 rpm on a rotary tumbler for 18 h. After the predetermined leaching time, the leachate was filtered through 0.20 µm syringe-driven membrane filters, and the filtrate was analyzed for dissolved Pb and Zn using ICP-AES.

5.3. Results and discussion

5.3.1. Coupled extraction-cementation of Pb and Zn from zinc plant leach residues using ZVAl

The concentrations of Pb and Zn as a function of time when 2.5 g ZPLRs were leached in a solution composed of 3 M NaCl and 0.05 M HCl with and without the addition of 0.1 g ZVAl is shown in Fig. 5.2a and 5.2b. The concentration of Pb when ZPLRs was leached without ZVAl reached an apparent equilibrium of around 8.5 mM (which represents 59% of total Pb) after just 15 minutes (Fig. 5-2a). Pb dissolution from ZPLRs involves the formation of lead-chloride complexes as explained by Eqs. 5-3 and 5-4 (Farahmand et al., 2009; Feng et al., 2015; Liu et al., 2010; Xie et al., 2019):

$$PbSO_4 + xCl^- = PbCl_x^{(2-x)} + SO_4^{2-} \quad (5\text{-}3)$$

$$PbCO_3 + 2H^+ + xCl^- = PbCl_x^{(2-x)} + CO_2 + H_2O \quad (5\text{-}4)$$

where $PbCl_x^{(2-x)}$ and x are lead-chloride complex(es) and integers from 1 to 4, respectively, all of which depended on the chloride concentration.

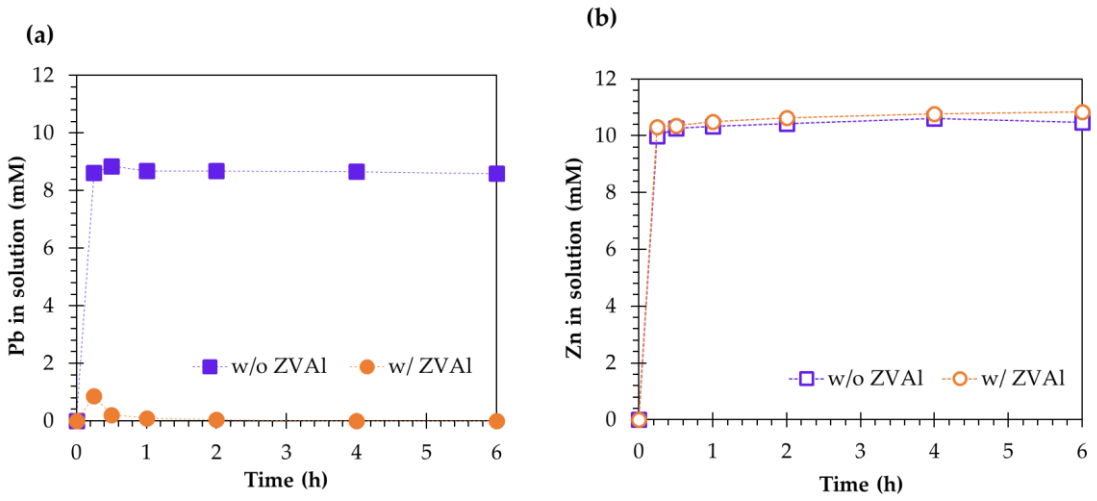

Fig. 5-2. The concentration of (a) Pb and (b) Zn dissolved in leaching solution as a function of time when ZPLRs were leached without and with ZVAl.

The concentration of dissolved Pb when ZVAl was added was 10-fold lower than when only ZPLRs were leached in the same solution. The dissolved concentration of Pb decreased further with increasing treatment time and reached below 0.048 mM (i.e. 0.1 mg/L) with ZVAl after 4 h. The dramatically lower dissolved concentration of Pb after 15 minutes and its continued decrease to below 0.1 mg/L with ZVAl could be attributed to its sequestration from solution via cementation. In other words, an additional chemical reaction—cementation described by the overall reaction (Eq. 5-7) which is the sum of two half-reactions (i.e., Eqs. 5-5 and 5-6)—occurred concurrently with dissolution reactions previously described.

$Al^{3+} + 3e^- = Al^0$ $\quad E^0 = -1.66\,V$ (5-5)

$Pb^{2+} + 2e^- = Pb^0$ $\quad E^0 = -0.126\,V$ (5-6)

$3Pb^{2+} + 2Al^0 = 3Pb^0 + 2Al^{3+}$ (5-7)

The overall reaction potential, ΔE^0, is calculating by subtracting the standard electrode potential of Eq. 5-5 from Eq. 5-6, that is, $\Delta E^0 - 0.126 — 1.66 = 1.534\,V$. The standard Gibbs free energy change, ΔG^0 (i. e. $\Delta G^0 = -nF\Delta E^0$, n number of electrons transferred, F is Faraday's constant and ΔE^0 is the galvanic cell potential), of Eq. 5-7 is negative (–888.047 *kJ/mol*) because ΔE^0 is positive indicating that cementation of dissolved Pb^{2+} from ZPLRs by ZVAl is thermodynamically spontaneous. Besides, the Al_2O_3 layer which inherent present on the surface of ZVAl and passivate

the cementation is removed at acidified chloride solution (Jeon et al., 2020; Seng et al., 2019). Hence, simultaneous cementation of dissolved Pb^{2+} from ZPLRs occurred, which could explain why Pb^{2+} was comparatively lower and was even below 0.1 mg/L with ZVAl during ZPLRs leaching.

Meanwhile, the concentration of dissolved Zn reached apparent equilibrium after 15 minutes at around 10.3 mM (i.e., equivalent to around 52% of total Zn) for without and with ZVAl (Fig. 5-2b). This implied that dissolved Zn from ZPLRs was not cemented on ZVAl as described by Eq. 5-10 (i.e., the summation of two half-cell reactions Eqs. 5-8 and 5-9) though it is thermodynamically feasible due to negative ΔG^0 (i.e., –519.282 *kJ/mol*).

$Al^{3+} + 3e^- = Al^0$ $\quad E^0 = -1.660\ V$ (5-8)

$Zn^{2+} + 2e^- = Zn^0$ $\quad E^0 = -0.763\ V$ (5-9)

$3Zn^{2+} + 2Al^0 = 3Zn^0 + 2Al^{3+}$ (5-10)

The cementation product that was obtained as +150 µm particles were characterized by SEM-EDX and XRD. Figure 5-3 shows that Pb was cemented on ZVAl and agglomerated. However, Zn was not detected, which confirms that dissolved Zn was not cemented by ZVAl. Further characterization of the cementation product by XRD (Fig. 5-4) showed that cemented Pb was mainly in zero-valent Pb (metallic Pb) form and a small amount of oxidized metallic Pb as PbO, which supports the chemical reaction expressed in Eq. 5-7.

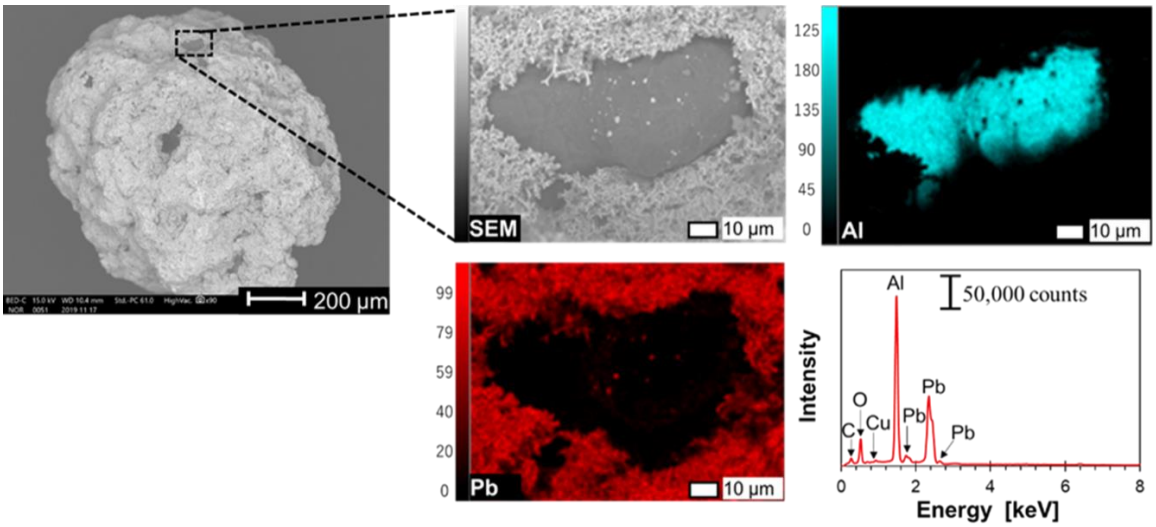

Fig. 5-3. SEM-EDX of ZVAl "coated" with Pb from the +150 µm particles obtained after sieving the leaching pulp when ZVAl was added during leaching of ZPLRs from Kabwe, Zambia.

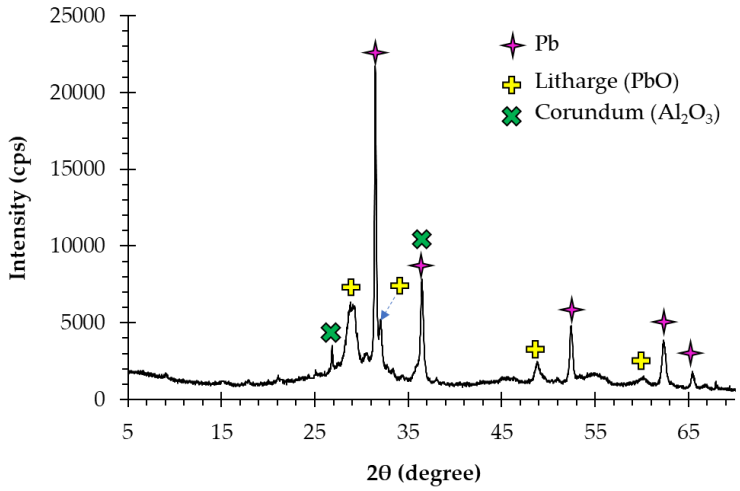

Fig. 5-4. XRD pattern of the +150 µm fraction obtained after sieving the leaching residue in the experiments with ZVAl.

The explanation to why Zn could not be cemented by ZVAl in leaching solution could be (1) the dissolution of cemented Zn by the proton (H^+) (Eq. 5-11) and (2) the reduction of H^+ to H_2 on ZVAl, which competes with the reduction of Zn^{2+} to Zn^0 (Eq. 5-12).

$$6\,H^+ + 3Zn \rightarrow 3H_2 + 3Zn^{2+} \quad (5\text{-}11)$$

$$6\,H^+ + 2Al \rightarrow 3H_2 + 2Al^{3+} \quad (5\text{-}12)$$

In an acidic region, the redox potential of the H^+/H_2 redox pair is higher than that of the Zn^{2+}/Zn redox pair, indicating that reaction depicted in Eq. 5-11 ($\Delta G^0 = -6121.203$ *kJ/mol*) occurred, and Zn once cemented on the ZVAl surface would be dissolved (St-Pierre and Piron, 1986). Similarly, since the redox potential of the H^+/H_2 redox pair is higher than that of the Al^{3+}/Al redox pair, the reaction as shown in Eq. 5-12 ($\Delta G^0 = -8168.614$ *kJ/mol*) also can take place. This reaction consumes the electron supplied from ZVAl and competes with Zn^{2+} reduction to Zn (Eq. 5-10). As a result, these reactions suppress the Zn cementation on ZVAl. The rates and equilibrium of these reactions (Eq. 5-11 and 5-12) depend on H^+ concentration, hence suppression of Zn cementation on ZVAl would decrease at higher pH.

To investigate the effects of H^+ concentration on cementation of Zn^{2+} from solution using ZVAl, simulated (model) acidic and alkaline solutions containing both 8 mM Pb^{2+} and 10 mM Zn^{2+}, and to mimic composition similar to what would be obtained by leaching ZPLRs, were prepared by

dissolving $ZnCl_2$ and $PbCl_2$ (Wako Pure Chemical Industries, Ltd., Japan) in acidified chloride solution (3 M NaCl and 0.05 M HCl, initial pH = 0.82) and alkaline solution (3 M NaOH, initial pH = 14.5), respectively. To cement both Pb and Zn, 0.15 g ZVAl was added after N_2 purging.

Figure 5-5a shows the percentage of cemented Pb and Zn from the simulated acidified chloride solution. Only Pb (around 99.7% after 30 min) was cemented out leaving Zn in solution, which is in line with the results obtained when ZVAl was added during ZPLRs leaching. However, in the alkaline solution around 99.8% of both Pb and Zn were cemented out of the solution Fig. 5-5b. The SEM-EDX analysis and mapping results showed that both Pb and Zn were deposited on the ZVAl surface (Fig. 5-6). The results confirm the suppression of Zn cementation, which depends on pH. In the acidic region, Zn cementation is strongly suppressed by the reactions shown in Eqs. 5-11 and 5-12, while in the alkaline region the suppressive effects become negligible because of low H^+ concentrations.

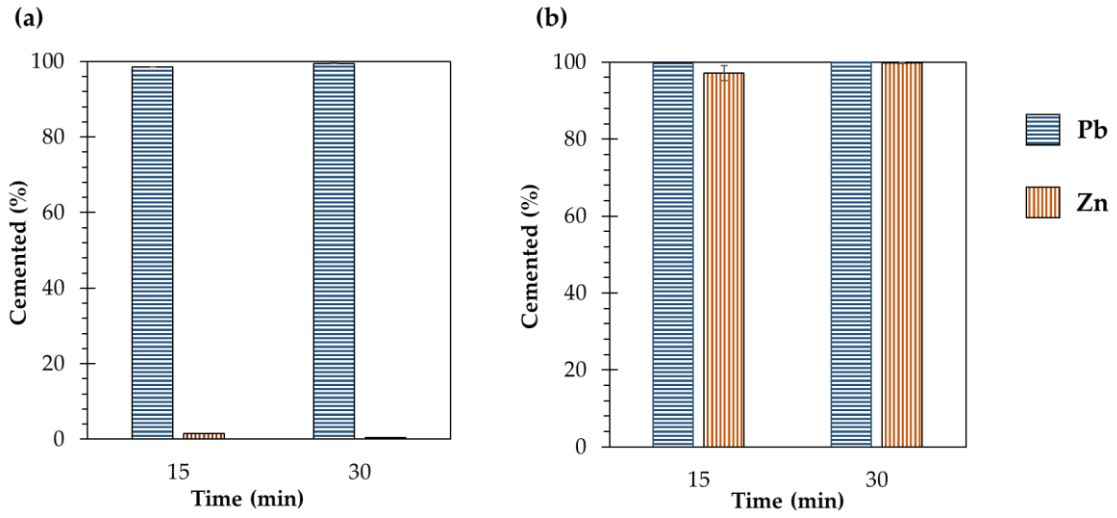

Fig. 5-5. Amount of Pb and Zn cemented out using ZVAl in model experiments under (a) the acidic chloride and (b) alkaline solutions.

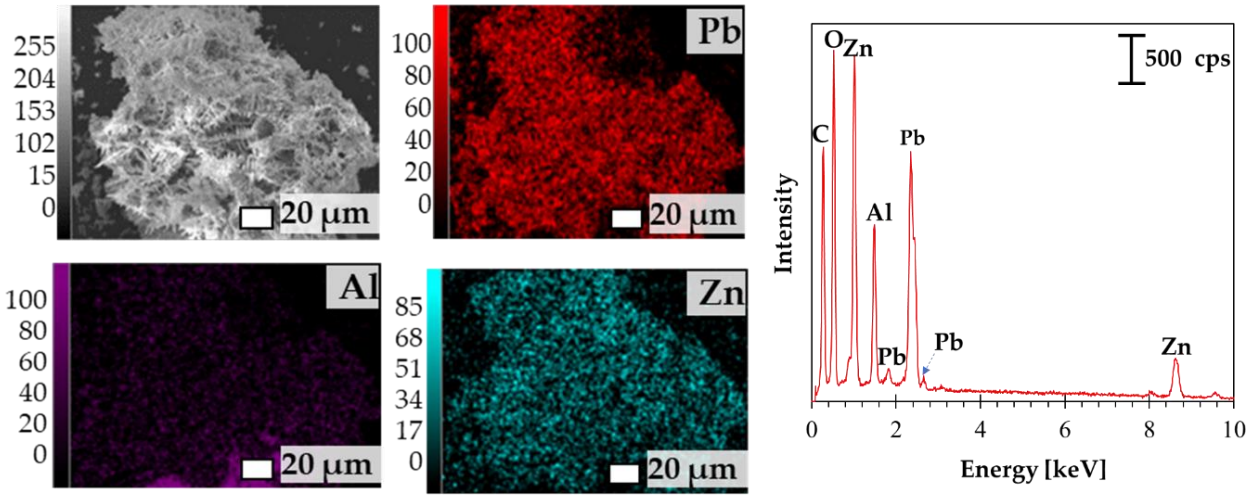

Fig. 5-6. SEM-EDX of cementation product of Pb and Zn by ZVAl from the alkaline model solution.

5.3.2. Effects of solution composition on Pb and Zn removal from zinc plant leach residues

Lead and Zn removal from ZPLRs was evaluated for different solution compositions and compared the removal efficiencies when ZPLRs were leached with and without ZVAl addition. When ZVAl was added during ZPLRs leaching, Pb was extracted into a leaching solution and concurrently cemented and agglomerated. The Pb distribution among the solution (i.e. extracted but uncemented Pb), +150 µm particles (i.e. cementation and agglomerated product), and –150 µm particles (unextracted Pb in residues). Since the amount of Pb that remained in the solution was negligible (in most cases below 0.1 mg/L), Pb removal in a case when ZVAl was added during ZPLRs leaching is referred to as Pb that was extracted, cemented, and separated as +150 µm particles. However, in the case when ZPLRs were leached without the addition of ZVAl, Pb removal is referred to as the Pb that was extracted into a leaching solution. The same definition was also applied to Zn removal with and without ZVAl addition since it was not cemented from the leaching solution as discussed previously.

Lead removal when ZPLRs were leached without the addition of ZVAl increased with increasing both HCl and NaCl concentration as shown in Fig. 4-7. Pb removal steadily increased from around 0 to 28, 0.5 to 58, and 0.5 to 72% for 0.01, 0.05, and 0.1 M HCl, respectively, when NaCl increased from 0 to 3 M, respectively. Lead dissolution from anglesite ($PbSO_4$) depends on (1) Cl^- concentration, (2) SO_4^{2-} concentration, and (3) solution pH (Fig. 4-8). For example, for a 1:1 ratio of Pb concentration to SO_4^{2-} concentration (i.e., assuming the source of SO_4^{2-} in the leaching system is from $PbSO_4$) Pb dissolution depends on the Cl^- concentration only to form Pb-Cl complexes and not

on pH (Eq. 4-3) (Fig. 5-8a and 5-8b). However, even in this case, some Pb from $PbSO_4$ would remain in solid form as $PbCl_2$(s) depending on the Cl^- concentration. The sample used in our study contains $CaSO_4 \cdot 2H_2O$ and $ZnSO_4$ these minerals contribute SO_4^{2-} in the system. At high SO_4^{2-} concentration Pb dissolution from $PbSO_4$ depends on pH (Fig. 5-8c). As the pH increases (i.e., H^+ concentration decreases) HSO_4^- speciates to form SO_4^{2-} which then reacts with dissolved lead in the leaching system to form $PbSO_4$ (Fig. 5-8c and 5-8d). Meaning at high SO_4^{2-} concentration $PbSO_4$ dissolution is limited at high pH. Meanwhile, the release of Pb from other Pb-minerals such as cerussite ($PbCO_3$) in ZPLRs requires an H^+ attack in addition to the Cl^- concentration as previously described in Eq. 5-4. This is the possible reason why Pb removal increased when NaCl and HCl concentrations were increased. The semi-quantitative analysis of the residues obtained after treating ZPLRs in 3 M NaCl and 0.05 M HCl solution with the addition of ZVAl by XRD shown the disappearance/decrease of peaks of anglesite, cerussite, gypsum, and other minerals.

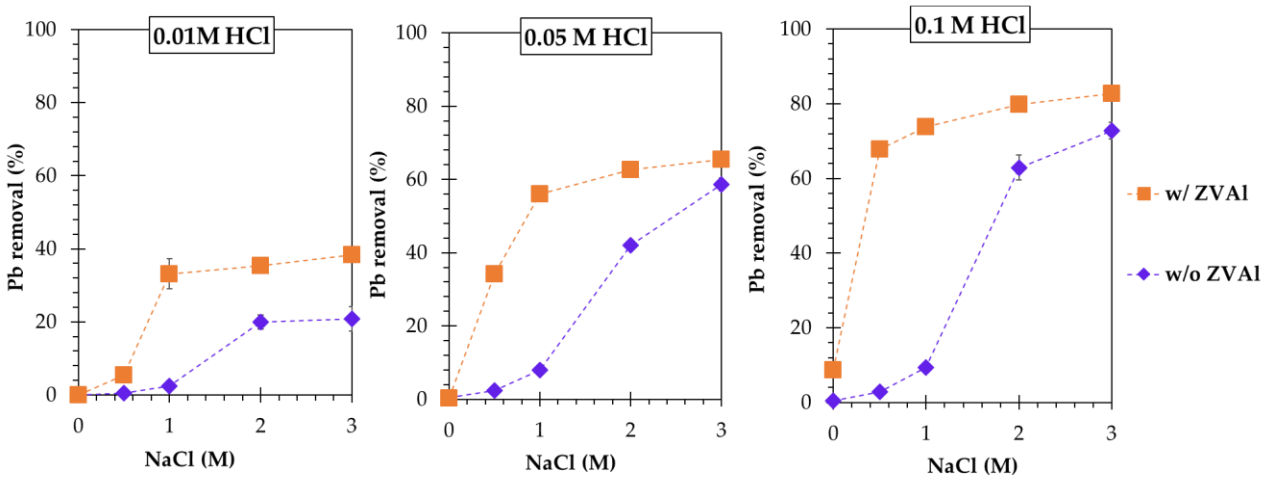

Fig. 5-7. Effects of solution compositions on Pb removal from ZPLRs with and without ZVAl addition.

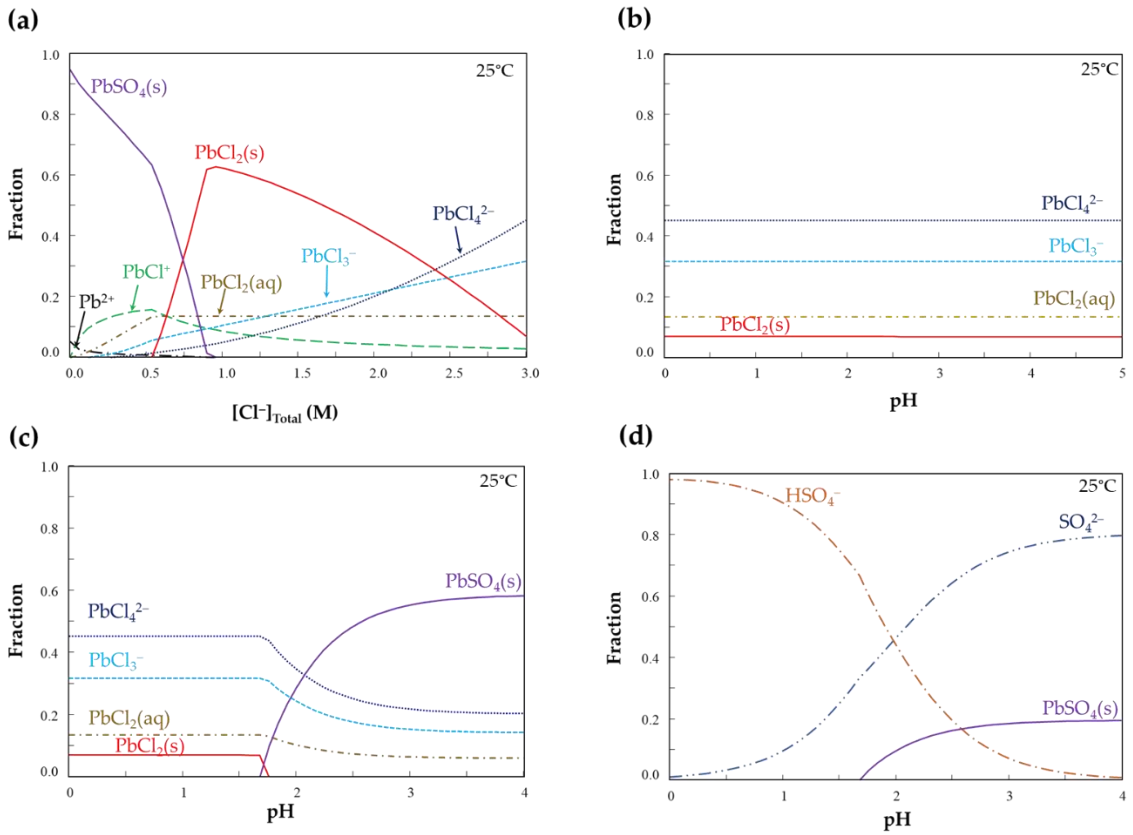

Fig. 5-8. Thermodynamic calculation of dissolution of $PbSO_4$, speciation of Pb-Cl complexes, and SO_4^{2-} at (a) Pb^{2+} = 8 mM, SO_4^{2-} = 8 mM, pH=1, (b) Pb^{2+} = 8 mM, SO_4^{2-} = 8 mM, Cl^- = 3 M, (c) Pb^{2+} = 8 mM, SO_4^{2-} = 24 mM, Cl^- = 3 M, and (d) Pb^{2+} = 8 mM, SO_4^{2-} = 12 mM, Cl^- = 3 M (created using the MEDUSA software (Puigdomenech, 2010))

The addition of ZVAl during leaching of ZPLRs significantly increased the Pb removal even at low NaCl concentration especially when HCl was increased from 0.01 to 0.05 and 0.1 M (Fig. 5-7). For example, while maintaining HCl at 0.05 M, the addition of ZVAl during ZPLRs leaching increased Pb removal from 2.5 to 35.5% and 8 to 57% for 0.5 and 1 M NaCl concentration, respectively. Meanwhile, for 0.1 M HCl, the addition of ZVAl during ZPLR leaching increased Pb removal from 3 to 69% and 9 to 72% for 0.5 and 1 M NaCl concentration, respectively. The dramatic increase of Pb removal at low NaCl concentration is attributed to the leaching solution not attaining saturated with dissolved Pb^{2+} and Pb-Cl complexes. In other words, when ZVAl was added during ZPLRs leaching, dissolved soluble Pb^{2+} and Pb-Cl complexes were simultaneously sequestered from the solution by cementation, hence more Pb could dissolve from host minerals (e.g. $PbSO_4$) as well

as the conversion of intermediate sparingly soluble solid, $PbCl_2$, to more Pb-Cl complexes (Figs 5-9a and 5-9b).

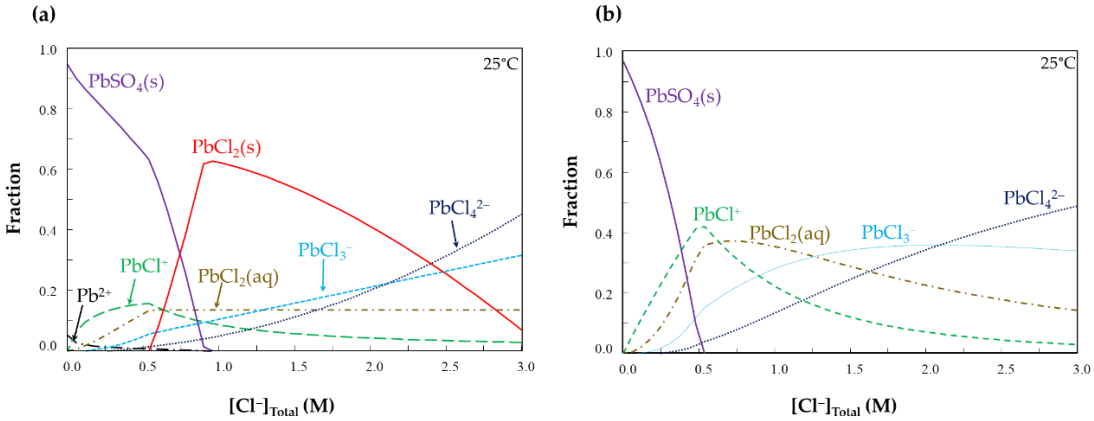

Fig. 5-9. Effects of Pb^{2+} concentration on solubility and speciation of Pb^{2+} and Pb-Cl complexes in Pb-Cl-SO_4^{2-}-H_2O system under the condition (a) Pb^{2+} = 8 mM, SO_4^{2-} = 8 mM, pH=1 and (b) Pb^{2+} = 1 mM, SO_4^{2-} = 8 mM, pH=1 (created using MEDUSA software)

Zinc removal was, however, independent of the increase of NaCl concentration as well as the addition of ZVAl but it increased when HCl concentration increased as shown in Fig. 4-10. When HCl increased from 0.01 to 0.05 and 0.1M, Zn removal increased from around 27 to 60 and 70 %, respectively. Increasing HCl concentration increased the H^+ concentration which in turn increased Zn solubilization from Zn host minerals in ZPLRs by H^+ attack mechanism (e.g., dissolution of Zn associated with amorphous iron oxyhydroxide phase fraction as discussed in Chapter 3). Zinc removal was not affected by NaCl concentration. Unlike Pb that forms an intermediate solid ($PbCl_2$) at low chloride concentration and dissolves as the chloride concentration increases, Zn does form solid Zn-Cl species, and it does not complex strongly with chloride. Additionally, Zn removal was not affected by the addition of ZVAl because it was not sequestered (remained in solution) from the solution as previously discussed. Since Zn was not be recovered by cementation using ZVAl from the leaching pulp, methods such as precipitation as ZnS (Ye et al., 2017) or electrowinning (Tuffrey et al., 1985) can be employed to recover Zn from solution. Unfortunately, these methods are beyond the scope of this study.

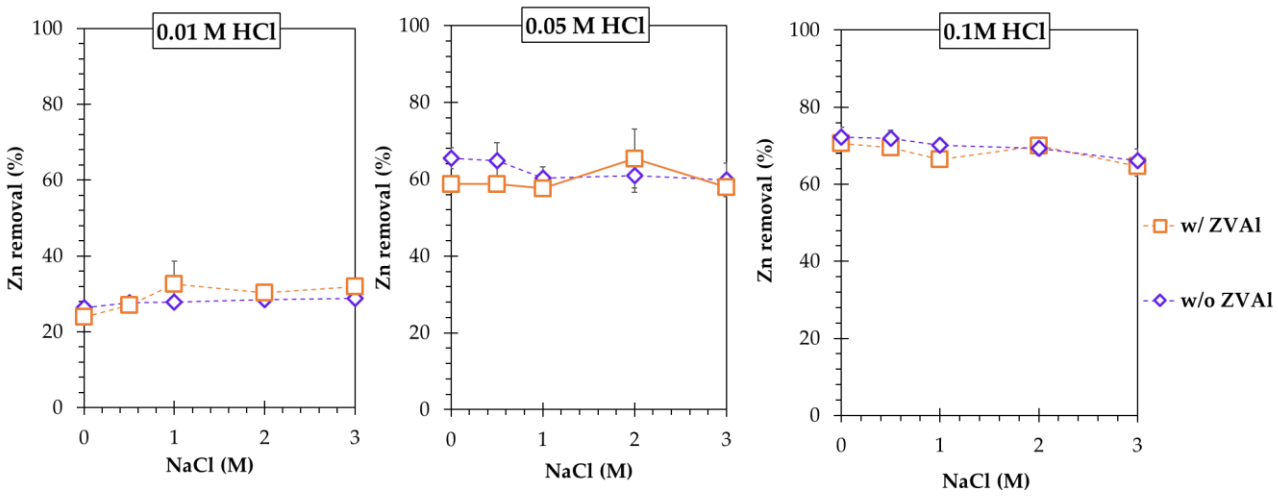

Fig. 5-10. Effects of solution compositions on Zn removal from ZPLRs with and without ZVAl addition.

5.3.3. Leachability of lead and zinc from regenerated residues after coupled extraction-cementation

To evaluate if the solid residues generated after treatment by concurrent dissolution-cementation meet environmental standards, the leachability of Pb and Zn using TCLP was examined out. The amounts of Pb and Zn leached before (untreated ZPLRs) and after treatment (treated by combined dissolution-cementation technique under the conditions 0.1M HCl, 2 M NaCl, and 0.1 g ZVAl) were compared with the regulatory thresholds. As illustrated in Table 5-1, the levels of Pb and Zn leached from untreated ZPLRs were substantially high: Pb was higher than environmental standards. In contrast, the amounts Pb and Zn that leached from the residues after treatment by the concurrent dissolution-cementation method were dramatically lower. Leachable Pb (which was about 0.12 mg/L) was lower than the regulatory threshold, which entails the detoxification of ZPLRs.

Table 5-1. TCLP leachability tests of untreated ZPLRs and treated residues after concurrent dissolution and cementation treatment.

	Untreated ZPLRs	Treated residues	Threshold (USEPA)
Pb	12.95 mg/L	0.12 mg/L	5 mg/L
Zn	473.5 mg/L	21.5 mg/L	–*

* No Zn TCLP regulatory threshold.

5.3.4. Conceptual flowsheet

Based on the results obtained in this study, the conceptual flowsheet for ZPLR treatment by a concurrent dissolution-cementation technique to remove/recover Pb and Zn by using HCl-NaCl solution with ZVAl is proposed (Fig. 5-11). The flowsheet involves the removal of Pb—more toxic heavy metal to human beings than Zn—by cementation using ZVAl before solid-liquid separation. Zn that remains in a solution can be recovered by precipitation or electrowinning. High removal of Pb and Zn can be achieved using less concentrated NaCl (even as low as 1 M) solution acidified with 0.1 M HCl by the addition of ZVAl. The generated solid residues may not necessarily need to be washed because the most toxic metal that remains in the solution as a result of the inherent incomplete solid-liquid separation is negligible. In addition, this approach shortens and simplifies the treatment of ZPLRs compared to the conventional approach (i.e., leach, solid-liquid separation, and finally recovery of dissolved metals).

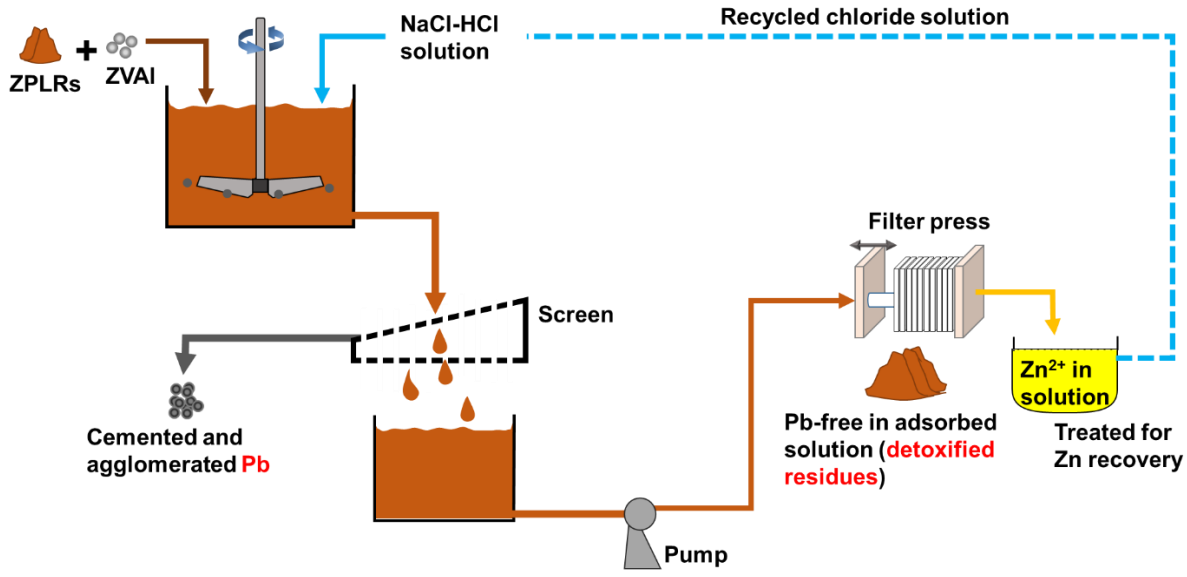

Fig. 5-11. A conceptual flowsheet of treatment of ZPLRs using the concurrent dissolution-cementation technique.

5.4. Conclusions

This chapter investigated Pb and Zn removal from ZPLRs using a concurrent dissolution- cementation technique in acidified chloride solution. The following is a summary of the findings:

1. Zinc removal from ZPLRs increased with increasing HCl concentration (i.e., increased from 27 to 60 and 70% when HCl concentration increased from 0.01 to 0.05 and 0.1 M, respectively) but it was neither affected by the increase of NaCl concentration nor the addition of ZVAl during leaching.

2. Zinc was not be sequestered from the acidified chloride leaching pulp by cementation using ZVAl and was attributed to dissolution of cemented Zn or preferential reduction of H^+ to H_2 by ZVAl over Zn^{2+} to Zn.

3. Lead removal from ZPLRs without the addition of ZVAl increased with increasing NaCl and HCl concentrations. Pb removal steadily increased from around 0 to 28, 0.5 to 58, and 0.5 to 72% for 0.01, 0.05, and 0.1 M HCl, respectively, when NaCl increased from 0 to 3 M, respectively. The increase of Pb removal with HCl concentration was attributed to an H^+ attack to dissolve Pb from carbonates as well as fixing free SO_4^{2-} as HSO_4^- thereby limiting the precipitation/formation of solid $PbSO_4$. Meanwhile, Pb removal increased at higher NaCl concentrations because of the formation of more soluble Pb-Cl complexes.

4. The addition of ZVAl during ZPLRs leaching (concurrent dissolution-cementation technique) dramatically increased the Pb removal even at low chloride concentration. Pb removal at 0.05 M HCl increased from 2.5 to 35.5% and 8 to 57% for 0.5 and 1 M NaCl concentration, respectively. Meanwhile, for 0.1 M HCl, the addition of ZVAl during ZPLR leaching increased Pb removal from 3 to 69% and 9 to 72% for 0.5 and 1 M NaCl concentration, respectively. The increase was attributed to shifting the equilibrium as the result of sequestration of dissolved Pb thereby enhancing dissolution lead host minerals and dissolution of intermediate sparling soluble solid, $PbCl_2$.

5. The most toxic metal, Pb, from ZPLRs was recovered and separated before solid-liquid separation, which simplifies the treatment flowsheet as well as eliminates the need for extensive washing of the solid residues generated.

This chapter was based on a research paper published under the following details: -

Silwamba, M., Ito, M., Hiroyoshi, N., Tabelin, C.B., Hashizume, R., Fukushima, T., Park, I., Jeon, S., Igarashi, T., Sato, T., Chirwa, M., Banda, K., Nyambe, I., Nakata, H., Nakayama, S., Ishizuka, M., 2020b. Recovery of Lead and Zinc from Zinc Plant Leach Residues by Concurrent Dissolution-Cementation Using Zero-Valent Aluminum in Chloride Medium. Metals 10, 531. https://doi.org/10.3390/met10040531.

References

Farahmand, F., Moradkhani, D., Safarzadeh, M.S., Rashchi, F., 2009. Brine leaching of lead-bearing zinc plant residues: Process optimization using orthogonal array design methodology. Hydrometallurgy 95, 316–324. https://doi.org/10.1016/j.hydromet.2008.07.012.

Feng, Q., Wen, S., Wang, Y., Zhao, W., Liu, J., 2015. Dissolution Kinetics of Cerussite in Acidic Sodium Chloride Solutions. Bull. Korean Chem Soc., 36, 1100–1107.

Guo, Z., Pan, F., Xiao, X., Zhang, L., Jiang, K., 2010. Optimization of brine leaching of metals from hydrometallurgical residue. Transactions of Nonferrous Metals Society of China 20, 2000–2005. https://doi.org/10.1016/S1003-6326(09)60408-8.

Jeon, S., Tabelin, C.B., Takahashi, H., Park, I., Ito, M., Hiroyoshi, N., 2020. Enhanced cementation of gold via galvanic interactions using activated carbon and zero-valent aluminum: A novel approach to recover gold ions from ammonium thiosulfate medium. Hydrometallurgy 191, 105165. https://doi.org/10.1016/j.hydromet.2019.105165.

Liu, W., Yang, T., Xia, X., 2010. Behavior of silver and lead in selective chlorination leaching process of gold-antimony alloy. Transactions of Nonferrous Metals Society of China 20, 322–329. https://doi.org/10.1016/S1003-6326(09)60141-2.

Needleman, H., 2004. Lead Poisoning. Annual Review of Medicine 55, 209–222. https://doi.org/10.1146/annurev.med.55.091902.103653.

Puigdomenech, I., 2010. Make equilibrium diagrams using sophisticated algorithms (MEDUSA), inorganic chemistry.

Ru, Z., Pan, C., Liu, G., Wang, X., Dou, G., Zhu, K., 2015. Leaching and recovery of zinc from leaching residue of zinc calcine based on membrane filter press. Transactions of Nonferrous Metals Society of China 25, 622–627. https://doi.org/10.1016/S1003-6326(15)63645-7.

Ruşen, A., Sunkar, A.S., Topkaya, Y.A., 2008. Zinc and lead extraction from Çinkur leach residues by using hydrometallurgical method. Hydrometallurgy 93, 45–50. https://doi.org/10.1016/j.hydromet.2008.02.018.

Seng, S., Tabelin, C.B., Kojima, M., Hiroyoshi, N., Ito, M., 2019. Galvanic Microencapsulation (GME) Using Zero-Valent Aluminum and Zero-Valent Iron to Suppress Pyrite Oxidation. Materials Transactions 60, 277–286. https://doi.org/10.2320/matertrans.M-M2018851.

Sethurajan, M., Huguenot, D., Jain, R., Lens, P.N.L., Horn, H.A., Figueiredo, L.H.A., van Hullebusch, E.D., 2017. Leaching and selective zinc recovery from acidic leachates of zinc metallurgical leach residues. Journal of Hazardous Materials, Selected papers presented at the 4th International Conference on Research Frontiers in Chalcogen Cycle Science and Technology, Delft, The Netherlands, May 28 - May 29, 2015 324, 71–82. https://doi.org/10.1016/j.jhazmat.2016.01.028.

St-Pierre, J., Piron, D.L., 1986. Electrowinning of zinc from alkaline solutions. J Appl Electrochem 16, 447–456. https://doi.org/10.1007/BF01008856.

Tuffrey, N.E., Jiricny, V., Evans, J.W., 1985. Fluidized bed electrowinning of zinc from chloride electrolytes. Hydrometallurgy 15, 33–54. https://doi.org/10.1016/0304-386X(85)90065-9

U.S. EPA, 1991. Toxicity Characteristic Leaching Procedure (TCLP), test method 1311- TCLP.

Xie, H., Zhang, L., Li, H., Koppala, S., Yin, S., Li, S., Yang, K., Zhu, F., 2019. Efficient recycling of Pb from zinc leaching residues by using the hydrometallurgical method. Mater. Res. Express 6, 075505. https://doi.org/10.1088/2053-1591/ab11b9.

Ye, M., Li, G., Yan, P., Zheng, L., Sun, S., Huang, S., Li, H., Chen, Y., Yang, L., Huang, J., 2017. Production of lead concentrate from bioleached residue tailings by brine leaching followed by sulfide precipitation. Separation and Purification Technology 183, 366–372. https://doi.org/10.1016/j.seppur.2017.04.020.

CHAPTER 6: GENERAL CONCLUSION AND FUTURE WORKS

6.1. Summary of the dissertation and conclusion

In this dissertation, an innovative method, a coupled extraction-cementation (CEC) process that combines two stages (i.e., extraction and recovery of extracted valuable/heavy metals thereby minimizing the operation stages and amounts of lixiviant), was investigated to detoxify high-Pb ZPLRs. The dissertation was divided into six (6) chapters in line with the global objective and the summary and conclusion of each chapter are as below: -.

Brief background of secondary resource and the environmental importance of ZPLRs are introduced in Chapter 1. Challenges of the conventional treatment of ZPLRs for metal removal/recovery are highlighted in the same Chapter 1. Finally, the major objective of this dissertation which is the "development of detoxification method for zinc plant leach residues by removing heavy metals using coupled extraction-cementation process" was stated.

Chapter 2 reviewed previous studies on methods and techniques used in the concentration of valuable minerals and recovery of valuable and critical metals from ZPLRs and other Zn hydrometallurgical solid wastes such as iron removal purification residues and metal cementation filter cake. Recovery of valuable and critical metals by hydrometallurgical route using acids (chloride and sulfuric acids) and alkaline solution by following conventional stages (i.e., leach→solid-liquid separation→ recovery of metal) requires aggressive and high amounts lixiviants as well as many operation stages to achieve satisfactory metal recovery/removal. Although critical and valuable metals are recovered from ZPLRs by a pyrometallurgical route at a high rate, the limitations are high energy consumption and production of toxic and greenhouse gases emission.

Chapter 3 reported on the detoxification of ZPLRs by CEC using micro-scale zero-valent iron (mZVI) and acidified chloride solution. Lead and Zn removal was evaluated in different solution compositions with and without the addition of mZVI. The addition of mZVI during ZPLRs leaching (i.e., CEC) increased Pb removal from 3% to 24%, 1.3% to 27.5%, 5.2% to 34.9%, and 6.5% to 55.8% when NaCl concentration was fixed at 0.86 M and HCl concentrations were 0 M, 0.01 M, 0.05 M and 0.1 M, respectively, after 12 h. Meanwhile, Zn removal was not affected by NaCl concentration and addition of mZVI but increased with increasing the HCl concentration. Extracted Zn remained in solution because it is thermodynamically unfavorable to be cemented by mZVI. Analysis of the Pb-loaded mZVI (magnetic fraction) by scanning electron microscopy with energy-dispersive X-ray spectroscopy (SEM-EDX) and X-ray photoelectron spectroscopy (XPS) revealed that Pb was recovered during leaching via cementation as zero-valent Pb (Pb^0). The toxicity characteristic

leaching procedure (TCLP) for Pb of ZPLRs before and after treatment decreased from 11.3 to 3.5 mg/L (below 5 mg/L threshold).

In Chapter 4, selective agglomeration of zero-valent Pb, Zn, Al was presented. This was necessary to evaluate the applicability of the Al-based CEC process for ZPLRs because the hypothesized cementation product (Pb-Zn-Al) cannot be separated physically from the leaching pulp using a magnet. When Zn, Al, and Pb metal powders were shaken in 0.1 M HCl, only Pb agglomerated. Further investigation showed that Pb agglomeration occurred in acidified chloride (HCl-NaCl) solution, but not in non-acidified chloride (NaCl) solution. Agglomeration was proposed to be as a result of the removal of the brittle oxide film and metallurgical bond formation ('solid-state cold welding') between Pb particles because Pb is a soft metal whose crystallization occurs even at room temperature. To investigate selective agglomeration of fine Pb metal particles in presence of other fine particles, fixed amounts of Pb metal powder were mixed with various amounts of fine quartz particles and Al metal powder to cement dissolved Pb^{2+}. Separation of agglomerated Pb from quartz was done by sieving. Around 98% of Pb metal powder was selectively agglomerated and could be separated effectively from quartz even in a high mass ratio of quartz to Pb metal as 24 g to 0.15 g. This implied that Al-based CEC could be applied to ZPLRs because the cementation product could be separated from the leaching pulp by sieving.

In Chapter 5, an investigation of the use of zero-valent aluminum (ZVAl) in the CEC process to detoxify ZPLRs in chloride solution was reported. The reasons for using ZVAl were (1) to cement both Pb and Zn since thermodynamic favorability shows ZVAl can cement Pb and Zn, and (2) to use a reducing agent metal whose standardized reduction potential is much low to increase the rate of the electrochemical reaction of cementation of Pb and Zn. The fact that ZVAl and cemented metals (i.e., Pb and Zn) are non-ferromagnetic, separation of cementation product from the leaching pulp was achieved via sieving since the cemented product agglomerated. The results showed that for 2 h Pb removal significantly increased when ZVAl was added at a low chloride concentration (e.g., for 0.1 M HCl, the addition of ZVAl increased Pb removal from 3% to 69% and 9% to 72% for 0.5 M and 1 M NaCl). The dramatic increase of Pb removal at low NaCl concentration was attributed to the leaching solution not attaining saturated with dissolved Pb^{2+} and Pb-Cl complexes. However, Zn removal, which was independent of NaCl concentration and addition of ZVAl, was not cemented out of the leaching pulp despite it being thermodynamic favorable. The suppression of cementation of Zn by ZVAl was attributed to proton (H^+) competition for electrons from ZVAl. The leachability test results using TCLP protocol for detoxified residues showed that Pb and Zn in solution were as low as 0.12

mg/L (below 5 mg/L threshold) and 21.5 mg/L (below 25 mg/L threshold), respectively. A treatment flowchart for detoxification of ZPLRs using Al-based CEC was proposed.

6.2. Future research works

i. The Al-based CEC process has the potential for industrial application to remove Pb, which is the most toxic metal in ZPLRs, before solid-liquid separation. However, there is a need to further optimization study of the process and investigate process kinetics.

ii. For the complete study, further research work on the recovery of Zn that remained in solution after recovery of cemented and agglomerated Pb is also recommended. Processes that can be explored, include precipitating Zn as ZnS, ZnO, or electrowinning.

iii. To increase the purity of cemented and agglomerated Pb there is a need to remove co-agglomerated Al metal powder. The removed Al metal powder can be recycled. Possible ways of removing Al metal powder by disintegration of agglomerate particles by ultrasonic and agglomeration experiments in low HCl concentrated solution.